# Aptamer−Protein Interactions: From Regulation to Biomolecular Detection

Cailing Ji, Junyuan Wei, Lei Zhang, Xinru Hou, Jie Tan,* Quan Yuan,* and Weihong Tan
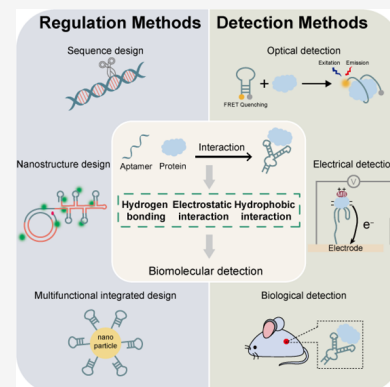
Read Online

ACCESS | Metrics & More | Article Recommendations

**ABSTRACT:** Serving as the basis of cell life, interactions between nucleic acids and proteins play essential roles in fundamental cellular processes. Aptamers are unique single-stranded oligonucleotides generated by in vitro evolution methods, possessing the ability to interact with proteins specifically. Altering the structure of aptamers will largely modulate their interactions with proteins and further affect related cellular behaviors. Recently, with the in-depth research of aptamer−protein interactions, the analytical assays based on their interactions have been widely developed and become a powerful tool for biomolecular detection. There are some insightful reviews on aptamers applied in protein detection, while few systematic discussions are from the perspective of regulating aptamer−protein interactions. Herein, we comprehensively introduce the methods for regulating aptamer−protein interactions and elaborate on the detection techniques for analyzing aptamer−protein interactions. Additionally, this review provides a broad summary of analytical assays based on the regulation of aptamer−protein interactions for detecting biomolecules. Finally, we present our perspectives regarding the opportunities and challenges of analytical assays for biological analysis, aiming to provide guidance for disease mechanism research and drug discovery.

## CONTENTS

## 1. INTRODUCTION

Intermolecular interactions influence biomolecule behaviors, regulating a broad range of biological processes to perform complex life activities.[1−4] Taking nucleic acid−protein interactions as an example, these interactions play pivotal roles in fundamental cellular processes such as replication, translation, transcription, and gene expression regulation.[5−7] Hence, nucleic acid−protein interactions are essential for normal cell function and the survival of any living organism. Aptamers are single-stranded oligonucleotides evolved by in vitro selection methods, capable of binding to proteins with superior specificity and affinity.[8−10] Aptamers interacting with

proteins are able to reveal information regarding spatiotemporal behaviors of target proteins, further offering profound insights into related biological processes.[11,12] For instance, utilizing their interactions with cytochrome c (Cyt c), fluorescent aptamer probes can visualize the cytosolic release of Cyt c, thus monitoring the apoptotic process.[13,14] Therefore, research on aptamer—protein interactions provides crucial feedback to thoroughly understand and appropriately manipulate vital life processes within biological systems, which is of great significance in the biomedical field.

Aptamers interact with proteins via hydrogen bonding, electrostatic interactions, hydrophobic interactions and van der Waals forces.[15–17] Changing the structure of aptamers can tune their binding affinity toward target proteins.[18–20] By way of illustration, the introduction of hydrophobic amino-acid-like side chains into aptamers can form additional hydrophobic contacts, enhancing the interactions of aptamers with thrombin dramatically and achieving highly sensitive detection of thrombin.[21–23] Notably, regulating the interactions between aptamers and disease-related proteins allows modulation of protein-mediated cell behaviors, assisting disease diagnosis, treatment and pathological assessment.[24–26] For example, aptamers are modified with hydrophobic small-molecule anticancer drugs to improve their interactions with target proteins, facilitating selective cellular uptake and thereby inhibiting tumor growth.[27] The regulation of aptamer—protein interactions thus serves as a universal platform not only for realizing the highly sensitive and selective detection of biomolecules, but also for boosting the discovery of disease biomarkers and potential drug targets.

Recently, the development of analytical assays based on aptamer—protein interactions has been greatly bolstered by in-depth understanding of the aptamer—protein interactions, including interaction sites, intensity, and mechanisms.[28–32] As plenty of groundbreaking work has been reported, many reviews on the application of aptamers for protein detection have also been published.[22,33–37] However, there has not been a systematic discussion about these analytical assays from the perspective of regulating aptamer—protein interactions. This review introduces various approaches to regulate aptamer—protein interactions. We focus largely on synthetic aptamers and their interactions with proteins, rather than aptameric RNA transcripts expressed in cells.[38–41] Subsequently, we provide a comprehensive summary of methods for determining structures of aptamer—protein complexes and for detecting the interactions of aptamers with target proteins. Additionally, the application of analytical assays based on the regulation of aptamer—protein interactions in bioanalytical detection is also systematically reviewed. We end with a discussion of challenges and perspectives in this field, aiming to provide guidance for disease diagnosis and drug development.

## 2. REGULATION METHODS OF APTAMER—PROTEIN INTERACTIONS

Aptamers are a special class of single-stranded oligonucleotides obtained by an in vitro selection process termed Systematic Evolution of Ligands by EXponential enrichment (SELEX), enabling binding to target proteins with high affinity and specificity.[42–44] The binding events are based on the characteristic of aptamers forming unique three-dimensional structures that allow specific interactions with target proteins, including hydrogen bonding, electrostatic interactions, hydrophobic interactions, $\pi$–$\pi$ stacking and van der Waals

forces.[15–17] The characteristics of these interactions are summarized in Table 1. Most aptamer—target protein

### Table 1. Summary of the Interactions between Aptamers and Proteins

| Interaction type | Main components that mediate the interaction |
|---|---|
| Hydrogen bonding | The side chains of proteins and either the nucleic acid bases or phosphate groups of aptamers |
| Electrostatic interactions | The negatively charged phosphate backbones of aptamers and the positively charged protein residues |
| Hydrophobic interactions | The aromatic rings of aptamers and the aliphatic side chains of proteins |
| $\pi$–$\pi$ stacking | Parallel aromatic rings of aptamers and proteins |
| van der Waals forces | Atoms, molecules, and surfaces of aptamers and proteins |

interactions are mediated by hydrogen bonding.[45] In addition to nucleic acid bases, phosphate groups also play an important role in the formation of hydrogen bonding. The phosphate groups in aptamers generally act as hydrogen bond acceptors, and the side chains of proteins serve as hydrogen bond donors.[46,47] Besides, owing to the negatively charged phosphate backbones, aptamers can attract the positively charged surface of target proteins, thereby inducing electrostatic interactions.[48,49] The hydrophobic interaction of aromatic rings with the aliphatic side chains of proteins is reported to be another force responsible for aptamer—target protein interactions.[23,50] In addition, aromatic rings are also confirmed to participate in $\pi$–$\pi$ stacking, mainly due to the overlapping of $\pi$ orbitals.[51–53] The final important binding interaction is the van der Waals force arising from the mutual attraction of dipoles and induced dipoles.[54] It has been reported that the strength of van der Waals forces heavily depends on the dimension of the interacting interface.[51] Regulation of aptamer—protein interactions can distinguish subtle differences in the structure and content of analytes, achieving the sensitive and specific detection of biomolecules.[37,55–57] Some studies have validated that changing the structure of aptamers changes their interactions with proteins.[18–20] In this section, we will give a detailed discussion about how to customize aptamer structures by sequence design, nanostructure design and multifunctional integrated design, thereby regulating aptamer—protein interactions.

### 2.1. Design of Aptamer Sequences

The main idea of aptamer sequence design is to transform their spatial structures via the reformation of aptamer sequences, thereby regulating the interactions between aptamers and proteins. Generally, full-length aptamers derived from the SELEX process are 70–130 nucleotides (nt) in length, consisting of a random region (30–50 nt) and two fixed primer regions.[58–60] Only a small fraction of nucleotides in a full-length aptamer, known as essential and supporting nucleotides, play critical roles in the interactions with target protein.[61,62] The remaining nucleotides that do not support aptamer—protein interactions are regarded as nonessential nucleotides.[63] These nonessential nucleotides not only produce unnecessary steric hindrance but also increase nonspecific interactions, affecting the affinity and specificity of aptamers to a certain extent.[64–66] Therefore, appropriately truncating aptamers to eliminate nonessential nucleotides is one of the important strategies to regulate aptamer—protein interactions. To determine which nucleotides can be deleted, analyzing the sequence and structure of aptamers is first
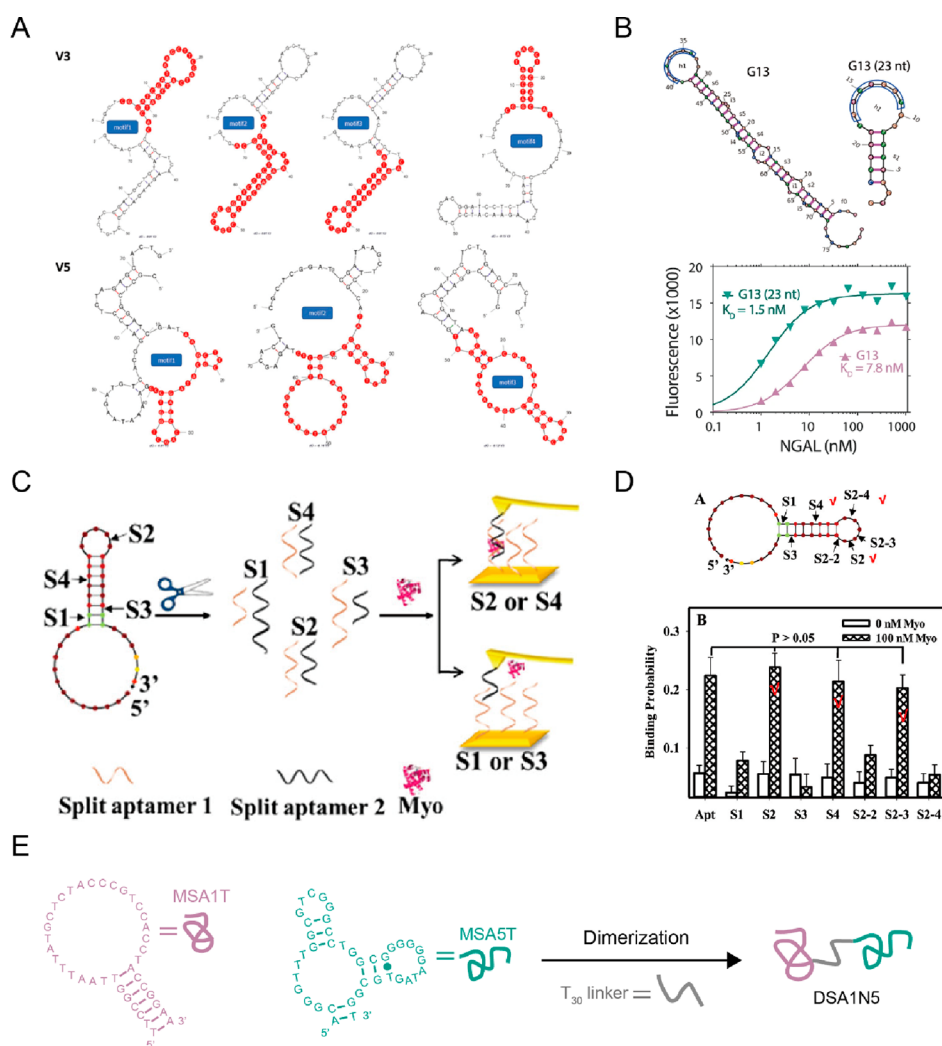
**Figure 1.** (A) Secondary structures of selected 74-mer vimentin aptamers. Seven potential binding motifs are shown in red. Reprinted with permission from ref 72. Copyright 2021 MDPI under CC BY 4.0 [https://creativecommons.org/licenses/by/4.0/]. (B) Secondary structures (top) and KD curves (bottom) of the full-length aptamer (purple line) and truncated aptamer (teal line). Adapted with permission from ref 74. Copyright 2021 Springer Nature under CC BY 4.0 [http://creativecommons.org/licenses/by/4.0/]. (C) Illustration of engineering Myo-binding split aptamers using AFM. (D) Binding probabilities of Myo and split aptamers cleaved at different sites. (C,D) Reprinted and adapted with permission from ref 87. Copyright 2020 American Chemical Society. (E) Schematic illustration of the spike-protein binding divalent aptamer DSA1N5 built with MSA1T (purple), MSA5T (teal), and T$_{30}$ linker. Adapted with permission from ref 90. Copyright 2021 John Wiley and Sons.

required.[67,68] In general, some available software algorithms, such as ClustalW and Mfold, are applied to conduct multiple sequence alignments or predict the secondary structure of aptamers, thereby deducing the essential sequences for interactions between aptamers and target proteins.[63,69,70] Subsequently, the aptamers are rationally truncated on the principle of preserving the required sequence. Many studies have demonstrated the effectiveness of aptamer truncation strategies. Macdonald et al. utilized the MFold to predict the secondary structure of transferrin receptor (TfR) aptamer, GS24 (64 nt), identifying the minimum sequence required to GS24-TfR interactions.[71] GS24 was finally truncated to a 14 nt sequence, exhibiting a significantly enhanced binding affinity for TfR. Several studies have demonstrated that special secondary structures such as stem-loops are central to target molecule recognition.[72,73] Accordingly, elimination of non-essential nucleotides in these regions can change the accessibility of targets to aptamers, regulating aptamer—protein interactions efficiently. Based on the predictive secondary

structures of 74 mer vimentin-binding aptamers (V3 and V5), Costello and co-workers conducted aptamer truncations on the stem-loop regions, resulting in seven truncated motifs with different binding affinities (Figure 1A).[72] Among them, truncated aptamers with ∼40 mer showed the highest binding affinity, revealing approximately 2-fold enhancements compared with the original aptamers. In recent years, with the rapid growth of computer science and computational biology, researchers have also applied machine learning to the identification and design of high-performance aptamers. In 2021, using affinity data of multiple full-length aptamers (∼80 nt) against neutrophil gelatinase-associated lipocalin (NGAL), Bashir's team trained machine learning models for affinity prediction of de novo and experimentally derived aptamers.[74] These machine learning models were used to identify core sequences necessary for the aptamer—NGAL protein interactions. On the basis of retaining the core sequence, the authors designed truncated aptamers 70% shorter and with a 5-
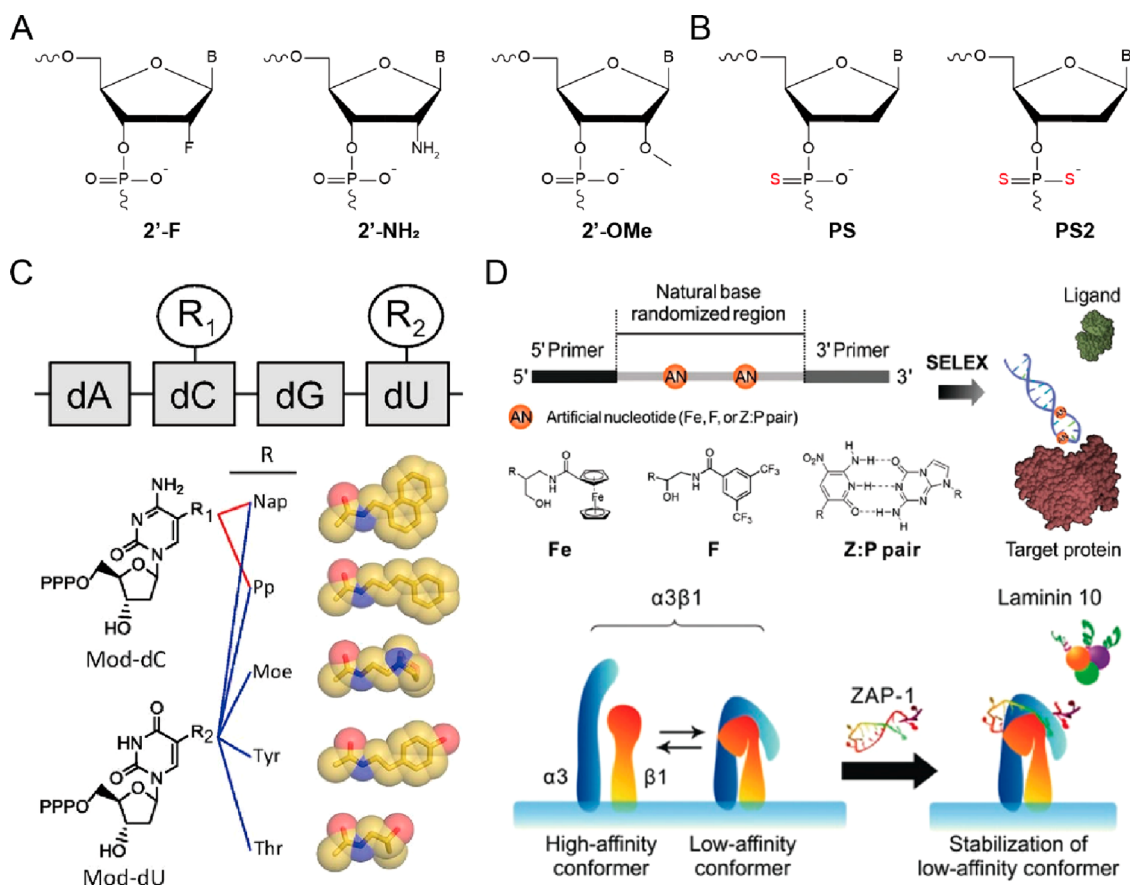
**Figure 2.** Modifications on the ribose (A) and phosphate backbone (B) of the aptamers. (C) Schematic of an aptamer with combinations of double modifications on dC and dU. Space-filling models of R groups as follows: Nap, 5-[N-(1-naphthylmethyl)carboxamide]-2′-deoxy; Pp, 5-[N-(phenyl-3-propyl)carboxamide]-2′-deoxy; Moe, 5-[N-(1-morpholino-2-ethyl)carboxamide]-2′-deoxy; Tyr, 5-[N-(4-hydroxyphenyl-2-ethyl)carboxamide]-2′-deoxy; and Thr, 5-[N-(S-2-hydroxypropyl)carboxamide]-2′-deoxy. R1 groups tested on dC were Nap and Pp (red lines), whereas R2 groups tested on dU were Nap, Pp, Moe, Tyr, and Thr (blue lines). Adapted with permission from ref 113. Copyright 2017 Natl Acad Sciences under PNAS Open Access License. (D) Molecular design of ZAP-1 aptamer derived from libraries containing P-Z base pairs (top) and conformational modulation of integrin $\alpha 3\beta 1$ by ZAP-1 binding (bottom). Reprinted with permission from ref 119. Copyright 2019 John Wiley and Sons.

fold higher binding affinity than the original aptamers (Figure 1B).

When binding to target proteins, the conformation of aptamers changes significantly to form various secondary structures, such as hairpin loops, stem-loops, or pseudoknots.[37,75] These structures play basic roles in contacting target proteins. However, in complex substrates, aptamer conformational changes are also susceptible to environmental factors like ions and pH, thus affecting their folding to the proper secondary structures.[76−78] To overcome this obstacle, researchers have designed and constructed split aptamers. Intact aptamers are split into two or more independent and nonfunctional fragments.[79] Only upon encountering target proteins are split aptamers selectively assembled into the specific binding conformations.[80,81] This effectively avoids unfavorable secondary structures and nonspecific interactions.[82,83] Moreover, split aptamers are much shorter than intact aptamers, showing the good anti-interference ability to steric hindrance.[84] Consequently, splitting aptamers provides an available strategy for regulating aptamer−protein interactions. Li et al. divided an intact aptamer for vascular endothelial growth factor (VEGF$_{165}$) into two short fragments and exploited single molecular force spectroscopy (SMFS) to measure the interaction force of aptamers with VEGF$_{165}$.[85] SMFS results demonstrated that no detectable signal was observed in the absence of VEGF$_{165}$. When VEGF$_{165}$ was present, split aptamers interacted specifically with VEGF$_{165}$, and the interaction force was approximately 20 pN higher than that of intact aptamer−VEGF$_{165}$. However, since binding mechanisms of most aptamers to proteins are not well understood, there are still few split aptamers reported so far.[86] To address this issue, researchers have developed multiple methods to guide the engineering of split aptamers in recent years. For instance, Li's group constructed split aptamers against myoglobin (Myo) with the help of atomic force spectroscopy (AFM).[87] As illustrated in Figure 1C, the intact Myo-binding aptamer was first randomly cleaved into split aptamer 1 and split aptamer 2 at different sites. Split aptamer 1 and split aptamer 2 were then attached to the AFM tip and gold substrate, respectively. Subsequently, the interaction between Myo and split aptamers was investigated using AFM, and three pairs of split aptamers that exhibited high affinity and specificity for Myo in human serum were successfully obtained (Figure 1D).

Apart from aptamer splitting, sequence splicing is also an attractive strategy for regulating aptamer−protein interactions. At present, a variety of linkage methods have been described to splice two or more aptamers to construct multivalent aptamers, thereby interacting with target proteins via multiple binding sites.[88] Shiang and co-workers constructed bivalent aptamers

by coupling two thrombin-binding aptamers (TBA15 and TBA29, which interact with positively charged exosites 1 and 2 of thrombin, respectively) onto Au nanoparticles.[89] Compared with free TBAs, these bivalent TBAs enhanced electrostatic interactions with thrombin, exhibiting significantly improved anticoagulant potency (ca. 50-fold). Zhang et al. chose two aptamers, MSA1T and MSA5T, targeting SARS-CoV-2 spike protein, and created divalent aptamers via a 30-mer polythymidine ($T_{30}$) linker linkage, as presented in Figure 1E.[90] The obtained divalent aptamers had binding affinities for spike proteins that were about 100- and 30-fold higher than MSA1T and MSA5T, respectively.

To achieve excellent multivalent interactions, most strategies for constructing multivalent aptamers need to identify two or more aptamers that bind to different sites on the same target protein and further optimize linkage methods, orientation, and distance between these monovalent aptamers.[91,92] However, owing to the gradual loss of aptamers targeting weakly binding sites during the selection process, almost all aptamers so far are specific to the same binding site on the target protein, limiting the widespread development of multivalent aptamers.[93] Addressing this, Zhou and co-workers introduced DNA nanostructures into conventional SELEX techniques and exploited an approach to directly screen bivalent aptamers with superior binding affinity.[94] Each strand in the library was designed as a single-strand DNA nanostructure, comprising fixed sequences that self-fold to form the two-helix stem region of the scaffold structure and two 20 nt random loop sequences. The closed random loop regions were supposed to form many complicated conformations to adequately interact with target proteins. The scaffold structure could not only offer stable structural support for the contact between two random loop regions and target proteins, but also adjust the relative orientation and distance between two aptamers, thus providing the optimal linkage mode. By designing the scaffolded library according to the size of thrombin, the authors identified via a simple seven-round screening a group of extremely high-affinity bivalent aptamers ($K_D \approx 340$ fM) that interact with two different binding sites on thrombin. In conclusion, compared with monovalent aptamers, multivalent aptamers can manipulate the interaction interface between aptamers and target proteins, further regulating aptamer−protein interactions.

Antibodies, conventional recognition molecules, are composed of 20 different amino acids with a variety of spatial structures.[95,96] In contrast, the limited components of natural nucleotides (A, G, C, T, or U) definitely restrict the structural and functional diversity of aptamers.[97,98] Introducing chemical groups not found in natural nucleotides not only allows the formation of aptamers with richer spatial conformations, but also provides additional interactions between aptamers and their target proteins.[99,100] Therefore, strategies regarding chemical modifications of aptamers are also well established for modulating aptamer−protein interactions. Many conceivable chemical modifications are not compatible with the conventional SELEX process involving RNA polymerase transcription and/or PCR depending on DNA polymerases.[101] Such modifications therefore cannot be included in random libraries and cannot be subjected to the selection process. This is a major obstacle to optimizing chemical modifications because ad hoc post-SELEX engineered modifications may or may not be optimal. Ideally, modifications would be present in the random library during the selection process, not added

later. This may provide new ideas for efficient aptamer selection.

On the basis of the diverse modification position, chemical modifications for aptamers can be divided into three categories: modifications on sugar rings, modifications on phosphates, and modifications on bases.[102,103] As illustrated in Figure 2A, modifications on sugar rings mainly involve 2′-ribose modifications, including 2′-amino (2′-$NH_2$), 2′-fluoro (2′-F), 2′-O-methyl (2′-O−$CH_3$), and so on.[36,104−106] Much evidence indicates that 2′-substitution on ribose moieties affects sugar pucker conformation, further having an impact on the tertiary structures of aptamers.[107,108] Therefore, for the same target proteins, aptamers with distinct sequences and structures will be identified from nucleic acid libraries with different 2′-ribose modifications. Comparatively, aptamers with more stable conformations exhibit higher binding affinity to their target proteins.[109] For example, Pagratis performed the selection process to obtain different 2′-modified aptamers against keratinocyte growth factor (KGF) from libraries containing modified RNA with 2′-$NH_2$ or 2′-F pyrimidines.[110] Since the intramolecular helices formed by 2′-F RNA are substantially stronger than that of 2′-$NH_2$ RNA, the 2′-F modified aptamers have more rigid structures. Thus, 2′-F modified aptamers exhibited binding affinity ($K_D \approx 0.3−3$ pM) for KGF superior to 2′-$NH_2$ modified aptamers ($K_D \approx 400$ pM). The phosphate moieties are typically well exposed on the surface of aptamer, allowing easy access to the target proteins.[111] Hence, common modifications on phosphate linkages presented in Figure 2B play a crucial role in regulating aptamer−protein interactions. Studies have shown that the two nonbridging oxygen atoms of phosphate groups in the aptamer backbone commonly interact with amino acid side chains of proteins via hydrogen bonding.[111] By replacing two non-bridging phosphate oxygen atoms by sulfur to yield a phosphorodithioate (PS2) linkage, Abeydeera et al. synthesized chemically modified aptamers targeting VEGF and thrombin, respectively.[111] Due to the introduction of hydrophobic interactions by sulfur substitution, PS2-modified aptamers had an approximately 1000-fold increase in affinity toward target proteins compared with unmodified aptamers. Indeed, some modifications not only bring remarkable enhancements in target affinity, but may also increase off-target affinities.[38,97]

Modifications on bases, that is, base substitutions or addition of unnatural bases, are widely studied chemical modification strategies. In general, base substitutions refer to replacing the 5′-position of pyrimidines with hydrophobic, hydrophilic, or charged groups, thereby introducing additional interactions into aptamer−protein interactions.[112] Gawande's group incorporated numerous hydrophobic and hydrophilic groups that resemble similar side chains in proteins into nucleic acid libraries.[113] Figure 2C shows various substitutions at 5′-position of cytidine (Nap and Pp) and uridine (Nap, Pp, Moe, Tyr, and Thr). Multiple doubly modified aptamers targeting proprotein convertase subtilisin/kexin type 9 (PCSK9), a representative human therapeutic protein target, were derived from libraries with pairwise combinations of these modifications. Compared with unmodified and single-modified aptamers, these doubly modified aptamers showed a significant improvement in affinity, in particular a hydrophobic modification (Nap or Pp) on deoxyuridine (dU) paired with Tyr-deoxycytidine (Tyr-dC).
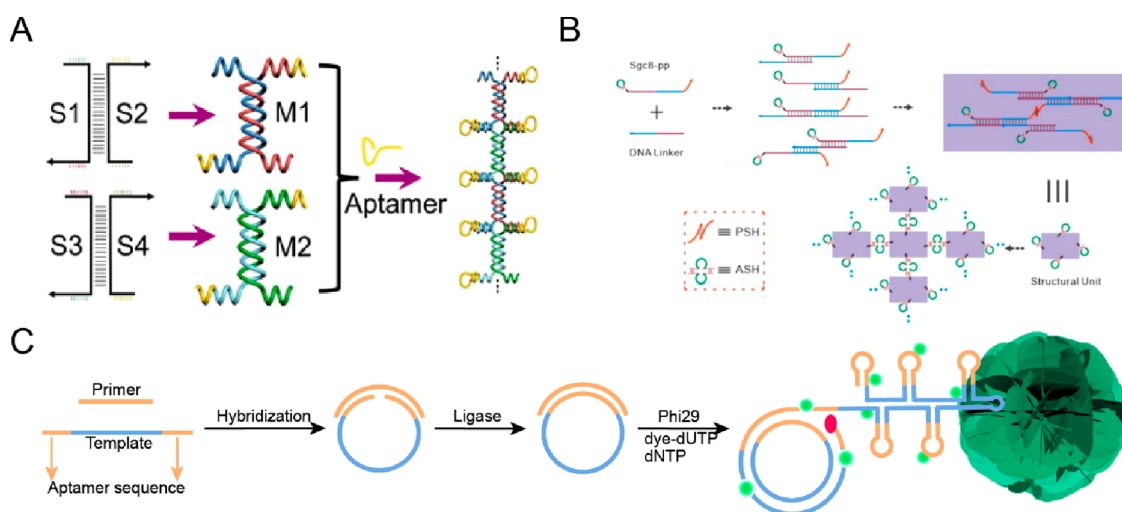
**Figure 3.** Stepwise assembly of 1D aptamer nanowires (A), 2D aptamer nanonetworks (B), and 3D aptamer nanoflowers (C). PSH and ASH denote the palindromic-self-hybridization and aptamer-self-hybridization, respectively. (A) Adapted with permission from ref 133. Copyright 2020 John Wiley and Sons. (B) Adapted with permission from ref 135. Copyright 2020 Elsevier.

Moreover, indole and methyl groups have also been applied in base modifications to modulate interactions between aptamers and target proteins. Dolot and colleagues synthesized 5-(indolyl-3-acetyl-3-amino-1-propenyl)-2-deoxyuridine (W) and 5-(methyl-3-acetyl-3-amino-1-propenyl)-2-deoxyuridine (K) as deoxythymidine (T) analogues.[114] Substituting T at position 4 of TBA15 by these T analogues afforded T4W and T4K. Compared with native TBA15, T4W and T4K introduced additional hydrophobic and hydrogen bonding interactions, respectively, promoting a significant increase in their binding affinity toward thrombin. Yoshikawa and Rangel introduced indole groups into aptamer screening.[115] The indole moieties of base-modified aptamers offered stable hydrophobic effects for aptamer−glycoprotein interactions, achieving the recognition and differentiation of specific protein glycoforms. Furthermore, multiple artificial base pairs, such as P{2-amino-8-(1-$\beta$-D-2-deoxyribofuranosyl)-Imidazo[1,2-$a$]-1,3,5-triazin-4(8H)one}−Z[6-amino-5-nitro-3-(1-$\beta$-D-2-deoxyribofuranosyl)-2(1H)-Pyridone] and Ds {7-(2-thienyl)-imidazo[4,5-$b$]pyridine}-Px(2-nitro-4-propynylpyrrole), have also been developed to increase the chemical diversity of nucleic acid libraries and regulate aptamer−protein interactions.[9,19,116] Among them, the P−Z base pair can lead to additional interactions of the nitro group on Z with proteins,[117,118] while the highly hydrophobic Ds base will strengthen interactions between aptamers and hydrophobic cavities in target proteins.[9] Our group selected the aptamer that targets integrin alpha3 (named ZAP-1) from nucleic acid libraries containing P−Z base pairs.[119] With high affinity and selectivity, ZAP-1 could effectively reduce integrin $\alpha3\beta1$−laminin binding, thus inhibiting $\alpha3\beta1$-mediated adhesion and migration of tumor cells (Figure 2D). Overall, owing to the improved chemical and structural diversity, chemically modified aptamers possess the capability to effectively regulate aptamer−protein interactions, further manipulating biomolecular behaviors.

## 2.2. Design of Aptamer Nanostructures

The binding affinity and specificity of aptamers toward target proteins rely on their unique three-dimensional folded conformations.[120,121] In recent years, researchers have focused on regulating aptamer−protein interactions in complex biological milieu to modulate diverse biological processes. However, in the crowded living environment, the folding process and conformational stability of aptamers are susceptible to interference from nucleases and nonspecific interactions with other biomolecules, thereby affecting the stable binding of aptamers to target proteins.[92,122] Therefore, it becomes difficult to regulate aptamer−protein interactions in living systems. As artificially synthesized nucleic acids, aptamers have been used as exceptional molecular building blocks for nanostructures, mainly due to their predictable and programmable conformations as well as intra- and intermolecular Watson−Crick base-pairing rules.[51,123,124] Several reports reveal that by utilizing convenient sequence designs and reliable assembly methods, all termini of aptamers can be stably encapsulated in nanostructures to restrict their flexibility, significantly enhancing the conformational stability of aptamers.[121,124−126] Meanwhile, the self-assembly of nanostructures driven by a number of noncovalent interactions is also capable of bringing many additional interactions, thus increasing the structural complexity and diversity of nanostructures.[127,128] Besides, customizing aptamer nanostructures can control the number, density and spatial arrangement of interaction sites, providing more possibilities for regulating aptamer−protein interactions.[129] In the past few decades, researchers have designed aptamer nanostructures varying in size and shape to effectively regulate aptamer−protein interactions under physiological conditions.

According to the dimensions of nanostructures, aptamer-based nanostructures can be divided into one-dimensional (1D), two-dimensional (2D), and three-dimensional (3D) nanostructures. Self-assembled 1D aptamer nanomaterials generally have a linear shape, such as nanowires, by placing free aptamers in designated distances and orientations along 1D compact DNA nanostructures.[129] Due to the introduction of multiple binding sites, constructing aptamer nanowires can effectively regulate aptamer−protein interactions via multivalent interactions.[130−132] Xue and Zhang connected multiple DNA double helices together to build a linear core backbone that exposed sequences complementary to the termini of aptamers at specific distances.[133] Then, targeting aptamers were regularly anchored perpendicularly on the core surface to
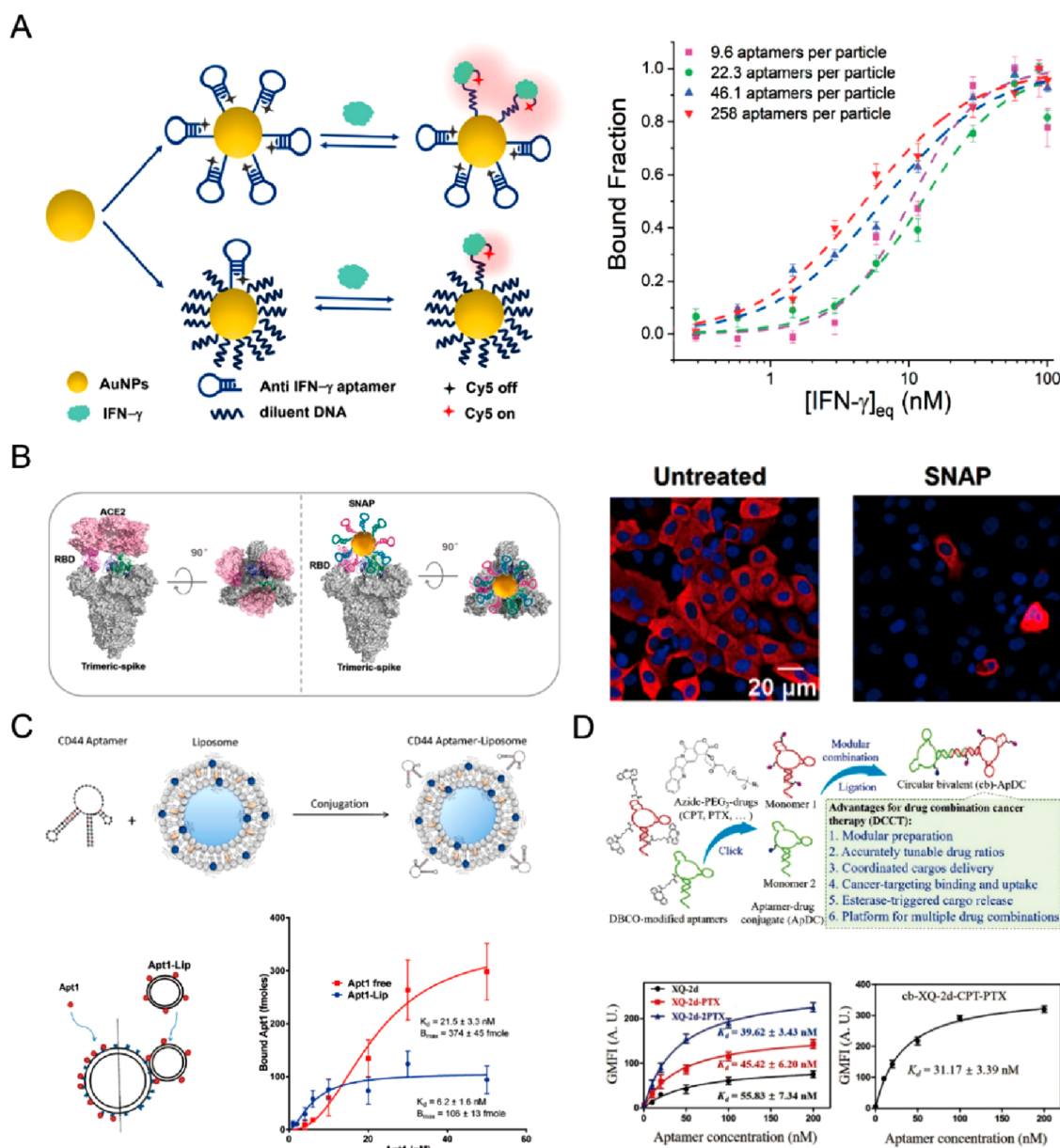
**Figure 4.** (A) Fabrication of aptamer−AuNPs conjugate with different surface coverage of aptamer and binding curves of these obtained aptamer−AuNPs conjugates to IFN-γ. Reprinted with permission from ref 148. Copyright 2021 American Chemical Society. (B) Inhibition mechanism and effects of SNAP conjugates against authentic SARS-CoV-2 infection. Adopted with permission from ref 149. Copyright 2021 American Chemical Society. (C) Fabrication of Apt1−Lip and binding affinity curves of Apt1−Lip to CD44. Adapted with permission from ref 159. Copyright 2015 American Chemical Society. (D) Fabrication and equilibrium dissociation constants of cb-ApDCs with accurate tunability of drug ratios. Adapted with permission from ref 163. Copyright 2019 John Wiley and Sons.

form a periodically ordered core/shell aptamer nanowire (Figure 3A). These nanowires effectively hid all termini of aptamers and displayed a large number of protein-binding sites, resulting in significantly enhanced nuclease-degradation resistance and binding affinity in the crowded intracellular milieu. Li et al. utilized hybridization chain reaction (HCR) to generate a DNA scaffold. The HCR used here contained three components: biotin-modified hairpin monomers (H1 and H2) and a DNA initiator strand.[134] Subsequently, biotinylated aptamers were coupled to the scaffold via streptavidin−biotin affinity interaction, thus forming the aptamer nanocentipede structure. Aptamer nanocentipedes exhibited higher selectivity and affinity than those of free aptamers. Additionally, the

binding affinity of aptamer nanocentipedes to target proteins could be adjusted by the length of HCR products.

Compared with 1D aptamer nanostructures, 2D nanostructures further expand the effective territory for immobilization of aptamers, thus enabling better regulation of their interaction with target proteins. For example, Wang's team extended the sequence of aptamer-targeting protein tyrosine kinase 7 (PTK7) to confer three functional regions, including an aptamer segment, a terminal palindrome, and a segment complementary to DNA linker.[135] As shown in Figure 3B, 2D aptamer nanonetworks were self-assembled from the extended aptamers and DNA linkers by utilizing DNA-linker-based horizontal hybridization and vertical self-hybridization. Eventually, the binding affinity of nanonetworks is increased by 3-

fold owing to the multivalent binding effect. With the rapid development of DNA nanotechnology, numerous 3D aptamer nanostructures have been designed and constructed to further promote the tunability of the interaction between aptamers and target proteins. Roloff and colleagues designed TBA—polymer amphiphiles that assembled into uniformly sized nanomicelles.[122] These micellar aptamers retained their native secondary structure in human serum and showed stronger inhibitory effects in blood clotting assays when compared to free aptamers. Lv's group described a comprehensive protocol for preparing aptamer nanoflowers via rolling-circle replication (RCR) of a designed template, as illustrated in Figure 3C.[136] The authors used aptamer Sgc8c, which can specifically recognize PTK7, as the model, designed the template and primer sequences reasonably, and employed RCR to generate long DNA building blocks containing multiple Sgc8c aptamers. Subsequently, these building blocks were gradually assembled to form Sgc8c-integrated nanoflowers by DNA liquid crystallization. Based on the multivalent effect, aptamer nanoflowers were endowed with higher affinity and selectivity than free aptamers. In conclusion, aptamer nanostructures can not only improve the conformational stability of aptamers, but also introduce multivalent interactions, opening a promising avenue for regulating aptamer—protein interactions.

## 2.3. Multifunctional Integrated Design of Aptamers

As aptamer technology and coupling technology continue to develop, aptamers can be coupled with a variety of functional carriers to form numerous composite materials with an increasingly diverse range of structures and functions.[137−140] Multifunctional integrated design strategies effectively merge the advantages and characteristics of functional carriers and aptamers while circumventing their disadvantages, providing a potential means to regulate aptamer—protein interactions. In this part, we give a detailed discussion about how functional modifications of aptamers affect aptamer—protein interactions.

As the most common functional carriers, inorganic nanomaterials possess unique properties such as large surface-area-to-mass ratio and easy biofunctionalization, making them capable of loading a number of aptamers to construct aptamer—inorganic hybrid nanomaterials.[141−143] The loading of aptamers on the one hand endows inorganic nanomaterials with specific recognition ability and improved biocompatibility.[144−146] On the other hand, inorganic nanomaterials can modulate the conformational stability, density, and number of loaded aptamers, thereby regulating the blood circulation times, nuclease resistance, and the ability to interact with proteins.[129,147] Chen's group immobilized different amounts of aptamers specific for interferon-gamma (IFN-$\gamma$) on the surface of gold nanoparticles (AuNPs), and investigated the effect of surface coverage of aptamer on the aptamer—target protein interactions (Figure 4A).[148] The binding affinity between aptamer—AuNPs conjugates and IFN-$\gamma$ enhanced 10-fold when increasing the number of aptamers from an average of 9.6 to 258 per particle. This indicated that the higher the surface coverage of aptamers on nanoparticles, the more protein binding sites will be provided, thus promoting the interaction between aptamers and proteins. For SARS-CoV-2 and associated mutant strains, Sun and Liu engineered a spherical cocktail neutralizing aptamer—gold nanoparticle (SNAP) to block the interaction between the receptor-binding domain (RBD) of trimeric-spike protein and host ACE2.[149] As presented in Figure 4B, multiple aptamers targeting distinct

epitopes on RBD were anchored on the same AuNP with high density, resulting in multivalent effects that significantly improved the binding affinity against spike proteins. Moreover, SNAP can simultaneously interact with three nonoverlapping epitopes on RBD, thus producing potent virus inhibition efficacy. More importantly, attributed to the inherent features of inorganic nanomaterials such as optical and electronic properties, inorganic nanomaterial—aptamer conjugates are able to serve as highly sensitive biosensor platforms.[141,150] This platform can convert information about the distribution and content of biomolecules into detectable optical or electrical signals, greatly facilitating the wide application of regulating aptamer—protein interactions in ultrasensitive biomolecule detection. Based on the unique optical properties of AuNPs, Wang et al. constructed TBA—AuNPs conjugates for simple, rapid, and ultrasensitive colorimetric detection of thrombin.[151] TBA—AuNPs conjugates showed excellent sensing performance in complex biological samples, and the colorimetric signals enhanced with the increase of thrombin concentrations in human plasma.

Considering that organic nanoparticles have excellent loading capacity, there is no doubt that they can also be utilized as functional carriers coupled with aptamers.[152−155] Hence, the integration of organic nanoparticles with aptamers provides an efficient direction for the regulation of aptamer—protein interactions by changing the loading density and quantity of aptamers. Different from inorganic nanoparticles, organic nanoparticles such as liposomes possess inherently high biocompatibility and low toxicity.[156−158] This further promotes the regulation of aptamer—protein interactions in the physiological environment using multifunctional integrated design strategies. Alshaer et al. constructed aptamer—liposome bioconjugates (Apt1-Lip) by integrating 2′-F-pyrimidine-containing RNA aptamer (Apt1), selected against CD44 receptor protein, to the surface of PEGylated liposomes using the thiol—maleimide click reaction (Figure 4C).[159] By inducing multivalent interactions with CD44, Apt1—Lip was shown to express higher binding affinity ($K_D \approx 6$ nM) compared to the affinity of free Apt1 ($K_D \approx 21$ nM). In addition, in crowded cellular environments, Apt1—Lip targeted CD44-expressing tumor cells with high specificity and selectivity, showing its great potential for versatile in vivo application. Farokhzad and colleagues covalently linked aptamers targeting prostate-specific membrane antigen (PSMA) to PEGylated polylactic acid (PLA) nanoparticles by EDCI reaction. The obtained bioconjugates showed 77-fold enhanced binding to PSMA-expressing cells compared with the control group.[160]

Apart from nanoparticles, drug molecules are attractive functional carriers for aptamers.[161−163] Given that most drug molecules are rich in nonpolar moieties, drug-integrated aptamers usually introduce additional hydrophobic effects in their interactions with proteins, thus affecting aptamer—protein interactions.[164,165] Meanwhile, the targeting ability of aptamers enables drug molecules to be delivered to particular sites to exert effects. Zhou and Wang prepared circular bivalent aptamer—drug conjugates (cb-ApDCs) with accurate tunability of drug ratios for drug combination cancer therapy.[163] As illustrated in Figure 4D, aptamer XQ-2d specifically recognizing transferrin receptor 1 was chosen as a model, and DBCO-functionalized XQ-2d was conjugated with various azide-functionalized drugs to form ApDCs with different drug combinations via a click reaction. Then, two ApDCs

**Table 2. Summary of the Optical Assays Used to Acquire Information on Aptamer−Protein Interactions**

| Optical property | Technique | Interaction informaton obtained | Advantages | Limitations |
|---|---|---|---|---|
| Refractive index | Surface plasmon resonance (SPR) | Equilibrium dissociation constant ($K_D$), kinetic parameters ($k_{on}$ and $k_{off}$), thermodynamic parameters ($\Delta H$ and $\Delta S$), analyte concentration | (1) Real-time monitoring of interaction processes; (2) High sensitivity and accuracy; (3) Label-free technique; (4) Simple operation | (1) Susceptible to interference from sample composition, temperature, and other factors; (2) Difficulty in distinguishing nonspecific adsorption; (3) Require the immobilization of one interaction partner |
| Scattering intensity | Surface-enhanced Raman scattering (SERS) | Aptamer conformational changes induced by protein binding | (1) High sensitivity; (2) Label-free technique; (3) Rapid measurement | (1) The recording of SERS spectra may be affected by the laser power, integration time, and analyte concentration; (2) Require the immobilization of one interaction partner |
| Interference pattern | Biolayer interferometry (BLI) | Equilibrium dissociation constant ($K_D$), kinetic parameters ($k_{on}$ and $k_{off}$), thermodynamic parameters ($\Delta H$ and $\Delta S$), analyte concentration | (1) High throughput; (2) Label-free technique | (1) Require the immobilization of one interaction partner |
| Polarization response | Fluorescence anisotropy (FA)/ fluorescence polarization (FP) | Equilibrium dissociation constant ($K_D$), binding nucleotide sites of aptamers | (1) High sensitivity; (2) High throughput; (3) Without immobilization of one interaction partner onto a solid substrate and the need for additional washing and separation steps; (4) Simple operation and rapid measurement | (1) Susceptible to fluorescence lifetime, molecular rotational rates, and other factors; (2) Sensitive to variations in buffer conditions; (3) High instrumental cost |
| | Circular dichroism (CD) | Equilibrium dissociation constant ($K_D$), aptamer conformational changes induced by protein binding | (1) Rapid measurement; (2) Allows operation on small amounts of samples in physiological buffers | (1) Only global features of macromolecules can be detected; (2) High sample preparation requirements; (3) High instrumental cost |
| Fluorescence resonance energy transfer (FRET) | FRET-based fluorescence technique such as the molecular beacon probe | Equilibrium dissociation constant ($K_D$), analyte concentration | (1) Rapid measurement; (2) High sensitivity and selectivity; (3) Provide real-time interaction information; (4) Allow measurement of binding parameters under various buffer conditions. | (1) Labeled aptamers are usually required; (2) Sensitive to variations in buffer conditions; (3) Possibility of false-positive results |

monomers were cyclized to generate a variety of cb-ApDCs based on Watson−Crick base-pairing. Introducing additional hydrophobic interactions, the conjugation of hydrophobic drugs significantly enhanced the binding affinity of XQ-2d that depended on the number of bound hydrophobic drugs. Due to their high affinity and specificity, cb-ApDCs showed excellent selective cytotoxicity, achieving good synergistic effects to inhibit cancer cell growth by tuning the drug ratios.

Taken together, by combining the unique properties of functional carriers with aptamers, the multifunctional integrated design of aptamers may offer an effective methodology to regulate aptamer−protein interactions in biosensing, disease diagnosis, and treatment.

## 3. DETECTION METHODS OF APTAMER−PROTEIN INTERACTIONS

Specific binding of aptamers to target proteins is mediated by many interactions.[166] The strength, kinetic, and thermodynamic parameters associated with these interactions are critical components that define aptamer−protein binding events. The interaction strength relates to the selectivity of aptamers for target proteins.[167,168] Kinetic analysis can provide association ($k_{on}$) and dissociation ($k_{off}$) rate constants to evaluate the stability of aptamer−protein interactions.[169,170] Thermodynamic analysis of aptamer−protein systems is usually carried out to acquire enthalpy changes ($\Delta H$) and entropy changes ($\Delta S$), showing instructive implications for understanding the molecular principles of aptamer−protein interactions.[171,172] Therefore, exploring basic binding parameters of aptamer−protein interactions can help to optimize or develop regulation strategies, further promoting the development of aptamer−protein interactions in analytical fields. More recently, numerous methods for characterizing aptamer−protein interactions have been exploited, and these methods will be introduced in this chapter.

### 3.1. Optical Assay

The optical signals are closely related to the optical properties of the analytical interface, including refractive index, scattering intensity, interference pattern, polarization response, and fluorescence resonance energy transfer (FRET).[173,174] The aptamer−protein interactions will change the optical properties of the analytical interface, resulting in the variation of optical signals.[175−180] Hence, many optical methods have been rationally designed to monitor changes of various optical effects upon the binding of aptamers to target proteins, acquiring detailed information about aptamer−protein interactions (Table 2).

Surface plasmon resonance (SPR) is one of the broadly applied techniques for studying aptamer−protein interactions.[181−184] The partner with the larger mass is usually in the flow in SPR, with the smaller partner immobilized, to maximize the change.[185−188] The kinetic parameters ($k_{on}$ and $k_{off}$) and equilibrium dissociation constant ($K_D$) of aptamer−protein interactions can be calculated based on time-dependent SPR signals during flow.[188,189] Li et al. constructed a five-component RNA aptamer microarray by modifying five protein factor IXa (fIXa)-binding aptamers with different structures onto a gold surface.[190] According to the SPR signals from fIXa binding at different aptamer array elements, the optimal aptamers that specifically interact with fIXa are selected out of the five RNA aptamer components. However, SPR also suffers

from some limitations, such as sensitivity to temperature and difficulty in distinguishing nonspecific adsorption.[191]

Surface-enhanced Raman scattering (SERS) is a surface-sensitive spectroscopic technique that can provide information on the process of aptamer−protein interactions at the analytical interface. In SERS measurements, aptamers are usually adsorbed on the rough surface of nanostructured metallic particles (typically gold, silver, and copper) to further enhance the Raman scattering, and the obtained SERS signals are closely associated with aptamer structures.[192−194] Aptamer−protein interactions are reported to usually cause changes in aptamer structures.[180,195] Hence, the SERS spectrum of aptamers attached to the rough metal surface will alter when binding to target proteins, thus reflecting the interaction of aptamers with proteins. For example, Muhammad's group built an AuNPs array-based SERS sensor to investigate the interaction between aptamer and interleukin-6 (IL-6).[196] A DNA aptamer adhered to the AuNPs array would change its conformation upon binding to target IL-6 in serum, thus inducing obvious alterations in the SERS spectrum.

Another optical method that requires the immobilization of one interaction partner is Biolayer interferometry (BLI).[197,198] Aptamers are covalently functionalized onto the surface of a fiber-optic biosensor.[199] Upon white light illumination, the two interfaces of optical film layer at the sensor tip will generate two reflected beams that are superimposed to form an interference spectrum.[200,201] The association and dissociation of aptamers with target proteins can cause changes in the thickness and density of the film, creating a wavelength shift of the interference spectrum.[202,203] By the real-time monitoring of the wavelength shift, BLI is capable of obtaining abundant information about aptamer−protein interactions, including steady-state affinity, kinetic, and thermodynamic parameters.[175]

As one of the main optical properties of analytical interface, variations in polarization can also be utilized to indicate aptamer−protein interactions. Fluorescence anisotropy (FA)/fluorescence polarization (FP) assay can monitor the interactions between fluorescently labeled aptamers and target proteins by measuring polarized fluorescence emission of the fluorophores under polarized excitation light.[204] When fluorescently labeled aptamers bind to proteins, increased molecular volume and restricted rotation of fluorophore will cause an enhancement in FA/FP signals.[205] Interestingly, monitoring the FA/FP signal upon the interaction between aptamer labeled with fluorescein at specific sites and proteins can further infer the binding sites on aptamers.[206] For instance, to identify the binding nucleotide sites of aptamers interacting with Immunoglobulin E (IgE), Zhao and colleagues constructed a series of aptamer probes with a single FAM label at different individual nucleotides.[207] Multiple possible close-contact nucleotide sites of aptamer were found by detecting the FA response of aptamer−IgE complexes. Concisely, these close-contact site-labeled aptamers showed high FA signals due to the confined local rotation of FAM, while distant site-labeled aptamers only produced weak signals. Besides, proteins and nucleic acids exhibit differential absorption of left and right circularly polarized light owing to the presence of asymmetric carbons in amino acid residues and ribose.[29,208] Based on the circular dichroism (CD) of proteins and aptamers, scientists developed CD spectroscopy to study aptamer−protein interactions by monitoring CD spectra upon binding. Never-
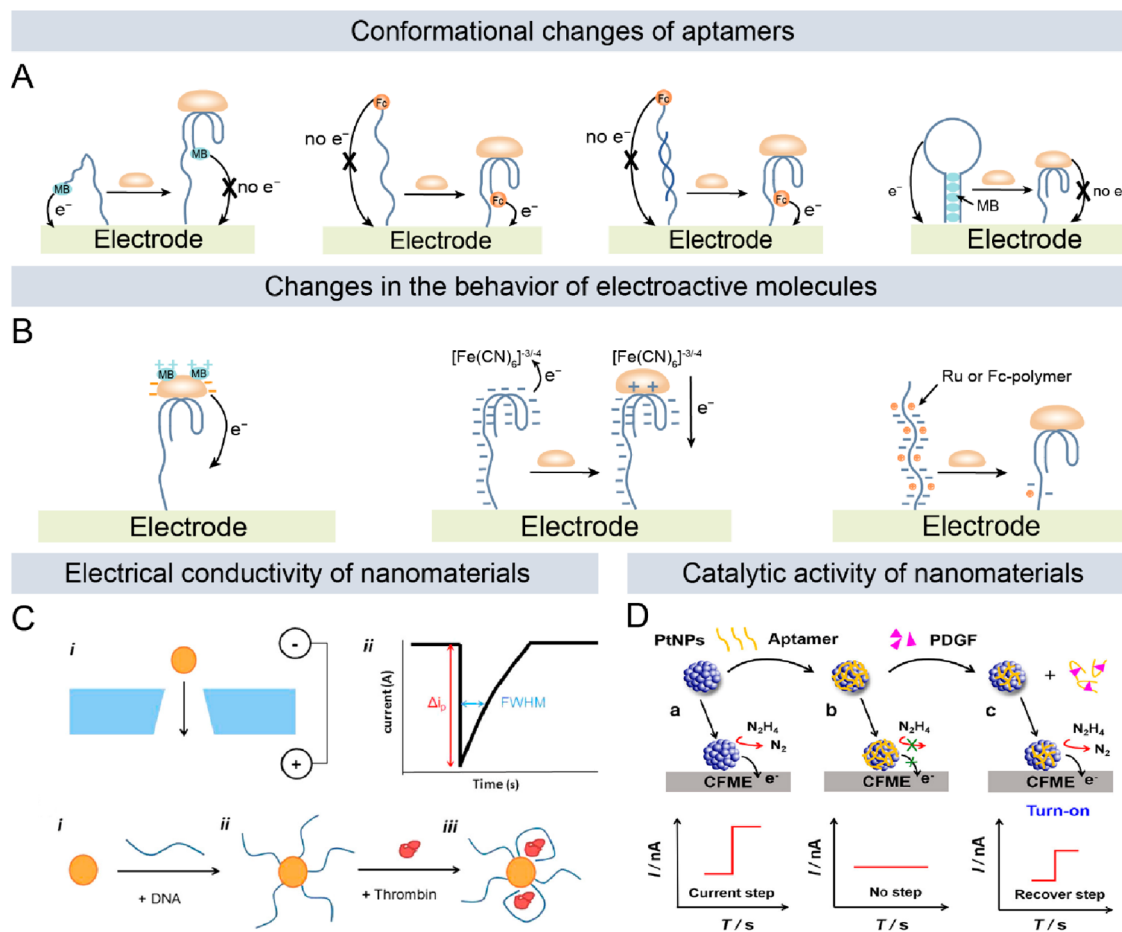
**Figure 5.** Schematic illustration of electrical assays based on (A) conformational changes of aptamers, (B) changes in the behavior of electroactive molecules, (C) electrical conductivity of nanomaterials, and (D) catalytic activity of nanomaterials. (C) Reprinted with permission from ref 260. Copyright 2014 American Chemical Society. (D) Reprinted with permission from ref 261. Copyright 2019 American Chemical Society.

theless, CD technology also has certain limitations, most notably the stringent sample preparation requirements.[46]

The FRET-based fluorescence technique is also an important optical assay for monitoring aptamer−protein interactions, allowing direct transduction of information on aptamer−protein interactions into alterations in FRET.[176,209,210] Taking the molecular beacon probe (MB) as an example, a fluorophore and a quencher are usually modified at both ends of the aptamer that possess a stem-loop structure, respectively.[211] In the absence of the target protein, MB maintain a closed stem-loop structure to keep the fluorophore and quencher in close proximity, allowing quenching to occur by FRET,[212,213] whereas the closed stem-loop structure of MB may be unraveled upon binding to the target protein.[214] The fluorophore is spatially separated from the quencher to produce a bright fluorescence signal.[215] By utilizing MBs, researchers have studied specific interactions between aptamers and various proteins, such as thrombin, platelet-derived growth factor (PDGF-BB), Tat protein of HIV-1, and so on.[216−218] Additionally, unique optical properties make optical nanomaterials another excellent candidate to develop optical assays.[219] By way of illustration, Ghosh's group synthesized DNA aptamers targeting glycated albumin (GA) with a quantum dot attached at one end and gold nanoparticle quencher at the other end.[220] Without the addition of GA, the aptamer folded to a hairpin loop structure and the quantum dot fluorescence was quenched by energy transfer to the gold

nanoparticle. With increasing GA concentration, an enhancement in photoluminescence was observed due to the opening of the aptamer hairpin loop.

## 3.2. Electrical Assay

Aptamers can be easily immobilized on various electrode surfaces by utilizing molecular modification strategies.[221−223] The aptamer−protein interactions on the electrode interface can induce electron transfer in the system, resulting in changes in electrical signals such as current, potential and impedance.[224,225] As the most direct method for electron transfer characterization, electrical methods can quantify interactions between aptamers and proteins by measuring changes in electrical signals.[226,227] Accordingly, numerous electrical methods have been developed, such as differential pulse voltammetry (DPV), alternating current voltammetry (ACV), cyclic voltammetry (CV), square wave voltammetry (SWV), electrochemical impedance spectroscopy (EIS), and amperometric detection.[228−233] In this section, we will display various electrical assays based on different detection principles for analyzing aptamer−protein interactions.

Emil Paleček revealed, for the first time, the inherent electrochemical activity of nucleic acids by showing reduction processes close to −1.4 V (vs SCE) of adenine and cytosine residues on mercury electrodes.[234] Furthermore, the electrochemical oxidation of guanine and adenine residues was observed on carbon and gold electrodes. These findings make

it possible to transduce aptamer−protein interactions into a detectable electronic signal using intrinsic aptamer electro-activity-based approaches. Inspired by that, Rodriguez modified aptamers against lysozyme on the surface of a carbon paste electrode and monitored changes in electrical signals after the addition of lysozyme utilizing the SWV technique.[235] They successfully translated the aptamer−lysozyme interactions into the decrease in the guanine and adenine electro-oxidation signals. However, electrical techniques based on intrinsic aptamer electroactivity are usually restricted to the use of mercury electrodes and carbon electrodes, hindering their further development in analytical fields.

Thanks to the property of easy modification, aptamers are able to covalently or noncovalently link to a variety of electroactive molecules, thus coupling aptamer−protein interactions to the efficiency of electron transfer between the electroactive molecule and the electrode.[236,237] According to the changes in electrical signals, the electroactive molecule-based electrical assays can be divided into two categories: one depends on the conformational transition of aptamers upon binding to their target proteins; the other relies on changes in the behavior of electroactive molecules initiated by aptamer−protein interactions. For the electrical detection methods based on conformational changes of aptamers, electroactive molecules such as methylene blue (MB) and ferrocene (Fc) are usually modified at the free end of the aptamers immobilized at the electrode surface (Figure 5A).[238,239] Upon interacting with proteins, conformational changes of the aptamers will alter the distance of the electroactive molecules to the electrode surface.[240,241] Correspondingly, the efficiency of electron transfer can also be influenced, resulting in a decrease or increase in the current.[242−244] For example, Li and co-workers covalently attached prostate-specific antigen (PSA)-binding aptamers labeled with MB to the gold electrode. In the absence of PSA, the intrinsically flexible conformation of the aptamers increased the possibility of collision between MB and the electrode surface, resulting in fast electron transfer kinetics.[245] After adding PSA, aptamer−PSA interactions induced aptamers to switch conformation, hampering the electron transfer between MB and the electrode surface. The authors applied the SWV technique to translate electron transfer kinetics alterations into the current changes, further obtaining the binding affinity of the aptamer−PSA interactions. Curti and Idili both employed AttoMB, an MB derivative, as an electrochemical indicator to modify the free end of aptamers that specifically bind to SARS-CoV-2 spike protein.[246,247] These two pieces of research enabled the monitoring of aptamer−SARS-CoV-2 spike protein interactions by short-ening or lengthening electron-transfer distances via conforma-tional changes of the aptamers, respectively. It is reported that MB is also known as DNA intercalator.[248,249] Thus, Bang et al. designed and constructed a hairpin-forming beacon aptamer that specifically binds to thrombin, and MB was intercalated into the double-stranded DNA domain of the beacon aptamer.[250] The interaction between thrombin and the beacon aptamer induces the opening of the hairpin structure, and subsequently the intercalated MB is released, resulting in a decrease in electrical current intensity in the voltammogram. Another class of electrical technique is associated with the behavior of electroactive molecules instead of the conforma-tional transition of aptamers, as illustrated in Figure 5B. In this method, the changes of electrical signals depend on the electrostatic attraction or repulsion of aptamers to electroactive

molecules with different charging properties before and after aptamer−protein interactions.[251] For instance, positively charged MB (a small organic molecule) can interact with negatively charged proteins, forming stable complexes.[252,253] Therefore, the formation of protein−MB complexes makes an increased redox current when target proteins bind to the aptamers immobilized at the electrode surface. According to the aforementioned principle, Hianik's group took advantage of CV and DPV methods to record the current change, realizing the detection of aptamer−thrombin interactions.[254] Metal−organic complexes are also often designed as electrical signal reporters for electrical assays attributed to their good chemical stability and strong redox responses.[255] Negatively charged aptamers will repel the negatively charged metal−organic complexes, such as $[Fe(CN)_6]^{4-/3-}$, in turn, hindering electron transfer between electroactive molecules and the electrode surface.[256] In the presence of positively charged target proteins, interactions of aptamers with target proteins can switch the electrode surface charge, thus decreasing the electron transfer resistance.[257] In light of the above-mentioned phenomena, aptamer−protein interactions can be monitored by utilizing the electrochemical impedance spectroscopy technique to detect changes in impedance before and after adding to the target proteins.[258] Positively charged organo-metallic complexes can bind to aptamers immobilized on the electrode via electrostatic interactions, generating CV responses. In the presence of target proteins, aptamer−protein interactions block the binding of the cationic electroactive reporters with the aptamers, resulting in significant changes in the CV response.

With rapid developments in nanochemistry, the application of nanomaterials sparks a new idea for the electrical detection of aptamer−protein interactions. For example, Maehashi's group fabricated a carbon nanotube field-effect transistor (CNT-FET) device to monitor the interaction process between aptamers and immunoglobulin E.[259] Moreover, nanopore-based tunable resistance pulse sensing (TRPS) technology has been developed to accurately determine the concentration, size, and surface charge of nanoparticles. Billinge et al. immobilized aptamers on the surface of superparamagnetic beads and then incubated these beads with thrombin proteins (Figure 5C).[260] Once bound to proteins, aptamers undergo conformational changes and lead to the shielding of the polyanion backbone. Thus, information about aptamer−thrombin interactions, such as binding affinity, can be obtained by monitoring variations in translocation time and pulse frequency of particles traversing the nanopore in real time. Zhang et al. conjugated Pt nanoparticles (PtNPs) with the platelet-derived growth factor (PDGF) recognition aptamer to inhibit the electrocatalytic oxidation of hydrazine ($N_2H_4$) by PtNPs.[261] As shown in Figure 5D, in the presence of PDGF, the stronger binding between the aptamer and the PDFG disturbs the aptamer/PtNPs conjugates. Subsequently, the electrocatalytic performance of PtNPs is recovered and PtNPs further catalyzes oxidation of $N_2H_4$ to form $N_2$, thereby providing a quantitative current response for the aptamer−PDGF interaction.

Collectively, correlating the signaling mechanism of electrical detection with aptamer conformation allows variations in electrical signals to arise exclusively from aptamer conformational change induced by protein binding. This effectively eliminates the interference of nonspecific inter-actions from other biomolecules. In addition, owing to their

excellent electrical conductivity and catalytic activity, nanomaterials can be employed as high-performance electrode-supporting materials, electroactive labels, and catalytic labels.[262−264] The introduction of nanomaterials enables more efficient conversion of information on aptamer−protein interactions into electrical signals, providing a more sensitive electrical detection platform for analysis of the aptamer−protein interactions.

## 3.3. Biological Assay

As synthetic "chemical antibodies", aptamers have a number of unique advantages over antibodies.[34,51,265] Since aptamer production is often a chemical process, it not only eludes the batch-to-batch variation but also reduces production costs.[266] Thus, unlike antibodies, aptamers can be more facile to modify at premeditated sites and synthesized on a large scale.[267] Moreover, aptamers possess excellent chemical stability.[268] After thermal denaturation, aptamers can refold into their native conformation to be reused, whereas the denaturation process of antibodies is irreversible.[269] These advantages enable aptamers to be contemplated as antibody replacements and promising protein affinity reagents to construct a variety of biological methods, such as enzyme-linked aptasorbent assay, immunoprecipitation, and others, for detecting aptamer−protein interactions. Each approach owns distinct superiorities and limitations (Table 3).

Enzyme-linked immunosorbent assay (ELISA) is one of the important detection techniques in biomedicine, converting the information of antibody−antigen interactions into visually detectable color change.[268,270] In 1996, Drolet introduced aptamers into ELISA for the first time to replace antibodies, developing an enzyme-linked aptamer assay (ELAA).[271] The accuracy and specificity of ELAA were analyzed to show equivalence to the typical ELISA. Subsequently, ELAA has been extensively studied to detect aptamer−protein interactions. Almeida et al. selected aptamers against zika virus nonstructural protein 1 (ZIKVNS1), termed ZIKV60, and performed ELAA to analyze ZikV60-ZikVNS1 interactions.[272] Specifically, ZIKVNS1 was incubated with horseradish peroxidase (HRP)-labeled ZIKV60 at different concentrations, followed by adding 3,5,3′,5′-tetramethylbenzidine (TMB) to initiate colorimetric reactions. Based on measurements of absorbance at 450 nm, the saturation−binding curve was plotted and showed that ZIKV60 presented a high binding affinity to ZIKVNS1 with a $K_D$ value of $2.28 \pm 0.28$ nM.

Immunoprecipitation (IP) is a classical method for protein detection based on antibody−antigen interactions.[273,274] Antibodies against target proteins are preimmobilized on insoluble supports, such as agarose beads, and then incubated with cell lysates containing the target proteins to form antigen−antibody immune complexes.[275] Subsequently, immune complexes are eluted from the supports for further property analysis.[275] Studies have shown that aptamers represent a viable alternative to antibodies on insoluble supports, allowing the utilization of IP assay for analyzing aptamer−protein interactions.[276,277] For example, to demonstrate the interaction of heat shock protein 70 (HSP70, a serous ovarian cancer biomarker) with aptamers (Tx-01), Hsu and co-workers performed an IP assay using Tx-01 aptamer-coated magnetic beads.[278] Besides, the pull-down assay is also a bioanalytical technique that requires solid-phase supports.[279,280] Proteins that interact with target proteins are preimmobilized as bait proteins to recognize and capture target

**Table 3. Summary of the Biological Assays Used to Acquire Information on Aptamer−Protein Interactions**

| Technique | Principle | Advantages | Limitations |
|---|---|---|---|
| Enzyme-linked aptamer assay (ELAA) | A solid-phase enzyme immunoassay | (1) Qualitative or quantitative analysis can be performed according to the color change; (2) High sensitivity and accuracy; (3) Low cost and simple operation | (1) Labeled aptamers are required; (2) Immobilization of aptamers onto a solid support is required |
| Immunoprecipitation assay (IP) | The immunoprecipitate is formed by aptamer−protein interactions. | (1) A well-established method | (1) Immobilization of aptamers onto a solid support is required; (2) Possibility that low-affinity interactions cannot be detected |
| Pull-down assay | Target proteins are absorbed by the aptamers immobilized on a solid-phase support, thus changing their elution conditions. | (1) Simple operation | (1) Immobilization of aptamers onto a solid support is required |
| Electrophoretic mobility-shift assay (EMSA) | Mobility differences of different molecules (unbound protein, unbound aptamer, and their complexes) in the gel matrix | (1) High sensitivity; (2) Accommodate a wide range of binding conditions; (3) Low cost, simple operation, and rapid measurement | (1) Rapid dissociation of the samples during electrophoresis can prevent the detection; (2) Electrophoretic mobility is affected by the inherent properties of target proteins |
| Footprinting assay | Aptamer−protein interactions protect the binding region of aptamers from DNAzyme hydrolysis. The region of complex formation will be masked on the gel pattern. | (1) Provide interaction information at the single nucleotide level; (2) High protein concentrations are required | (1) Enzyme activity is susceptible to environmental factors; (2) Low cost and simple operation |
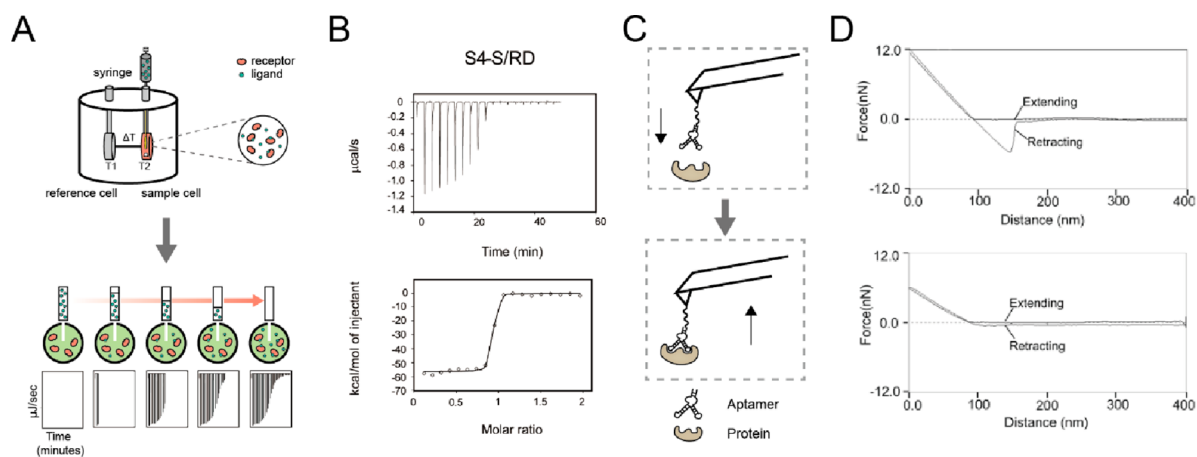
**Figure 6.** (A) Schematic diagram of an ITC experiment. (B) ITC data for S4−S−RD interaction. Reprinted with permission from ref 302. Copyright 2016 American Chemical Society. (C) Schematic diagram of an AFM experiment. (D) Typical force−distance curves of aptamer−IgE (top) and scramble oligo−IgE (bottom). Reprinted with permission from ref 322. Copyright 2003 American Chemical Society.

proteins for investigating protein−protein interactions.[281,282] Likewise, the aptamer−protein interactions can be detected by replacing the bait proteins with aptamers.[10,283]

In addition, to reveal the critical regulatory role of nucleic acid−protein interactions within the organism for life processes, several biological methods have been developed to study the interactions between DNA/RNA and proteins, including electrophoretic mobility shift assay (EMSA) and footprinting assay, among others (Table 3).[284−286] These conventional assays have, in turn, been further extended for the analysis of aptamer−protein interactions. EMSA is a common analytical technique to investigate aptamer−protein interactions based on the mobility differences of different molecules in the gel matrix.[287] Aptamers are polyanions and have strong electrophoretic mobility.[187] Comparatively, the net charges and molecular size of proteins greatly render their movement in the gel matrix greatly impeded.[29] Aptamer−protein complexes thus possess a slower electrophoretic mobility compared to free aptamers.[288] Consequently, information about aptamer−protein interactions, such as the interaction strength, can be obtained by observing the shift of bands.[289] As another classical biological technique, the unique advantage of footprinting assay is its ability to report the accurate binding sites of aptamers to proteins at the single nucleotide level.[290,291] Aptamers can be cleaved by DNAzymes when they are not bound to target proteins, while aptamers interact with proteins to form complexes that can protect the binding region of aptamers from DNAzyme hydrolysis.[292] Hence, interaction sites can be evaluated by comparing footprinting experiments in the presence and absence of the target proteins. For instance, Chinnapen et al. successfully identified aptamers capable of binding cytochrome c and hemin simultaneously.[293] By utilizing footprinting assay, they proved that the binding site of an aptamer to cytochrome c was immediately adjacent to its guanine-rich hemin-binding site. Chen and Corn developed a DNAzyme footprinting based on the site-specific nucleic acid cleavage activity of DNAzyme for visualizing the interactions of single-stranded DNA aptamers and target proteins.[292] Single-stranded aptamers are cleaved by the DNAzyme when not bound to the target proteins, while the formation of aptamer−protein complexes can block the access of the DNAzyme to the cleavage site and prevent hydrolysis. Using thrombin as a model protein, they investigated the

aptamer−thrombin interactions utilizing a DNAzyme that cleaves the thrombin aptamer at the thymine base position 7 in the aptamer sequence.

### 3.4. Other Assays

Apart from the three categories of assays described above, several other methods exist for detecting aptamer−protein interactions, including Isothermal Titration Calorimetry (ITC), Microscale Thermophoresis (MST), Quartz Crystal Microbalance (QCM), and Atomic Force Microscopy (AFM).[294−297]

ITC and MST are two essential thermodynamic techniques for monitoring aptamer−protein interactions.[77,298] For ITC, the formation of aptamer−protein complexes is a process that is accompanied by a certain degree of heat change.[299,300] The principle and stepwise progress of ITC experiments are shown in Figure 6A. By directly measuring the heat change during the interaction at a constant temperature, ITC is able to provide information about aptamer−protein interactions, such as binding affinity, thermodynamic parameters, and the number of binding sites.[28,301] For instance, Amano's team screened and obtained the aptamer S4−S, specific to the Runt domain (RD, DNA-binding domain) of AML1 protein.[302] Further, ITC was applied to analyze the thermodynamics of the interactions between S4−S and AML1 (Figure 6B), and information about their interaction was obtained, including thermodynamic parameters ($\Delta H = -56 \pm 1$ kcal mol$^{-1}$, $-T\Delta S = -45 \pm 1$ kcal mol$^{-1}$ at 298 K) and affinity constants ($K_D = 3.5 \pm 0.4$ nM). The main principle of MST analysis is based on the directional movement of molecules along temperature gradients.[303] The intrinsic properties of molecules, including their size, charge, and hydration shell, determine their thermophoretic movements.[304,305] In general, when the binding of aptamers to target proteins occurs, the above-mentioned properties of aptamers change and thus alter their movement.[306] Information on aptamer−protein interactions can be obtained by monitoring the distribution and intensity changes in fluorescence signals of fluorescent dye-labeled aptamers.[307,308]

QCM is a microgravimetric sensing strategy for determining aptamer−protein interactions.[309−311] Utilizing the piezoelectric effect of quartz crystals, QCM converts the surface mass change of the quartz crystal electrode into frequency shift of the quartz crystal resonator.[312−314] In a typical QCM
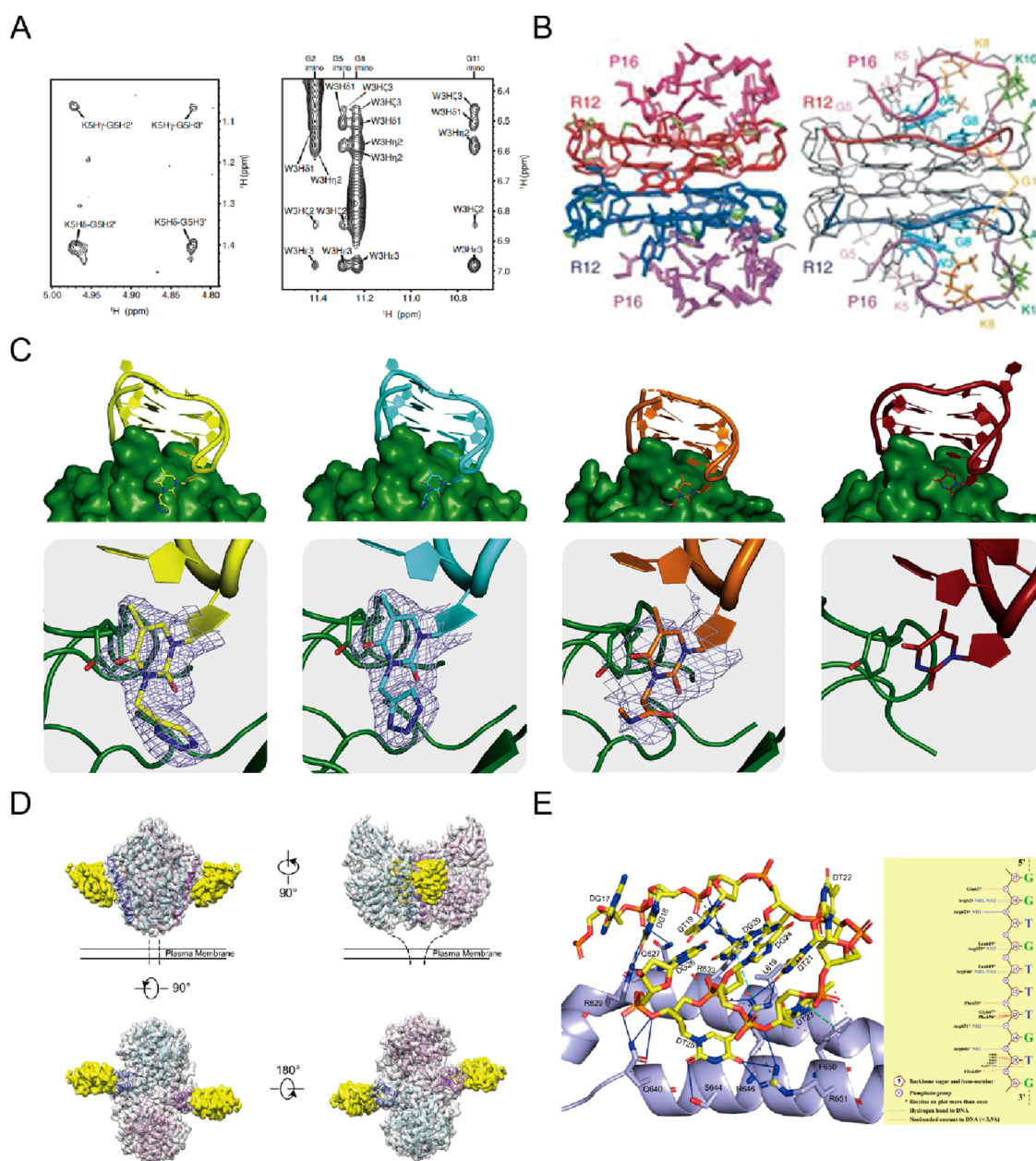
**Figure 7.** (A) Intermolecular NOESY cross peaks observed for the K5 (F) and W3 (G) residues of P16, respectively. (B) NMR structure ensemble of the R12:P16 complex. The two R12 monomers are colored red and blue, respectively. The two P16 monomers are colored magenta and purple, respectively. (A,B) Reprinted with permission from ref 337. Copyright 2012 Oxford University Press under CC BY-NC 3.0 [https://creativecommons.org/licenses/by-nc/3.0/]. (C) Structural characteristics of the interaction interfaces between chemically modified TBA15 and thrombin. Reprinted with permission from ref 348. Copyright 2021 Cell Press under CC BY-NC-ND 4.0 [http://creativecommons.org/licenses/by-nc-nd/4.0/]. (D) Cryo-EM density map and refined structure of tJBA8.1-bound TfR1. (E) Molecular interactions at the tJBA8.1−TfR1 interface. (D,E) Reprinted with permission from ref 355. Copyright 2022 American Chemical Society.

experiment, the binding of aptamers immobilized on the crystal surface and their target proteins will introduce a mass change of the QCM surface, allowing the highly sensitive detection of aptamer−protein interactions.[315,316] Lin et al. generated two mutated aptamer sequences, RBD-1CM1 and RBD-1CM2, based on a known aptamer that specifically recognizes SARS-CoV-2 spike protein (S protein).[317] Next, QCM was performed to characterize the interactions between these mutant aptamers and the S protein. The results indicated that the RBD-1CM1 aptamer produced larger signals in mass change and displayed a significant binding affinity to the S protein ($K_D = 1.2 \times 10^5$ $M^{-1}$).

Using microcantilevers that are extremely sensitive to weak force as signal transducers, AFM enables probing the binding affinity and recognition properties of aptamers to target proteins at the molecular level.[95,318,319] Typically, the aptamer is linked to the tip of the AFM probe.[320] The strength of aptamer−protein interactions is evaluated by detecting the unbinding events between the functionalized tip and the protein-modified substrate (Figure 6C).[77,321] Jiang and Zhu presented the first study of the interaction strength between proteins and aptamers.[322] As show in Figure 6D, the specific interaction between human immunoglobulin E (IgE) and its DNA aptamer was measured directly by atomic force

microscopy. Furthermore, the aptamer or anti-IgE monoclonal antibody was modified at the AFM tip. AFM was then applied to measure the forces required to separate the interaction between individual aptamer/anti-IgE and IgE. In comparison with the binding affinity of IgE−anti-IgE (∼139 ± 43 pN), the aptamer−IgE interactions exhibited comparable or stronger binding affinity (∼160 ± 29 pN).

## 4. STRUCTURE DETERMINATION OF APTAMER−PROTEIN INTERACTION SITES

Protein surfaces present multiple interaction sites that can be specifically recognized and bound by aptamers.[323] Aptamers can fold into specific three-dimensional structures for specific molecular recognition.[10,40] Characteristic structural motifs are employed as scaffolds on the surfaces of three-dimensional structures to precisely organize and display nucleotides bound to specific sites on proteins.[50,323] Structural determination of aptamer−protein complexes can provide characteristic information such as interaction sites, providing detailed information on the molecular basis for understanding the specific interactions between aptamers and their target proteins.[324−326] Combining the methods of structural determination with the approaches of interaction detection described above can offer more precise regulatory strategies for aptamer−protein interactions.

Nuclear magnetic resonance spectroscopy (NMR) has been one of the main methods to provide atomic resolution structures and information about interaction interfaces of aptamer−protein complexes.[207] Aptamer−protein interactions can give rise to variations in chemical environment around the atoms at the interface, thus inducing chemical shift perturbations in NMR spectra.[327,328] Consequently, tracking assays for changes in chemical shifts, in combination with isotope labeling strategies (most commonly $^1$H, $^{15}$N, $^{13}$C, and so on), allow information on interaction interfaces such as binding sites to be determined.[226,329−331] Conformational changes upon aptamers binding to their targets have been reported to cause additional peaks in the imine proton region (10−15 ppm), and these peaks can serve as a reporting signal for aptamer−ligand binding.[324,332] For instance, Weisshoff et al. found several DNA-susceptible peptide structures in the spike protein of SARS-CoV-2 and exploited NMR to examine the actual binding effect of these sequences with the aptamer, BC 007.[333] Specific binding of BC 007 to these peptide sequences was able to generate typical imino signal-patterns. Subsequent analysis in combination with the protein data bank entries of the full proteins identified BC 007−spike protein interaction sites. Besides, the nuclear Overhauser effect (NOE) is also an important parameter in NMR experiments.[334,335] NOE phenomena are usually observed when two atoms are in close spatial proximity (<0.5 nm).[336] Thus, two-dimensional NOE (HOESY) experiments can give information about the spatial distance between atoms, making it possible to apply NMR to resolve three-dimensional structures of aptamer−protein complexes. Mashima's group elucidated the structural basis for tight interactions between prion proteins (PrPs) and their aptamer R12 utilizing NMR techniques.[337] Specifically, residues 108−119 (GQWNKPSKPKTN, designated as P16) of bPrP were identified as specific binding sequences for R12. R12/P16 molar ratios in the complex were determined to be 1:1 by monitoring the chemical shifts of imino protons. Furthermore, the NOESY cross peaks were acquired to further illustrate that the structure of the R12:P16 complex consisted

of two R12 monomers and two P16 monomers, and three lysine residues of P16 were involved in the electrostatic interaction with phosphate groups of R12 (Figures 7A−B). In addition to the commonly used $^1$H, $^{15}$N, and $^{13}$C, fluorine-19 ($^{19}$F) NMR can also be used for structural characterization of aptamer−protein complexes. The high susceptibility of the $^{19}$F nucleus to changes in the environment makes it an ideal tool to study conformational changes.[338,339] Moreover, $^{19}$F is absent in natural compounds, and its integration into nucleic acid sequences yields readily interpretable spectra.[340,341] Based on these advantages of $^{19}$F NMR, Baranowski et al. used $^{19}$F-labeled oligonucleotides as NMR probes to study the G-quadruplex formation of TBA15 and TBA15−thrombin interactions.[342] The above studies indicated that NMR techniques are vitally instructive for revealing high-resolution information on aptamer−protein interaction interfaces. Whereas, NMR techniques are confined to high-resolution structures of the molecules with relatively small molecular weights (<30−40 kDa), owing to the overlap mapping of the complex NMR data.[343−345]

X-ray crystallography is a technique employed in the precise determination of three-dimensional structures of aptamer−protein complexes. In contrast to NMR, X-ray crystallography is more suitable for analyzing aptamer−protein complexes with larger molecular weights, providing detailed information on aptamer−protein interactions.[323,325] The crystal structure of a ternary complex formed by one protein and two aptamers was first proposed by Pica et al.[346] Aptamers TBA15 and TBA29 have been reported to bind specifically to thrombin exosites I and II, respectively. Thus, using thrombin as well as TBA15 and TBA29 as study models, they performed X-ray crystallography to resolve the structural features of this ternary complex. The conformation of TBA29 differs subtly in the ternary complex from that in the TBA29−thrombin binary complex, shedding light on the cooperative mechanisms generated by the interactions of TBA15 and TBA29 with thrombin. Crystal structure determination of aptamer−protein complexes can not only understand the interaction mechanism at the molecular level, but also provide theoretical guidance for regulatory strategies of the interactions such as chemical modification. Kato's team identified RB011, an aptamer capable of specifically inhibiting the activity of ATX, a plasma lysophospholipase D.[347] X-ray crystallographic analyses of the ATX−RB011 complex showed that RB011 bound near the hydrophobic pocket of ATX via specific interactions, preventing the binding of ATX to the catalytic substrates due to steric hindrance. Comparatively, the small-compound inhibitors were found to occupy the hydrophobic pocket of ATX by their hydrophobic scaffold, thereby inhibiting catalytic activity of ATX. In view of this, *p*-methyl and *p*-isopropyl groups were introduced into the backbone phosphate between C12 and C13 of RB011, generating RB012 and RB013, respectively. These chemical modifications effectively occluded the hydrophobic pocket of ATX and further enhanced the inhibitory activity of the anti-ATX aptamer. Further, X-ray crystallography can also be exploited to capture structural information on chemically modified aptamer−protein complexes, providing profound insights into the regulation of interactions at the molecular level. Smirnow and co-workers utilized X-ray crystallography to display the structural features of the chemically modified TBA15−thrombin interface (Figure 7C).[348] It was found that chemical modification of the T3 residue was able to regulate TBA15−thrombin interactions by

modulating the contacts of the oligonucleotide with exosite I. Additionally, by combining X-ray crystallography with the above-mentioned assays to detect interactions such as EMSA and ITC, Grau et al. offered comprehensive information on the interactions between the bacterial repressor TetR and the TetR-binding aptamer, including binding affinity constants ($K_D$ = 5.6 nM), thermodynamic parameters ($\Delta H$ = −156.0 kJ $mol^{-1}$, $\Delta S$ = −365.2 J $mol^{-1}$ $K^{-1}$), and interaction sites (important residues includes Arg28, Gln38, and Tyr42).[349] In fact, despite X-ray crystallography providing a molecular basis for understanding aptamer−protein interactions, this technique also suffers from certain limitations. In the whole process of resolving aptamer−protein complexes using X-ray crystallography, the most crucial step is the acquisition of the diffraction crystals.[350,351] Nevertheless, since cocrystallization relies on many factors such as the purity and conformation of the aptamer, as well as the ratio between the aptamer and its target protein, it is often difficult to obtain high-quality aptamer−protein crystals.[323,325]

With recent technological advances, cryo-electron microscopy (Cryo-EM) has been developed to determine three-dimensional structures of aptamer−protein complexes. Cryo-EM rapidly converts aptamer−protein complexes from a solution state to a glass-like state by means of fast-freezing techniques to maintain the native structure of complexes.[352,353] Obviating the need to obtain high-quality crystals, Cryo-EM enables structural analysis of aptamer−protein complexes in the near-natural state to gain high-resolution information on aptamer−protein interactions.[354] Kacherovsky and Yang developed a DNA aptamer, SNAP1, capable of binding to SARS-CoV-2 S protein with high affinity and specificity.[175] Cryo-EM was utilized to further identify that SNAP1 was only bound to the S N-terminal domain (NTD) including a part of an antigenic supersite targeted by NTD-binding antibodies. These findings revealed the importance of NTD in immunotherapy and vaccine design. Recently, aptamer tJBA8.1 that specifically binds to transferrin receptor 1 (TfR1) was reported by Cheng et al.[355] They presented for the first time a cryo-EM map of TfR1 in complex with an aptamer, revealing details of the tJBA8.1−TfR1 interface: a binding site shared by tJBA8.1 and holo-transferrin (the natural ligand of TfR1) on TfR1 (Figure 7D). The types of interactions that occur at the tJBA8.1−TfR1 binding interface between individual protein residues and nucleotides include hydrophobic interactions between Leu619 and the base of T21 as well as Phe650 and the base and sugar of T23 (Figure 7E). Kim's group developed two chemically modified aptamers, A43 and A62, as agonists of the insulin receptor (IR) to modulate IR autophosphorylation and downstream signaling pathways.[356] The structure of A43/A62-IR complex was determined by cryo-EM in the range of 3.62 to 4.27 Å resolution. The obtained structural information elucidated the conformational dynamics of IR activation related to signaling pathways, providing a structural basis for the design of functionally selective agonists for IR. Taken together, Cryo-EM can help to reveal the structural characteristics of aptamer−protein interactions and offer structural guidance to design the regulatory strategies for the interactions. Nevertheless, the widespread application of Cryo-EM technology is still limited by many factors. Requiring large sample molecular weight (limit of detection ∼0.1 MDa), Cryo-EM is not appropriate to study most aptamer−protein interactions.[46,325] Besides, given that biological samples are vulnerable to radiation damage from the electron beam, low electron doses are used in Cryo-EM experiments and result in low-resolution image features.[357−359] In addition, ultrahigh-resolution cryo-EM maps demand sufficient data collection that usually takes hours or even days, and the subsequent data analysis is complicated.[360,361] Ultimately, cryo-EM facilities are extremely sophisticated and costly, requiring massive capital and labor investment in installation, maintenance, and operation.[362] Thereby, Cryo-EM technology is still under development and needs further improvement.

## 5. ANALYTICAL ASSAYS BASED ON THE REGULATION OF APTAMER−PROTEIN INTERACTIONS

Regulation of aptamer−protein interactions enables the selective analysis of biomolecules and affords new insights into the fundamental processes of various life activities. Moreover, it can also identify clinically important biomarkers, providing a guide not only for the study of molecular mechanisms of human diseases but also for the diagnosis and treatment of diseases.[35] Therefore, numerous analytical methods based on the regulation of aptamer−protein interactions have been rationally designed and developed.

### 5.1. Detection Based on Hydrogen Bond Interactions

Hydrogen bonding is considered to be the most common interaction between aptamers and target proteins, representing the main driving force in the aptamer−protein binding processes.[45] Recently, based on hydrogen bond interactions between aptamers and their target proteins, various analytical assays have been developed for the detection of key biomolecules. Thrombin is a serine protease that plays a crucial role in numerous physiological and pathological processes in the body.[363,364] Studies have demonstrated that arginine in thrombin exhibits the potential as a hydrogen bond donor due to the positively charged guanidine group, endowing thrombin with the ability to form multiple hydrogen bonds.[346,365,366] As an aptamer that specifically binds to thrombin, TBA15 is able to fold into G-quadruplex structures for specific interaction with thrombin.[367] The crystallographic structure of TBA−thrombin complexes presents that the interaction interface consists of the nucleobases in two TT loops of TBA15 (T3-T4 and T12-T13 loops) as well as thrombin residues inserted between these two loops.[114] Moreover, TBA−thrombin interactions mainly rely on hydrogen bonding interactions.[368,369] Hence, TBA15 has been utilized to design multiple sensing strategies for highly sensitive and specific detection of thrombin by regulating hydrogen bond interactions of TBA15 with thrombin.[368] Xiong's group combined MPA-Mn:ZnS quantum dots (QDs) with BHQ2-tagged TBA15 (TBA-BHQ2) to form QDs/TBA-BHQ2 complexes.[370] In the QDs/TBA-BHQ2 system, phosphorescent QDs acted as the energy donors, and TBA-BHQ2 served as the energy acceptors. The close proximity of QDs and TBA-BHQ2 made this system nonluminescent in phosphorescence resonance energy transfer (PRET). Upon the addition of thrombin, the strong interaction between TBA15 and thrombin forced QDs away from the QDs/TBA-BHQ2 complex, leading to the phosphorescence recovery. Consequently, the concentration of thrombin could be determined by measuring the restoring phosphorescence intensity change value. Prostate-specific membrane antigen (PSMA) is a well-characterized tumor marker related to neovascularization in
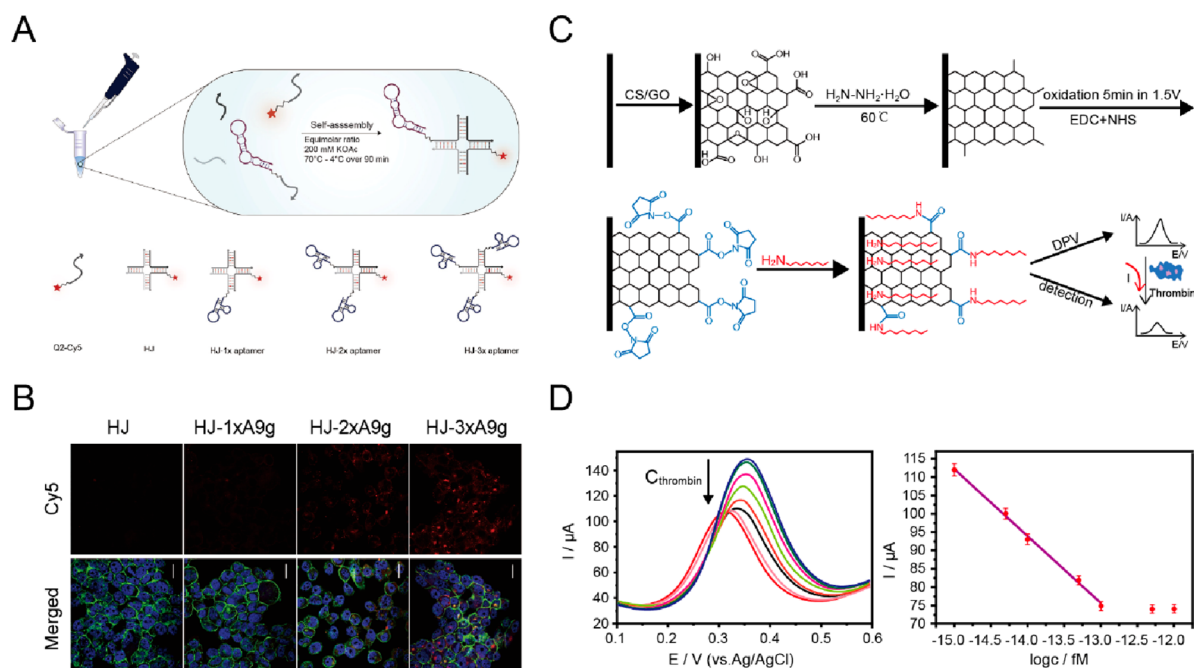
**Figure 8.** (A) Schematic illustration of the self-assembly process of HJ coupled with different amounts of A9g. (B) Confocal microscopy images of PC3+ cells treated with different amounts of A9g. (A,B) Reprinted with permission from ref 374. Copyright 2020 Cell Press under CC BY-NC-ND 4.0 [http://creativecommons.org/licenses/by-nc-nd/4.0/]. (C) Schematic diagram of the construction of the GR−TBA-based aptasensor and its sensing mechanism. (D) The relationship between the DPV response and thrombin concentration (left) and the calibration curve between the current response and thrombin concentration (right). (C,D) Adapted with permission from ref 379. Copyright 2012 Royal Society of Chemistry.

prostate cancer and most solid tumors; thus, the highly sensitive detection of PSMA is of great significance.[371,372] The analysis of the interface between PMSA and its aptamer A9g indicated the formation of an extensive network of hydrogen bonding, including direct and water-mediated.[373] These hydrogen bonding interactions play a dominant role in the specific binding of A9g to PSMA. On this basis, Omer et al. implemented click chemical reaction to splice multiple A9g on the Holliday junction (HJ) labeled with Cy5 for imaging detection of PMSA, as shown in Figure 8A.[374] As the amount of A9g increased, the fluorescence intensity improved significantly owing to the enhanced multivalent interactions (Figure 8B). Furthermore, regulating the hydrogen bonding between aptamers and proteins can not only achieve sensitive detection of biomolecules, but also further alter the behavior of biomolecules. It has been reported that fluorine atoms can be regarded as hydrogen bond acceptors in principle by virtue of high electronegativity.[375−377] In view of this, Bao et al. introduced 8-trifluoromethyl-2′-deoxyguanosine (FG) at different sites of TBA15, such as G5 and G14, respectively. They further monitored the anticoagulant activity of different-site-modified TBA15 by means of optical coagulation analyzer.[378] The results indicated that, owing to the formation of an additional hydrogen bond between the trifluoromethyl group and side chains of thrombin, the modification of FG near the TT loops significantly enhanced the anticoagulant activity of TBA15. Hence, it is a potential therapeutic strategy that introducing fluorine atoms to regulate the activity of thrombin via hydrogen-bonding modulation.

In addition to optical detection methods, electrical detection methods based on hydrogen-bonding regulation have also been widely applied in biomolecule detection. This is because the regulation of hydrogen bonding interactions between aptamers and proteins can transduce biomolecular information into

changes in electrical signals. For example, Wang and colleagues constructed a unique nanocomposite by covalently attaching TBA15 on graphene for thrombin sensing, as illustrated in Figure 8C.[379] In the presence of thrombin, a quadruplex−thrombin complex is formed based on hydrogen bond interactions of TBA15 with thrombin. This complex increases the steric hindrance and severely inhibits electron transfer for redox probes $[Fe(CN)_6]^{3-/4-}$. As the concentration of thrombin increased, the DPV current peaks gradually decrease, thus achieving highly sensitive detection of thrombin (limit of detection ∼0.45 fM) (Figure 8D).

In summary, the extensive hydrogen bonding network between aptamers and proteins is the primary driving force of their binding processes. Analytical methods based on the regulation of hydrogen bond interactions can significantly improve the sensitivity of biomolecular detection, making great contributions to their development in the field of bioanalysis.

## 5.2. Detection Based on Electrostatic Interactions

Electrostatic interaction is another important force that mediates the aptamer−protein binding processes.[380,381] Studies have confirmed that electrostatic interactions mainly occur between negatively charged phosphate backbones and positively charged protein residues.[44,45] Altering the structure of aptamers can alter the electrostatic interactions between aptamers and proteins. On this basis, plenty of methods have been established to accomplish biomolecule detection with high sensitivity and specificity.

Optical methods have become one of the most utilized approaches in analytical fields for their pronounced sensitivity.[382] Electrostatic interactions between aptamers and proteins can induce changes in the optical properties of interaction interfaces, thereby transforming biomolecular information into alterations in various optical signals. As a consequence, numerous optical assays have been developed for the detection
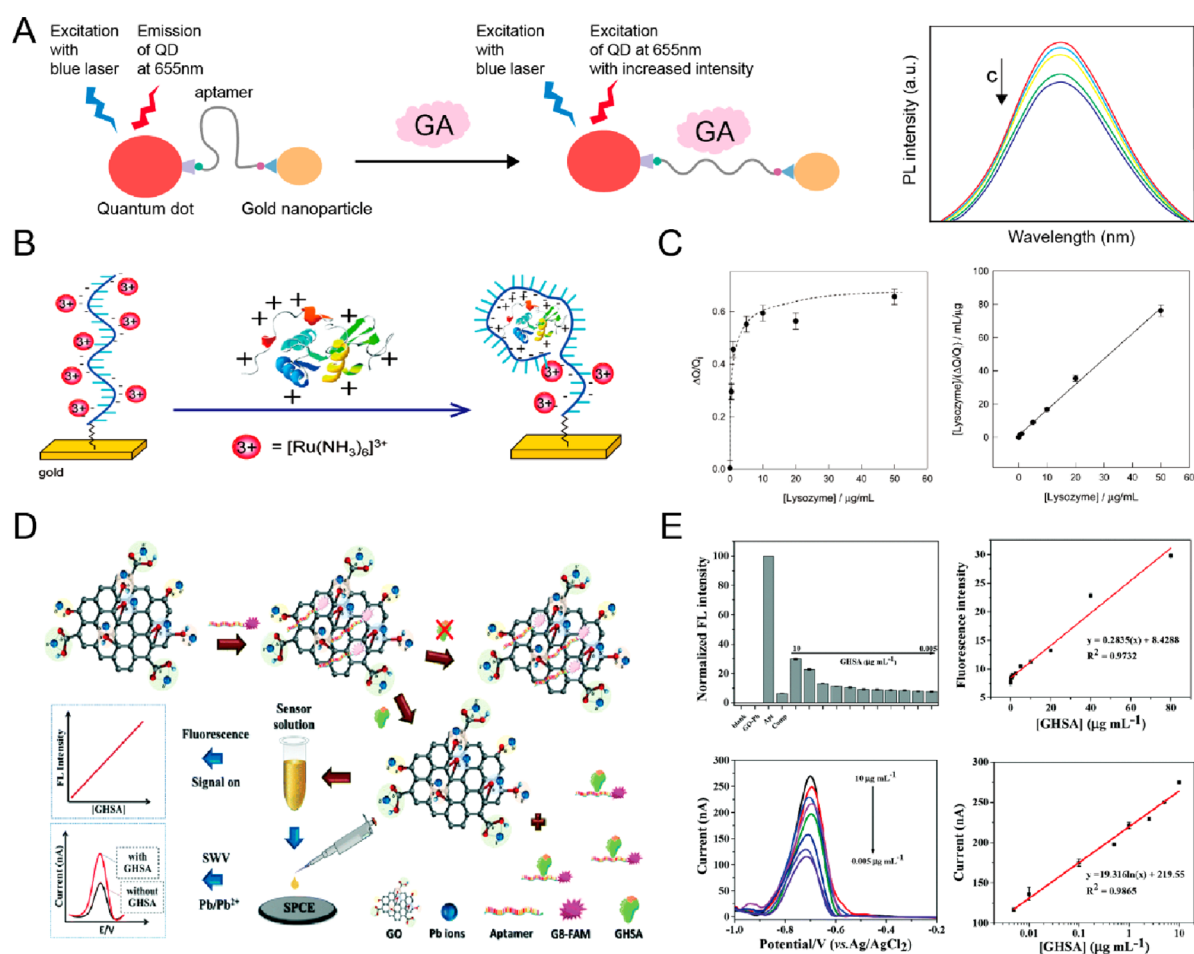
**Figure 9.** (A) Schematic diagram of aptamer-based FRET sensor for the detection of glycated albumin. (B) Schematic diagram of antilysozyme aptamers immobilized on gold electrodes for lysozyme detection. (C) Variations in the relative decrease in the integrated charge (reduction signal) as the concentration of lysozyme increases (left). Linearized adsorption isotherm of lysozyme binding to antilysozyme aptamers on gold electrodes based on the Langmuir model (right). (B,C) Reprinted and adapted with permission from ref 258. Copyright 2007 American Chemical Society. (D) Schematic diagram of fluorescence−electrochemical dual detection technique for the quantification of GA. (E) Fluorescence and electrochemical characteristics of the developed dual detection technique. (D,E) Reprinted and adapted with permission from ref 398. Copyright 2021 Royal Society of Chemistry.

of crucial biomolecules. The specific detection of manganese superoxide dismutase (MnSOD), a specific liver cancer biomarker, is of great significance for clinical diagnosis.[383,384] MnSOD-targeting aptamers were found to bind MnSOD in solution. It was found that the binding process of MnSOD-targeting aptamers to MnSOD in solution is dominated by electrostatic interactions, conferring on aptamers the ability to act as recognition elements for the MnSOD biosensors.[385] Thus, Cottat et al. constructed a SERS nanobiosensor with high specificity and sensitivity by coating MnSOD-binding aptamers on a nanoantenna surface.[386] This SERS nanobiosensor was able to detect MnSOD in different body fluids (serum and saliva) at concentrations in the nanomolar range. Glycated albumin (GA) is a key biomarker in the diagnosis and treatment of diabetes mellitus.[387−389] To improve the specificity and accuracy of GA detection, researchers have identified aptamers that specifically bind to GA. Utilizing the SPR technique, Sun and co-workers revealed for the first time that the interaction mechanism between GA, and its aptamer is driven by electrostatic force.[390] Considering this interaction mechanism, Ghosh et al. combined GA aptamers with semiconductor quantum dots (QDs) as well as AuNPs for the optical detection of GA.[220] As shown in Figure 9A, the GA

aptamer was designed into a molecular beacon structure with two ends attached to the QD and AuNP, respectively, to construct a FRET sensor. When the GA concentration increases within the range of 0 nM to 14500 nM, a linear increase in photoluminescence intensity of this sensor was observed. The results showed that the average LOD for the sensor was 0.067 $\mu g\ mL^{-1}$, meeting practical detection needs.

Electrical methods exhibit broad development prospects in rapid and on-site detection due to their advantages such as high sensitivity and fast response.[391] Aptamer−protein electrostatic interactions are able to induce changes in electrical signals, making them applicable to electrical detection. Hence, many electrical detection methods based on electrostatic interactions have been constructed to acquire biomolecular information. Platelet-derived growth factor-BB (PDGF-BB) plays an important role in angiogenesis and is closely related to the development of various tumors.[392,393] Reportedly, the specific binding interaction between PDGF-BB aptamer and PDGF-BB could be applied in the regulation of angiogenesis.[394] The structural characterization of the aptamer−PDGF-BB complex revealed that dimeric forms of PDGF-BB present two identical binding sites to interact electrostatically with aptamers.[395] In light of this, Wang's group developed an
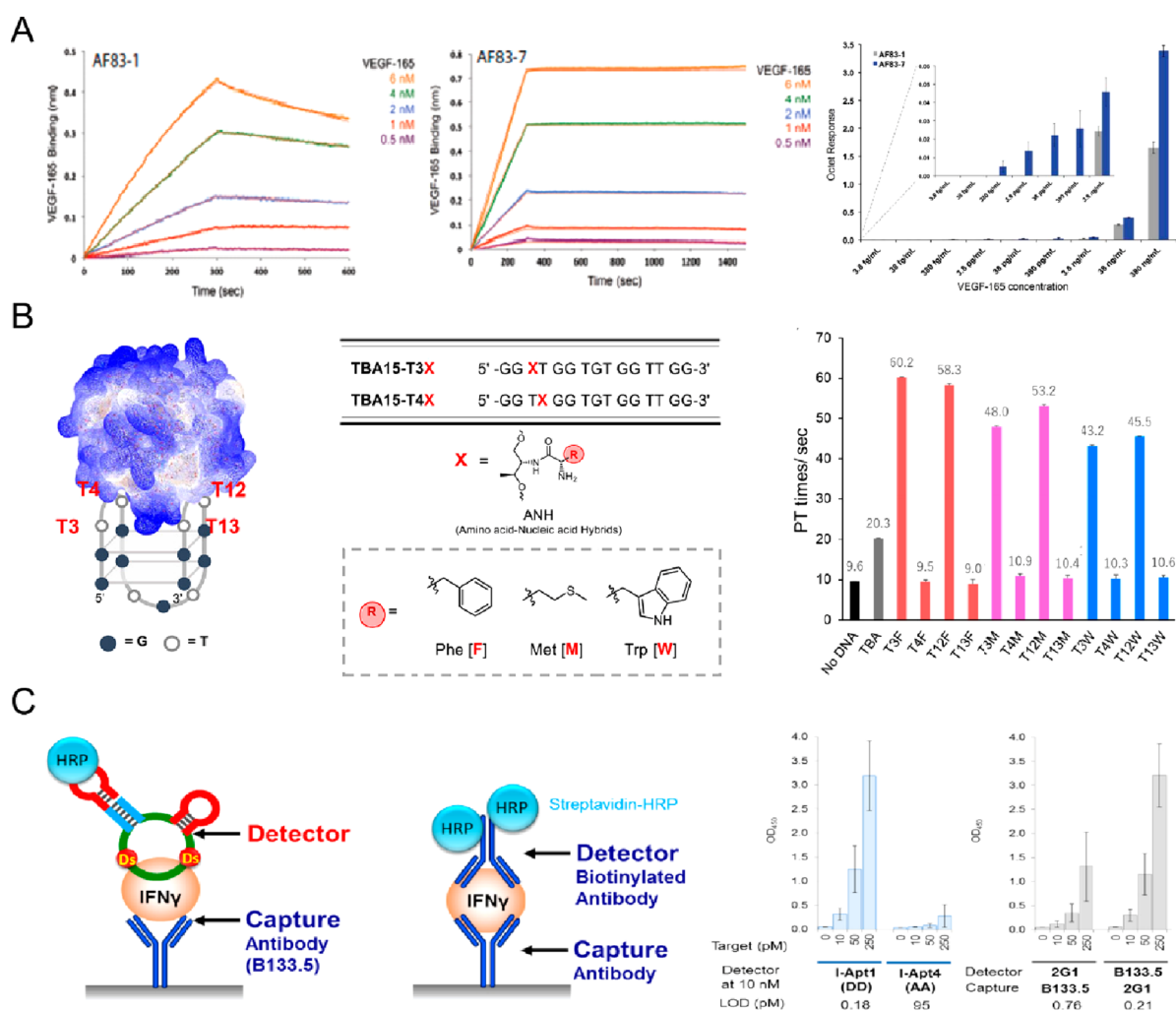
**Figure 10.** (A) The binding and LOD of native aptamer (AF83−1) and PS2-modified aptamers (AF83−7) to VEGF$_{165}$ as observed by BLI. Adopted with permission from ref 111. Copyright 2016 Oxford University Press under CC BY-NC 4.0 [http://creativecommons.org/licenses/by-nc/4.0/]. (B) Schematic illustration of TBA15 functionalized with hydrophobic amino acid residues and prothrombin time assay results of various hydrophobic residue-modified TBA15. Adopted with permission from ref 409. Copyright 2021 American Chemical Society. (C) The sandwich-type ELAA assay for IFN-$\gamma$ detection. Adopted with permission from ref 410. Copyright 2019 Oxford University Press under CC BY 4.0 [http://creativecommons.org/licenses/by/4.0/].

electrical detection method based on a "sandwich" structure by immobilizing aptamers of PDGF-BB onto the substrate gold electrode and the surface of AuNPs, respectively.[396] When PDFG-BB is present, one site binds to the aptamer immobilized on the substrate gold electrode, and another site binds to the aptamer loaded onto the surface of the AuNPs, thus forming a "sandwich" structure. The subsequent addition of positively charged electroactive molecule [Ru-(NH$_3$)$_5$Cl]$^{2+}$ provided significantly enhanced electrochemical readout signals by electrostatic interaction with multiple negatively charged aptamers on the surface of AuNPs via electrostatic attraction. By means of CV, an observable electrochemical response was obtained even for PDGF-BB concentrations as low as 0.01 pM. Likewise, Cheng and Ge also combined aptamer-modified gold electrodes with the CV method for quantitative detection of target proteins (Figure 9B).[258] The high specificity and sensitivity of this electrical assay can be mainly attributed to the electrostatic interactions between the antilysozyme DNA aptamer and lysozyme.[397] As presented in Figure 9C, with [Ru(NH$_3$)$_6$]$^{3+}$ as the signaling molecule, the quantification of lysozyme in unknown samples

was achieved by monitoring CV responses in the presence of lysozyme at different concentrations.

Additionally, integrating optical and electrical strategies based on aptamer−protein electrostatic interactions to construct dual-mode detection techniques can further improve the accuracy and sensitivity of biomolecular analysis.[398] As illustrated in Figure 9D, Putnin's group fabricated a composite comprising Pb ions adsorbed on graphene oxide (GO-Pb), serving either as a quencher probe for fluorescence detection or as a signal probe for electrochemical detection.[398] Fluorescence−electrochemical dual detection technique for the quantification of GA was subsequently established by modifying this complex with FAM-labeled GA aptamer. When the FAM-aptamer binds to the GO-Pb complex, fluorescence quenching of FAM occurred due to FRET, and the oxidation of Pb via electron transfer at the electrode ceases. In contrast, strong electrostatic interactions between FAM-aptamer and GA mediated their specific binding in the presence of GA, leading to the detachment of FAM-aptamer from the complex. While the fluorescence recovered, electrochemical signal increases significantly due to the free GO-Pb complex. The

fluorescence—electrochemical dual detection technique rendered a linear relationship with GA concentrations varying from 0.001 to 80 $\mu$g mL$^{-1}$ and 0.005 to 10 $\mu$g mL$^{-1}$, respectively, with detection limits of 8.80 ng mL$^{-1}$ and 0.77 ng mL$^{-1}$ correspondingly (Figure 9E). Finally, the dual technique also exhibited excellent GA detection capability when deployed to clinical samples from diabetes patients, showing potential to be applied as a diagnostic device for diabetes mellitus in the clinical environment.

Overall, on the basis of the electrostatic interactions between aptamers and proteins, numerous detection strategies can be exploited for highly sensitive and specific analysis of key biomolecules. These detection techniques also have tremendous potential in the analysis of clinical samples.

## 5.3. Detection Based on Hydrophobic Interactions

Hydrophobic interactions have also been reported to facilitate specific binding between aptamers and target proteins. In general, hydrophobic interactions mostly involve the hydrophobic aromatic rings of aptamers and the aliphatic or aromatic side chains of protein residues.[23,50,114] Since nucleic acids are usually hydrophilic, aptamers may not efficiently interact with hydrophobic cavities of specific proteins.[399] Integration of unnatural hydrophobic groups into aptamers can regulate aptamer—protein hydrophobic interactions.[400] This section will discuss how to construct analytical assays based on the regulation of aptamer—protein hydrophobic interactions to realize the specificity analysis of biomolecules.

The phosphate backbone in aptamers is usually exposed and easily contacts proteins, playing a crucial role in mediating aptamer—protein interactions.[111] Therefore, hydrophobic modifications on the phosphate backbone can effectively manipulate the hydrophobic interactions between aptamers and proteins. Some reports have demonstrated that PS2 modifications of aptamers can increase their hydrophobic interactions with proteins, enabling aptamers to bind to target proteins with higher binding affinity.[401−403] Pursuant to this, Abeydeera's group incorporated PS2 substitution at the G7 position of VEGF$_{165}$-targeting aptamers to dramatically increase VEGF$_{165}$ binding affinity by ~1000-fold (Figure 10A).[111] Further, they found that BLI assay based on PS2-modified aptamers was able to be used for highly sensitive detection of VEGF$_{165}$, with a LOD ($\leq$0.38 pg mL$^{-1}$) significantly lower than that of native aptamer-based BIL assay ($\leq$3800.0 pg mL$^{-1}$). This research demonstrated that, owing to the enhanced hydrophobic interactions, aptamers modified with hydrophobic groups exhibited remarkably improved target binding affinity and detection capabilities.

The introduction of unnatural hydrophobic groups into bases has also been confirmed to effectively regulate hydrophobic interactions between aptamers and proteins. Due to poor or lack of enzymatic recognition capabilities, many base modifications cannot be compatible with traditional SELEX techniques and cannot be included in random libraries. This is a major challenge for the development of chemical modification strategies. If the modification appears in the random library during the selection process rather than being added later, it may provide new insights into the regulation of aptamer—protein interactions. Reportedly, the groups that can effectively regulate aptamer—protein hydrophobic interactions generally possess hydrophobic aromatic character.[23] The common hydrophobic moieties resemble amino acid side chains in proteins, including 3-indole-2-ethyl (Trp), Nap, Pp,

and so on.[113] Such hydrophobic-group-modified nucleotides are capable of producing unique motifs in direct contact with proteins, thereby realizing the regulation of aptamer—protein interactions.[404] Taking advantage of aptamers modified with Nap or Pp groups, Gawande et al. developed a sandwich-type optical assay for detecting proprotein convertase subtilisin/kexin type 9 (PCSK9, an effective therapeutic target for hypercholesterolemia).[113] Specifically, aptamers with a single modification (dC/Pp-dU) and aptamers with two modifications (Nap-dC/Nap-dU) were used as capture and detection probes for PCSK9, respectively. This sandwich-type assay showed PCSK9 concentration-dependent signals. Moreover, the authors also successfully applied the hydrophobic interaction-based analytical strategy to PCSK9 measurements in human plasma, demonstrating the practical effectiveness of this strategy. Given the remarkable detection performance of optical assays based on the regulation of aptamer—protein hydrophobic interactions, researchers further combined them with microarray technologies for quantitative detection of various disease biomarkers, including EGFR, interleukin-6 (IL-6), matrix metalloproteinase-2 (MMP-2), and neurogenic locus notch homologue protein 3 (NOTCH 3).[405−408] Besides, the regulation of hydrophobic interactions based on modifications with protein-like side chains can also be used to modulate the activity of critical proteins within living organisms. Previously reported crystallographic studies revealed that the TT loops of TBA15 play a crucial role in TBA15—thrombin binding.[114,368,369] Consequently, modifying hydrophobic groups on the TT loops will cause the further enhancement of TBA15—thrombin interactions. Yum and Ishizuka significantly enhanced thrombin inhibition properties of TBA15 by incorporating hydrophobic amino acid residues (phenylalanine, methionine, and tryptophan) at the T3 and T4 positions in the loop region (Figure 10B).[409]

Furthermore, the development of artificial hydrophobic bases also provides an alternative idea for constructing analytical assays based on aptamer—protein hydrophobic interactions.[34] Kimoto et al. introduced unnatural hydrophobic bases into the SELEX technique and yielded the interferon $\gamma$ (IFN-$\gamma$)-targeting aptamer I-Apt1 containing two Ds bases.[410] The incorporation of Ds bases augments the capacity of aptamers to interact with hydrophobic residues of target proteins. Accordingly, the authors employed the combination of I-Apt1 and antibody to construct a sandwich-type ELAA assay for IFN-$\gamma$ detection, as illustrated in Figure 10C. Compared to native IFN-$\gamma$ aptamer—antibody and antibody—antibody sandwich systems, the sandwich-type ELAA platform using the aptamer variants presented a higher detection sensitivity and was successfully applied for the detection of IFN-$\gamma$ in human serum.

Altogether, the introduction of additional hydrophobic groups into aptamers is able to alter their hydrophobic interactions with target proteins. The analytical assays based on hydrophobic interactions can achieve highly sensitive detection of key biomolecules, providing a promising avenue for clinical diagnosis.

## 5.4. Detection Based on Other Interactions

Other interactions between aptamers and proteins, such as metal chelation interactions, $\pi$−$\pi$ stacking, and van der Waals forces, also drive the specific binding events of aptamers to target proteins.[411,412] Therefore, plentiful detection methods
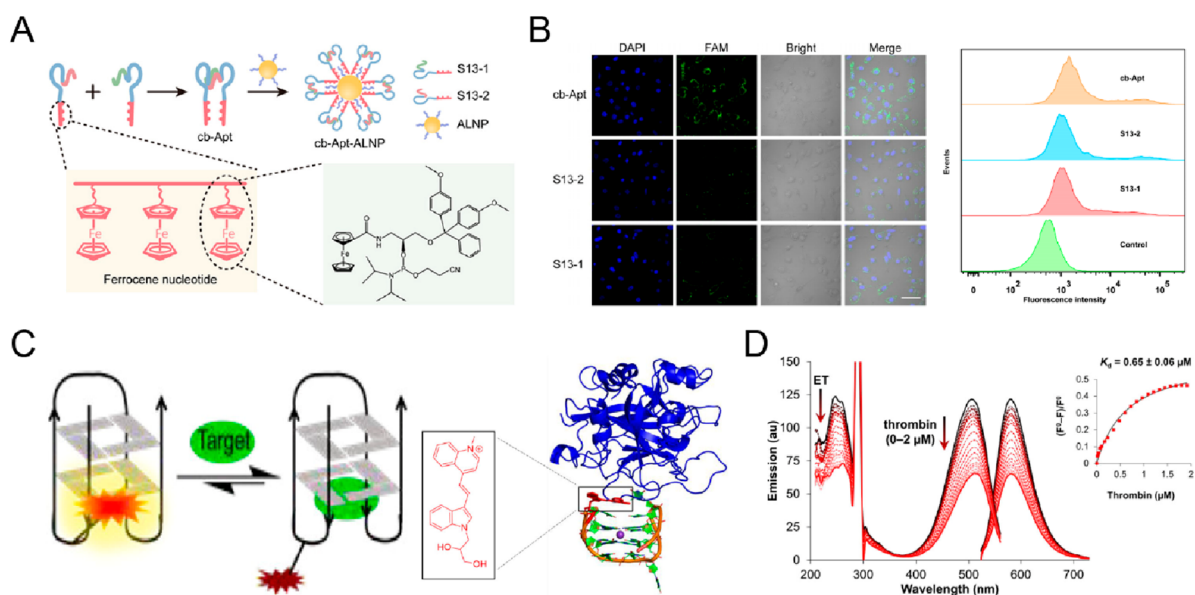
**Figure 11.** (A) Schematic of the synthesis process of cb-Apt-ALNPs. (B) Confocal microscopy and flow cytometric assays were utilized to characterize the binding ability of cb-Apt and monovalent aptamers to A549 cells. (A,B) Reprinted with permission from ref 428. Copyright 2022 American Chemical Society. (C) Schematic illustration of 4QI-displacement at the T3 position of TBA15. (D) Fluorescence titration of 4QI-TBA$_{16}$ with thrombin. (C,D) Reprinted and adapted with permission from ref 431. Copyright 2020 American Chemical Society.

based on other interactions have been exploited to detect key biomolecules.

In recent years, research on the formation mechanism of metal−amino acid−nucleoside ternary compounds facilitate the in-depth understanding of aptamer−protein chelation mediated by metal ions.[413−415] Metal ions can be contained in proteins or aptamers, driving the metal chelation between aptamers and proteins to promote their binding.[414,416] Thus, a series of analytical strategies based on metal chelation have been established for biomolecular detection. The zinc finger structure is a $Zn^{2+}$-dependent folded finger-like domain.[417,418] Proteins with zinc finger structures (zinc-finger proteins) are usually functional proteins involved in the regulation of gene expression.[419,420] For instance, as a key biomarker of human immunodeficiency virus type 1 (HIV-1), nucleocapsid protein 7 (NCp7) contains two zinc-finger structures and plays a critical role in viral reverse transcription.[421,422] To achieve high-sensitivity detection of NCp7, an aptamer tightly bound to NCp7 was developed, and their interaction was found to be strongly dependent on $Zn^{2+}$.[423,424] Based on the specific interactions between NCp7 and its aptamer, Niedzwiecki et al. combined the nanopore technique with the resistive-pulse technique for NCp7 quantification.[425] With increasing concentrations of NCp7, the amplitude of current blockades enhanced proportionally, thus achieving highly sensitive detection of NCp7. Moreover, integrating additional metal chelation into aptamer−protein interactions has also been proven to effectively modulate their binding. Taking aptamers containing ferrocene bases (Fe bases) as an example, since ferric irons can be coordinated to metal-binding sites of proteins, the introduction of Fe bases can offer new chelation effects for aptamer−protein interactions.[119,426] Tan et al. modified the EGFR-targeting aptamer containing Fe bases on the surface of persistent luminescence nanoparticles (PLNPs) to construct a highly sensitive and specific nanoprobe for the optical detection of phosphorylated EGFR (P-EGFR).[427] Concentration-dependent sensitivity analysis showed that this

nanoprobe exhibited a comparable sensitivity (∼20 ng mL$^{-1}$) to other strategies (such as fluorescence resonance energy transfer and surface-enhanced Raman scattering), satisfying stringent detection requirements in biological systems. Further, real-time monitoring of dynamic changes in P-EGFR during cell proliferation was achieved using this nanoprobe. On this basis, Zhang and Chu designed an optimized P-EGFR optical detection probe based on metal chelation (cb-Apt PLNPs).[428] In this strategy, a circular bivalent aptamer (cb-Apt) containing Fe bases were assembled on the surface of PLNPs, as is depicted in Figure 11A. Confocal microscopy and flow cytometric assays revealed that the cb-Apt displayed stronger EGFR binding affinity than the monovalent aptamer (Figure 11B). This is mainly attributed to the additional metal chelation introduced by the incorporation of Fe bases. Moreover, the authors further employed cb-Apt-PLNPs to in situ monitor the transport of P-EGFR from the cytoplasm to the nucleus to the nucleus and its distribution in the nucleus. The process of P-EGFR translocation has been reported to be closely associated with abnormal proliferation, migration, and antiapoptosis of tumor cells, and visualization of EGFR nuclear translocation can lay the foundation for revealing the molecular mechanism of tumor progression.[429]

$\pi-\pi$ stacking is a stable noncovalent interaction that primarily occurs between parallel aromatic rings.[51−53,430] To acquire biomolecular information with high efficiency, researchers have also engineered analytical assays based on the regulation of $\pi-\pi$ stacking. For example, Gray and Deore replaced the T3 base of TBA15 with a fluorescent base analogue for thrombin detection.[431] Concretely, a cyanine-indole-quinolinium (4QI) hemicyanine dye tethered to an acyclic 1,2-propanediol linker was used as the fluorescent base analogue to construct a chemically modified thrombin aptamer 4QI-TBA$_{16}$. Most importantly, 4QI adopted a unique conformation in the aptamer via $\pi-\pi$ stacking interactions with T4 and T13, resulting in bright fluorescence (Figure 11C). Structural elucidation of 4QI-TBA$_{16}$−thrombin com-

plexes revealed that 4QI incorporation disrupted the stacking interactions between T3 base in native TBA and residues Tyr141 of thrombin. In the presence of thrombin, the binding of thrombin to 4QI-TBA$_{16}$ diminished $\pi-\pi$ stacking interactions between 4QI and the GQ structure, causing a turn-off emission intensity response. Based on the regulation of $\pi-\pi$ stacking, highly sensitive and specific fluorescence detection of thrombin can be achieved with an LOD of 150 nM by utilizing 4QI-TBA$_{16}$ (Figure 11D).

Besides, van der Waals forces are a ubiquitous class of intermolecular interaction that are involved in mediating aptamer−target binding.[54,432] For example, Nomura et al. determined the crystal structure of the Fc fragment of human IgG1 (hFc1) complexed with an anti-Fc RNA aptamer and found that binding was mainly due to van der Waals forces and hydrogen bonding interactions.[433] Therefore, the synergistic regulation of van der Waals forces and other interactions on aptamer−protein binding process can also open a new avenue for the development of biomolecular detection strategies.

## 6. SUMMARY AND OUTLOOK

Aptamers are able to fold into special three-dimensional structures to interact with proteins via hydrogen bonding, electrostatic interactions, hydrophobic interactions, $\pi-\pi$ stacking, and van der Waals forces. Modulating the structure of aptamers can regulate aptamer−protein interactions and further have an impact on the behaviors of biomolecules. Many studies gradually turn their attention to the regulation of aptamer−protein interactions, promoting its potential development in analytical fields. In recent years, various analytical assays based on the regulation of aptamer−protein interactions have been rationally designed for the highly sensitive and selective detection of key biomolecules in biological systems, aiming to give vital guidance for studying the molecular mechanisms of diseases. In this review, we surveyed methods to regulate aptamer−protein interactions. Then, approaches for analyzing aptamer−protein interactions as well as resolving structures of aptamer−protein complexes were summarized in detail. Furthermore, we gave a thorough elaboration on the analytical assays based on the regulation of aptamer−protein interactions and their applications in biomolecular detection.

Although considerable achievements have been made in bioanalysis using assays based on the regulation of aptamer−protein interactions, several challenges remain in this field. The structural stability of aptamers is considered to be a vital factor that has broad implications for aptamer−protein interactions.[18,434,435] Chemical modification, nanostructure design and multifunctional integrated design of aptamers can influence their structural stability and, in turn, regulate their interaction with proteins. Indeed, these strategies are still at the research stage in extending the bioanalytical applications of assays based on the regulation of aptamer−protein interactions. To advance this frontier, researchers might focus on the following areas. For chemical modification, the types of chemical groups currently used for chemical modifications are limited, and partially chemical modified aptamers are subjected to the compatibility of conventional screening techniques. Regarding nanostructure design, the future development of aptamer nanostructures is speculated to follow a trend of increasing scale and complexity. This will undoubtedly increase the difficulty in designing aptamer nanostructures. Moreover, the regulatory effectiveness of multifunctional integrated design strategies on aptamer−protein interactions is largely influenced by the coverage density of aptamers, yet there is still a lack of simple and accurate methods for measuring aptamer density. Currently, the optimum loading density usually requires many in vitro and in vivo experiments. Hence, to expand the applicability of analytical assays based on the regulation of aptamer−protein interactions, regulatory strategies for aptamer−protein interactions need to be further optimized or developed to improve the sensitivity and accuracy of these assays.

Structural determination of aptamer−protein complexes enables insights into the characteristic information about the interactions of aptamers with proteins from a molecular perspective, helping to reveal the molecular mechanisms of the interactions. However, in most cases, the characterization of aptamer−protein interactions has been confined to affinity evaluation, and only few high-resolution structures of aptamer−protein complexes have been reported. Currently, NMR spectroscopy, X-ray crystallography, and Cryo-EM play major roles in probing aptamer−protein interactions and render detailed information on the molecular basis of the interactions between aptamers and target proteins. Despite this, all three methods suffer from limitations: NMR spectroscopy is limited to structure resolution of relatively small biomolecules (<30−40 kDa); for X-ray crystallography, obtaining high-quality crystals is still a huge challenge to be addressed in most cases; and Cryo-EM is also limited by a number of shortcomings, such as the high detection limit (~0.1 MDa), cumbersome data processing, expensive equipment, and high maintenance costs. These limitations mean that, in applicability, none of the above approaches are versatile structural analysis tools for accessing the detailed structural features of aptamer−protein complexes described to date. Recently, with the rapid development of computer science, various molecular docking simulation programs have also been utilized to study aptamer−protein interactions, such as molecular operating environment (MOE) and collaborative computational project number 4 (CCP4).[50,436−438] These computer simulation procedures are generally performed to predict potential interaction sites and interaction modes. In some cases where structural characteristics of aptamer−protein complexes are not available, simulation software may help us to better understand how aptamers interact with target proteins. Nevertheless, these simulation programs are unable to predict actual binding processes, and the prediction accuracy of binding modes is limited.[439−442] As a neural-network-based method, AlphaFold can regularly predict protein structures with atomic accuracy even when similar structures are not known.[443,444] However, there is currently no artificial-intelligence-based tool comparable to Alphafold for aptamer tertiary structure prediction and interaction analysis. Therefore, there is still a need to improve and develop versatile analytical tools to provide more accurate and comprehensive information on aptamer−protein interactions, including the types of interactions, spatial configurations, and binding sites.

Overall, design strategies for aptamer−protein interactions have evolved considerably over the past two decades, yielding a range of analytical assays based on the regulation of aptamer−protein interactions. These analytical assays have brought surprising and vastly unexplored avenues of research in analytical science and biomedical science. It is believed that collaborative efforts and cooperation between scientists with different research backgrounds will bring innovations and breakthroughs to the field in the near future, advancing the

development of these analytical assays toward practical implementations.

## AUTHOR INFORMATION

### Corresponding Authors

**Quan Yuan** − *Molecular Science and Biomedicine Laboratory (MBL), State Key Laboratory of Chemo/Biosensing and Chemometrics, College of Chemistry and Chemical Engineering, Hunan University, Changsha 410082, China;* ⓞ orcid.org/0000-0002-3085-431X; Email: yuanquan@whu.edu.cn

**Jie Tan** − *Molecular Science and Biomedicine Laboratory (MBL), State Key Laboratory of Chemo/Biosensing and Chemometrics, College of Chemistry and Chemical Engineering, Hunan University, Changsha 410082, China;* ⓞ orcid.org/0000-0002-0909-2904; Email: tanjie0416@hnu.edu.cn

### Authors

**Cailing Ji** − *Molecular Science and Biomedicine Laboratory (MBL), State Key Laboratory of Chemo/Biosensing and Chemometrics, College of Chemistry and Chemical Engineering, Hunan University, Changsha 410082, China*

**Junyuan Wei** − *Molecular Science and Biomedicine Laboratory (MBL), State Key Laboratory of Chemo/Biosensing and Chemometrics, College of Chemistry and Chemical Engineering, Hunan University, Changsha 410082, China*

**Lei Zhang** − *Molecular Science and Biomedicine Laboratory (MBL), State Key Laboratory of Chemo/Biosensing and Chemometrics, College of Chemistry and Chemical Engineering, Hunan University, Changsha 410082, China*

**Xinru Hou** − *Molecular Science and Biomedicine Laboratory (MBL), State Key Laboratory of Chemo/Biosensing and Chemometrics, College of Chemistry and Chemical Engineering, Hunan University, Changsha 410082, China*

**Weihong Tan** − *Molecular Science and Biomedicine Laboratory (MBL), State Key Laboratory of Chemo/Biosensing and Chemometrics, College of Chemistry and Chemical Engineering, Hunan University, Changsha 410082, China; The Cancer Hospital of the University of Chinese Academy of Sciences (Zhejiang Cancer Hospital), Hangzhou Institute of Medicine (HIM), Chinese Academy of Sciences, Hangzhou, Zhejiang 310022, China;* ⓞ orcid.org/0000-0002-8066-1524

Complete contact information is available at:
https://pubs.acs.org/10.1021/acs.chemrev.3c00377

### Notes

The authors declare no competing financial interest.

### Biographies

Cailing Ji received her B.S. degree in chemistry from Hunan University in 2019. She is currently pursuing her Ph.D. degree under the supervision of Prof. Quan Yuan at Hunan University. Her research focuses on the development of functional nucleic acids for bioanalysis.

Junyuan Wei obtained her B.S. degree in pharmaceutical engineering from Yunnan Minzu University in 2021. Now she is a Master's student in Prof. Quan Yuan's group at Hunan University. Her research interest is focused on the sensitive detection of biomolecules based on DNA nanotechnology.

Lei Zhang obtained her B.S. degree from Henan Normal University in 2018. She is currently a Ph.D. candidate in Prof. Quan Yuan's research group at Hunan University. Her research interests include the design and applications of chemically modified nucleic acids.

Xinru Hou received her B.S. degree from Hebei University (2022) and is currently a Master's student at Hunan University, under the supervision of Prof. Quan Yuan. Her research focuses on the multifunctional design of nucleic acid probes.

Jie Tan is an associate professor of College of Chemistry and Chemical Engineering at Hunan University. She earned her B.S. degree (2011) and Ph.D. degree (2016) from Zhejiang University. From 2017 to 2019, she pursued postdoctoral research with Prof. Weihong Tan at Hunan University. Her main research interest is focused on the design of chemically modified nucleic acids for biosensing.

Quan Yuan is a professor in Hunan University. She received her B.S. degree from Wuhan University in 2004 and Ph.D. degree in inorganic chemistry from Peking University in 2009. Afterwards, she worked as a postdoctoral researcher in the group of prof. Weihong Tan at the University of Florida (2009−2011). Her research focuses on the bioassays of complex samples.

Weihong Tan, Distinguished Professor of Chemistry and Professor of Physiology and Functional Genomics, earned his M.S. (1985) and Ph.D. degrees (1993) from the Chinese Academy of Sciences and the University of Michigan, respectively. Since 2019, Dr. Tan has worked as the director of Hangzhou Institute of Medicine (HIM), Chinese Academy of Sciences. Dr. Tan's research interest is the development and applications of novel nucleic acid probes for bioanalytical chemistry, chemical biology, and molecular medicine. His group developed cell-SELEX technology to select aptamers for specific recognition and molecular signature discrimination of diseased living cells. With their selected aptamers, Tan's group have designed a variety of DNA molecular tools for molecular recognition, bioseparation, ultrasensitive bioanalysis, and targeted cancer therapy.

## REFERENCES

(1) Van Roey, K.; Uyar, B.; Weatheritt, R. J.; Dinkel, H.; Seiler, M.; Budd, A.; Gibson, T. J.; Davey, N. E. Short Linear Motifs: Ubiquitous and Functionally Diverse Protein Interaction Modules Directing Cell Regulation. *Chem. Rev.* **2014**, *114*, 6733−6778.

(2) Vickers, T. A.; Crooke, S. T. Development of a Quantitative BRET Affinity Assay for Nucleic Acid-Protein Interactions. *PLoS One* **2016**, *11*, No. e0161930.

(3) Miyoshi, D.; Sugimoto, N. Molecular Crowding Effects on Structure and Stability of DNA. *Biochimie* **2008**, *90*, 1040−1051.

(4) Schwidetzky, R.; Lukas, M.; YazdanYar, A.; Kunert, A. T.; Poschl, U.; Domke, K. F.; Frohlich-Nowoisky, J.; Bonn, M.; Koop, T.; Nagata, Y.; et al. Specific Ion-Protein Interactions Influence Bacterial Ice Nucleation. *Chem.—Eur. J.* **2021**, *27*, 7402−7407.

(5) Camborde, L.; Jauneau, A.; Briere, C.; Deslandes, L.; Dumas, B.; Gaulin, E. Detection of Nucleic Acid-Protein Interactions in Plant Leaves Using Fluorescence Lifetime Imaging Microscopy. *Nat. Protoc.* **2017**, *12*, 1933−1950.

(6) Pires, D. E. V.; Ascher, D. B. Mcsm-Na: Predicting the Effects of Mutations on Protein-Nucleic Acids Interactions. *Nucleic Acids Res.* **2017**, *45*, W241−W246.

(7) Tuszynska, I.; Magnus, M.; Jonak, K.; Dawson, W.; Bujnicki, J. M. Npdock: A Web Server for Protein-Nucleic Acid Docking. *Nucleic Acids Res.* **2015**, *43*, W425−W430.

(8) Iwano, N.; Adachi, T.; Aoki, K.; Nakamura, Y.; Hamada, M. Generative Aptamer Discovery Using Raptgen. *Nat. Comput. Sci.* **2022**, *2*, 378−386.

(9) Kimoto, M.; Yamashige, R.; Matsunaga, K.; Yokoyama, S.; Hirao, I. Generation of High-Affinity DNA Aptamers Using an Expanded Genetic Alphabet. *Nat. Biotechnol.* **2013**, *31*, 453−457.

(10) Wu, L.; Wang, Y.; Xu, X.; Liu, Y.; Lin, B.; Zhang, M.; Zhang, J.; Wan, S.; Yang, C.; Tan, W. Aptamer-Based Detection of Circulating Targets for Precision Medicine. *Chem. Rev.* **2021**, *121*, 12035−12105.

(11) Shi, H.; Lei, Y.; Ge, J.; He, X.; Cui, W.; Ye, X.; Liu, J.; Wang, K. A Simple, pH-Activatable Fluorescent Aptamer Probe with Ultralow Background for Bispecific Tumor Imaging. *Anal. Chem.* **2019**, *91*, 9154−9160.

(12) Xun, K.; Sun, Y.; Zhang, Q.; Wen, N.; Wang, Z.; Qiu, L.; Tan, W. Aptamer-Based Analysis and Manipulation of the Protein Activity in Living Cells. *Anal. Chem.* **2022**, *94*, 4352−4358.

(13) Chen, T. T.; Tian, X.; Liu, C. L.; Ge, J.; Chu, X.; Li, Y. Fluorescence Activation Imaging of Cytochrome C Released from Mitochondria Using Aptameric Nanosensor. *J. Am. Chem. Soc.* **2015**, *137*, 982−989.

(14) Tang, J.; Huang, C.; Shu, J.; Zheng, J.; Ma, D.; Li, J.; Yang, R. Azoreductase and Target Simultaneously Activated Fluorescent Monitoring for Cytochrome C Release under Hypoxia. *Anal. Chem.* **2018**, *90*, 5865−5872.

(15) Kadam, U. S.; Hong, J. C. Advances in Aptameric Biosensors Designed to Detect Toxic Contaminants from Food, Water, Human Fluids, and the Environment. *Trends Environ. Anal. Chem.* **2022**, *36*, No. e00184.

(16) Tao, X.; Huang, Y.; Wang, C.; Chen, F.; Yang, L.; Ling, L.; Che, Z.; Chen, X. Recent Developments in Molecular Docking Technology Applied in Food Science: A Review. *Int. J. Food Sci. Technol.* **2020**, *55*, 33−45.

(17) Yan, J.; Xiong, H.; Cai, S.; Wen, N.; He, Q.; Liu, Y.; Peng, D.; Liu, Z. Advances in Aptamer Screening Technologies. *Talanta* **2019**, *200*, 124−144.

(18) Li, L.; Xu, S.; Yan, H.; Li, X.; Yazd, H. S.; Li, X.; Huang, T.; Cui, C.; Jiang, J.; Tan, W. Nucleic Acid Aptamers for Molecular Diagnostics and Therapeutics: Advances and Perspectives. *Angew. Chem., Int. Ed.* **2021**, *60*, 2221−2231.

(19) Matsunaga, K. I.; Kimoto, M.; Hirao, I. High-Affinity DNA Aptamer Generation Targeting von Willebrand Factor A1-Domain by Genetic Alphabet Expansion for Systematic Evolution of Ligands by Exponential Enrichment Using Two Types of Libraries Composed of Five Different Bases. *J. Am. Chem. Soc.* **2017**, *139*, 324−334.

(20) Ni, S.; Yao, H.; Wang, L.; Lu, J.; Jiang, F.; Lu, A.; Zhang, G. Chemical Modifications of Nucleic Acid Aptamers for Therapeutic Purposes. *Int. J. Mol. Sci.* **2017**, *18*, 1683.

(21) Avino, A.; Fabrega, C.; Tintore, M.; Eritja, R. Thrombin Binding Aptamer, More Than a Simple Aptamer: Chemically Modified Derivatives and Biomedical Applications. *Curr. Pharm. Des.* **2012**, *18*, 2036−2047.

(22) Nimjee, S. M.; White, R. R.; Becker, R. C.; Sullenger, B. A. Aptamers as Therapeutics. *Annu. Rev. Pharmacol. Toxicol.* **2017**, *57*, 61−79.

(23) Rohloff, J. C.; Gelinas, A. D.; Jarvis, T. C.; Ochsner, U. A.; Schneider, D. J.; Gold, L.; Janjic, N. Nucleic Acid Ligands with Protein-Like Side Chains: Modified Aptamers and Their Use as Diagnostic and Therapeutic Agents. *Mol. Ther. Nucleic Acids* **2014**, *3*, No. e201.

(24) Hu, L.; Liu, K.; Ren, G.; Liang, J.; Wu, Y. Progress in DNA Aptamers as Recognition Components for Protein Functional Regulation. *Chem. Res. Chin. Univ.* **2022**, *38*, 894−901.

(25) Wang, J.; Wei, Y.; Hu, X.; Fang, Y. Y.; Li, X.; Liu, J.; Wang, S.; Yuan, Q. Protein Activity Regulation: Inhibition by Closed-Loop Aptamer-Based Structures and Restoration by Near-IR Stimulation. *J. Am. Chem. Soc.* **2015**, *137*, 10576−10584.

(26) Xie, S.; Du, Y.; Zhang, Y.; Wang, Z.; Zhang, D.; He, L.; Qiu, L.; Jiang, J.; Tan, W. Aptamer-Based Optical Manipulation of Protein Subcellular Localization in Cells. *Nat. Commun.* **2020**, *11*, 1347.

(27) Li, F.; Lu, J.; Liu, J.; Liang, C.; Wang, M.; Wang, L.; Li, D.; Yao, H.; Zhang, Q.; Wen, J.; et al. A Water-Soluble Nucleolin Aptamer-Paclitaxel Conjugate for Tumor-Specific Targeting in Ovarian Cancer. *Nat. Commun.* **2017**, *8*, 1390.

(28) Qi, S.; Duan, N.; Sun, Y.; Zhou, Y.; Ma, P.; Wu, S.; Wang, Z. High-Affinity Aptamer of Allergen B-Lactoglobulin: Selection, Recognition Mechanism and Application. *Sensors Actuators B: Chem.* **2021**, *340*, 129956.

(29) Thevendran, R.; Citartan, M. Assays to Estimate the Binding Affinity of Aptamers. *Talanta* **2022**, *238*, 122971.

(30) Valero, J.; Civit, L.; Dupont, D. M.; Selnihhin, D.; Reinert, L. S.; Idorn, M.; Israels, B. A.; Bednarz, A. M.; Bus, C.; Asbach, B.; et al. A Serum-Stable RNA Aptamer Specific for SARS-CoV-2 Neutralizes Viral Entry. *Proc. Natl. Acad. Sci. U. S. A.* **2021**, *118*, No. e2112942118.

(31) Wu, X.; Liu, H.; Han, D.; Peng, B.; Zhang, H.; Zhang, L.; Li, J.; Liu, J.; Cui, C.; Fang, S.; et al. Elucidation and Structural Modeling of CD71 as a Molecular Target for Cell-Specific Aptamer Binding. *J. Am. Chem. Soc.* **2019**, *141*, 10760−10769.

(32) Zhao, Q.; Tao, J.; Feng, W.; Uppal, J. S.; Peng, H.; Le, X. C. Aptamer Binding Assays and Molecular Interaction Studies Using Fluorescence Anisotropy - A Review. *Anal. Chim. Acta* **2020**, *1125*, 267−278.

(33) Adachi, T.; Nakamura, Y. Aptamers: A Review of Their Chemical Properties and Modifications for Therapeutic Application. *Molecules* **2019**, *24*, 4229.

(34) Dunn, M. R.; Jimenez, R. M.; Chaput, J. C. Analysis of Aptamer Discovery and Technology. *Nat. Rev. Chem.* **2017**, *1*, 0076.

(35) Ma, H.; Liu, J.; Ali, M. M.; Mahmood, M. A.; Labanieh, L.; Lu, M.; Iqbal, S. M.; Zhang, Q.; Zhao, W.; Wan, Y. Nucleic Acid Aptamers in Cancer Research, Diagnosis and Therapy. *Chem. Soc. Rev.* **2015**, *44*, 1240−1256.

(36) Ni, S.; Zhuo, Z.; Pan, Y.; Yu, Y.; Li, F.; Liu, J.; Wang, L.; Wu, X.; Li, D.; Wan, Y.; et al. Recent Progress in Aptamer Discoveries and Modifications for Therapeutic Applications. *ACS Appl. Mater. Interfaces* **2021**, *13*, 9500−9519.

(37) Zhou, J.; Rossi, J. Aptamers as Targeted Therapeutics: Current Potential and Challenges. *Nat. Rev. Drug Discovery* **2017**, *16*, 181−202.

(38) Zavyalova, E.; Turashev, A.; Novoseltseva, A.; Legatova, V.; Antipova, O.; Savchenko, E.; Balk, S.; Golovin, A.; Pavlova, G.; Kopylov, A. Pyrene-Modified DNA Aptamers with High Affinity to Wild-Type EGFR and EGFRvIII. *Nucleic Acid Ther.* **2020**, *30*, 175−187.

(39) Manuel, B. A.; Sterling, S. A.; Sanford, A. A.; Heemstra, J. M. Systematically Modulating Aptamer Affinity and Specificity by Guanosine-to-Inosine Substitution. *Anal. Chem.* **2022**, *94*, 6436−6440.

(40) Cassiday, L. A.; Maher, L. J. In Vivo Recognition of an RNA Aptamer by Its Transcription Factor Target. *Biochemistry* **2001**, *40*, 2433−2438.

(41) Huang, D. B.; Vu, D.; Cassiday, L. A.; Zimmerman, J. M.; Maher, L. J.; Ghosh, G. Crystal Structure of Nf-Kappa B (p50)(2) Complexed to a High-Affinity RNA Aptamer. *Proc. Natl. Acad. Sci. U. S. A.* **2003**, *100*, 9268−9273.

(42) Alkhamis, O.; Xiao, Y. Systematic Study of in Vitro Selection Stringency Reveals How To Enrich High-Affinity Aptamers. *J. Am. Chem. Soc.* **2023**, *145*, 194−206.

(43) Wu, Y. Y.; Hsieh, I. S.; Tung, C. H.; Weng, C. H.; Wu, J. E.; Yu, J. S.; Hong, T. M.; Chen, Y. L. A Novel DNA Aptamer Targeting Lung Cancer Stem Cells Exerts a Therapeutic Effect by Binding and Neutralizing Annexin A2. *Mol. Ther. Nucleic Acids* **2022**, *27*, 956−968.

(44) Zhang, L.; Wan, S.; Jiang, Y.; Wang, Y.; Fu, T.; Liu, Q.; Cao, Z.; Qiu, L.; Tan, W. Molecular Elucidation of Disease Biomarkers at the Interface of Chemistry and Biology. *J. Am. Chem. Soc.* **2017**, *139*, 2532−2540.

(45) Mairal, T.; Cengiz Ozalp, V.; Lozano Sanchez, P.; Mir, M.; Katakis, I.; O'Sullivan, C. K. Aptamers: Molecular Tools for Analytical Applications. *Anal. Bioanal. Chem.* **2008**, *390*, 989−1007.

(46) Cai, S.; Yan, J.; Xiong, H.; Liu, Y.; Peng, D.; Liu, Z. Investigations on the Interface of Nucleic Acid Aptamers and Binding Targets. *Analyst* **2018**, *143*, 5317−5338.

(47) Almazar, C. A.; Mendoza, M. V.; Rivera, W. L. In Silico Approaches for the Identification of Aptamer Binding Interactions to Leptospira spp. Cell Surface Proteins. *Trop. Med. Infect. Dis.* **2023**, *8*, 125.

(48) Law, M. J.; Linde, M. E.; Chambers, E. J.; Oubridge, C.; Katsamba, P. S.; Nilsson, L.; Haworth, I. S.; Laird-Offringa, I. A. The Role of Positively Charged Amino Acids and Electrostatic Interactions in the Complex of U1A Protein and U1 Hairpin II RNA. *Nucleic Acids Res.* **2006**, *34*, 275−285.

(49) McBain, S. C.; Yiu, H. H. P.; El Haj, A.; Dobson, J. Polyethyleneimine Functionalized Iron Oxide Nanoparticles as Agents for DNA Delivery and Transfection. *J. Mater. Chem.* **2007**, *17*, 2561−2565.

(50) Gelinas, A. D.; Davies, D. R.; Janjic, N. Embracing Proteins: Structural Themes in Aptamer-Protein Complexes. *Curr. Opin. Struct. Biol.* **2016**, *36*, 122−132.

(51) Krissanaprasit, A.; Key, C. M.; Pontula, S.; LaBean, T. H. Self-Assembling Nucleic Acid Nanostructures Functionalized with Aptamers. *Chem. Rev.* **2021**, *121*, 13797−13868.

(52) Riwar, L. J.; Trapp, N.; Kuhn, B.; Diederich, F. Substituent Effects in Parallel-Displaced Pi-Pi Stacking Interactions: Distance Matters. *Angew. Chem., Int. Ed.* **2017**, *56*, 11252−11257.

(53) Hermann, J.; Alfe, D.; Tkatchenko, A. Nanoscale Pi-Pi Stacked Molecules Are Bound by Collective Charge Fluctuations. *Nat. Commun.* **2017**, *8*, 14052.

(54) Ambrosetti, A.; Ferri, N.; DiStasio Jr, R. A.; Tkatchenko, A. Wavelike Charge Density Fluctuations and Van Der Waals Interactions at the Nanoscale. *Science* **2016**, *351*, 1171−1176.

(55) Sun, H.; Tan, W.; Zu, Y. Aptamers: Versatile Molecular Recognition Probes for Cancer Detection. *Analyst* **2016**, *141*, 403−415.

(56) Ahmad, T.; Fiuzat, M.; Felker, G. M.; O'Connor, C. Novel Biomarkers in Chronic Heart Failure. *Nat. Rev. Cardiol.* **2012**, *9*, 347−359.

(57) Han, D.; Zhu, Z.; Wu, C.; Peng, L.; Zhou, L.; Gulbakan, B.; Zhu, G.; Williams, K. R.; Tan, W. A Logical Molecular Circuit for Programmable and Autonomous Regulation of Protein Activity Using DNA Aptamer-Protein Interactions. *J. Am. Chem. Soc.* **2012**, *134*, 20797−20804.

(58) He, X.; Guo, L.; He, J.; Xu, H.; Xie, J. Stepping Library-Based Post-SELEX Strategy Approaching to the Minimized Aptamer in SPR. *Anal. Chem.* **2017**, *89*, 6559−6566.

(59) Ma, P.; Ye, H.; Guo, H.; Ma, X.; Yue, L.; Wang, Z. Aptamer Truncation Strategy Assisted by Molecular Docking and Sensitive Detection of T-2 Toxin Using SYBR Green I as a Signal Amplifier. *Food Chem.* **2022**, *381*, 132171.

(60) Wang, T.; Chen, C.; Larcher, L. M.; Barrero, R. A.; Veedu, R. N. Three Decades of Nucleic Acid Aptamer Technologies: Lessons Learned, Progress and Opportunities on Aptamer Development. *Biotechnol. Adv.* **2019**, *37*, 28−50.

(61) Alsager, O. A.; Kumar, S.; Zhu, B.; Travas-Sejdic, J.; McNatty, K. P.; Hodgkiss, J. M. Ultrasensitive Colorimetric Detection of 17beta-Estradiol: The Effect of Shortening DNA Aptamer Sequences. *Anal. Chem.* **2015**, *87*, 4201−4209.

(62) Wu, Y.; Belmonte, I.; Sykes, K. S.; Xiao, Y.; White, R. J. Perspective on the Future Role of Aptamers in Analytical Chemistry. *Anal. Chem.* **2019**, *91*, 15335−15344.

(63) Nadal, P.; Svobodova, M.; Mairal, T.; O'Sullivan, C. K. Probing High-Affinity 11-mer DNA Aptamer against Lup an 1 (Beta-Conglutin). *Anal. Bioanal. Chem.* **2013**, *405*, 9343−9349.

(64) Hu, H.; Ding, Y.; Gao, Z.; Li, H. S1 Nuclease Digestion-Based Rational Truncation of PD-L1 Aptamer and Establishment of a Signal

Dual Amplification Aptasensor. *Sensors Actuators B: Chem.* **2021**, *331*, 129442.

(65) Vu, C. Q.; Rotkrua, P.; Tantirungrotechai, Y.; Soontornworajit, B. Oligonucleotide Hybridization Combined with Competitive Antibody Binding for the Truncation of a High-Affinity Aptamer. *ACS Comb. Sci.* **2017**, *19*, 609−617.

(66) Aljohani, M. M.; Chinnappan, R.; Alsager, O. A.; AlZabn, R.; Alhoshani, A.; Weber, K.; Cialla-May, D.; Popp, J.; Zourob, M. Mapping the Binding Region of Aptamer Targeting Small Molecule: Dabigatran Etexilate, an Anti-Coagulant. *Talanta* **2020**, *218*, 121132.

(67) Kong, Q.; Yue, F.; Liu, M.; Huang, J.; Yang, F.; Liu, J.; Li, J.; Li, F.; Sun, X.; Guo, Y.; et al. Non-Immobilized GO-SELEX of Aptamers for Label-Free Detection of Thiamethoxam in Vegetables. *Anal. Chim. Acta* **2022**, *1202*, 339677.

(68) Wei, H.; Cai, R.; Yue, H.; Tian, Y.; Zhou, N. Screening and Application of a Truncated Aptamer for High-Sensitive Fluorescent Detection of Metronidazole. *Anal. Chim. Acta* **2020**, *1128*, 203−210.

(69) Lavu, P. S.; Mondal, B.; Ramlal, S.; Murali, H. S.; Batra, H. V. Selection and Characterization of Aptamers Using a Modified Whole Cell Bacterium SELEX for the Detection of Salmonella Enterica Serovar Typhimurium. *ACS Comb. Sci.* **2016**, *18*, 292−301.

(70) Li, J.; Zhang, Z.; Gu, J.; Stacey, H. D.; Ang, J. C.; Capretta, A.; Filipe, C. D. M.; Mossman, K. L.; Balion, C.; Salena, B. J.; et al. Diverse High-Affinity DNA Aptamers for Wild-Type and B.1.1.7 SARS-CoV-2 Spike Proteins from a Pre-Structured DNA Library. *Nucleic Acids Res.* **2021**, *49*, 7267−7279.

(71) Macdonald, J.; Houghton, P.; Xiang, D.; Duan, W.; Shigdar, S. Truncation and Mutation of a Transferrin Receptor Aptamer Enhances Binding Affinity. *Nucleic Acid Ther.* **2016**, *26*, 348−354.

(72) Costello, A. M.; Elizondo-Riojas, M. A.; Li, X.; Volk, D. E.; Pillai, A. K.; Wang, H. Selection and Characterization of Vimentin-Binding Aptamer Motifs for Ovarian Cancer. *Molecules* **2021**, *26*, 6525.

(73) Hasegawa, H.; Savory, N.; Abe, K.; Ikebukuro, K. Methods for Improving Aptamer Binding Affinity. *Molecules* **2016**, *21*, 421.

(74) Bashir, A.; Yang, Q.; Wang, J.; Hoyer, S.; Chou, W.; McLean, C.; Davis, G.; Gong, Q.; Armstrong, Z.; Jang, J.; et al. Machine Learning Guided Aptamer Refinement and Discovery. *Nat. Commun.* **2021**, *12*, 2366.

(75) Ruff, K. M.; Snyder, T. M.; Liu, D. R. Enhanced Functional Potential of Nucleic Acid Aptamer Libraries Patterned to Increase Secondary Structure. *J. Am. Chem. Soc.* **2010**, *132*, 9453−9464.

(76) Rothlisberger, P.; Hollenstein, M. Aptamer Chemistry. *Adv. Drug Delivery Rev.* **2018**, *134*, 3−21.

(77) Tan, S. Y.; Acquah, C.; Sidhu, A.; Ongkudon, C. M.; Yon, L. S.; Danquah, M. K. SELEX Modifications and Bioanalytical Techniques for Aptamer-Target Binding Characterization. *Crit. Rev. Anal. Chem.* **2016**, *46*, 521−537.

(78) Wang, C. H.; Chang, C. P.; Lee, G. B. Integrated Microfluidic Device Using a Single Universal Aptamer to Detect Multiple Types of Influenza Viruses. *Biosens. Bioelectron.* **2016**, *86*, 247−254.

(79) Debiais, M.; Lelievre, A.; Smietana, M.; Muller, S. Splitting Aptamers and Nucleic Acid Enzymes for the Development of Advanced Biosensors. *Nucleic Acids Res.* **2020**, *48*, 3400−3422.

(80) Citartan, M. The Dynamicity of Light-up Aptamers in One-Pot in Vitro Diagnostic Assays. *Analyst* **2021**, *147*, 10−21.

(81) Liu, X.; Shi, L.; Hua, X.; Huang, Y.; Su, S.; Fan, Q.; Wang, L.; Huang, W. Target-Induced Conjunction of Split Aptamer Fragments and Assembly with a Water-Soluble Conjugated Polymer for Improved Protein Detection. *ACS Appl. Mater. Interfaces* **2014**, *6*, 3406−3412.

(82) Yu, H.; Canoura, J.; Guntupalli, B.; Lou, X.; Xiao, Y. A Cooperative-Binding Split Aptamer Assay for Rapid, Specific and Ultra-Sensitive Fluorescence Detection of Cocaine in Saliva. *Chem. Sci.* **2017**, *8*, 131−141.

(83) Qi, X.; Zhao, Y.; Su, H.; Wang, L.; Li, L.; Ma, R.; Yan, X.; Sun, J.; Wang, S.; Mao, X. A Label-Free Colorimetric Aptasensor Based on Split Aptamers-Chitosan Oligosaccharide-AuNPs Nanocomposites for

Sensitive and Selective Detection of Kanamycin. *Talanta* **2022**, *238*, 123032.

(84) Wang, Y.; Zhu, F.; Yin, L.; Qu, G.; Ma, D.-L.; Leung, C.-H.; Lu, L. Ratiometric Fluorescent Detection of Pesticide Based on Split Aptamer and Magnetic Separation. *Sensors Actuators B: Chem.* **2022**, *367*, 132045.

(85) Li, S.; Zheng, Y.; Liu, Y.; Geng, X.; Liu, X.; Zou, L.; Wang, Q.; Yang, X.; Wang, K. Investigation of the Interaction between Split Aptamer and Vascular Endothelial Growth Factor 165 Using Single Molecule Force Spectroscopy. *J. Mol. Recognit.* **2020**, *33*, No. e2829.

(86) Tang, J.; Shi, H.; He, X.; Lei, Y.; Guo, Q.; Wang, K.; Yan, L.; He, D. Tumor Cell-Specific Split Aptamers: Target-Driven and Temperature-Controlled Self-Assembly on the Living Cell Surface. *Chem. Commun.* **2016**, *52*, 1482−1485.

(87) Li, S.; Zheng, Y.; Zou, Q.; Liao, G.; Liu, X.; Zou, L.; Yang, X.; Wang, Q.; Wang, K. Engineering and Application of a Myoglobin Binding Split Aptamer. *Anal. Chem.* **2020**, *92*, 14576−14581.

(88) Naseri, M.; Halder, A.; Mohammadniaei, M.; Prado, M.; Ashley, J.; Sun, Y. A Multivalent Aptamer-Based Electrochemical Biosensor for Biomarker Detection in Urinary Tract Infection. *Electrochim. Acta* **2021**, *389*, 138644.

(89) Shiang, Y. C.; Hsu, C. L.; Huang, C. C.; Chang, H. T. Gold Nanoparticles Presenting Hybridized Self-Assembled Aptamers That Exhibit Enhanced Inhibition of Thrombin. *Angew. Chem., Int. Ed.* **2011**, *50*, 7660−7665.

(90) Zhang, Z.; Pandey, R.; Li, J.; Gu, J.; White, D.; Stacey, H. D.; Ang, J. C.; Steinberg, C. J.; Capretta, A.; Filipe, C. D. M.; et al. High-Affinity Dimeric Aptamers Enable the Rapid Electrochemical Detection of Wild-Type and B.1.1.7 SARS-CoV-2 in Unprocessed Saliva. *Angew. Chem., Int. Ed.* **2021**, *60*, 24266−24274.

(91) Riccardi, C.; Napolitano, E.; Musumeci, D.; Montesarchio, D. Dimeric and Multimeric DNA Aptamers for Highly Effective Protein Recognition. *Molecules* **2020**, *25*, 5227.

(92) Wang, D. X.; Wang, J.; Wang, Y. X.; Du, Y. C.; Huang, Y.; Tang, A. N.; Cui, Y. X.; Kong, D. M. DNA Nanostructure-Based Nucleic Acid Probes: Construction and Biological Applications. *Chem. Sci.* **2021**, *12*, 7602−7622.

(93) Song, Y.; Song, J.; Wei, X.; Huang, M.; Sun, M.; Zhu, L.; Lin, B.; Shen, H.; Zhu, Z.; Yang, C. Discovery of Aptamers Targeting the Receptor-Binding Domain of the SARS-CoV-2 Spike Glycoprotein. *Anal. Chem.* **2020**, *92*, 9895−9900.

(94) Zhou, Y.; Qi, X.; Liu, Y.; Zhang, F.; Yan, H. DNA-Nanoscaffold-Assisted Selection of Femtomolar Bivalent Human Alpha-Thrombin Aptamers with Potent Anticoagulant Activity. *ChemBioChem.* **2019**, *20*, 2494−2503.

(95) O'Donoghue, M. B.; Shi, X.; Fang, X.; Tan, W. Single-Molecule Atomic Force Microscopy on Live Cells Compares Aptamer and Antibody Rupture Forces. *Anal. Bioanal. Chem.* **2012**, *402*, 3205−3209.

(96) Bruno, J. G. Predicting the Uncertain Future of Aptamer-Based Diagnostics and Therapeutics. *Molecules* **2015**, *20*, 6866−6887.

(97) Chen, Z.; Luo, H.; Gubu, A.; Yu, S.; Zhang, H.; Dai, H.; Zhang, Y.; Zhang, B.; Ma, Y.; Lu, A.; et al. Chemically Modified Aptamers for Improving Binding Affinity to the Target Proteins via Enhanced Non-Covalent Bonding. *Front. Cell Dev. Biol.* **2023**, *11*, 1091809.

(98) Elskens, J. P.; Elskens, J. M.; Madder, A. Chemical Modification of Aptamers for Increased Binding Affinity in Diagnostic Applications: Current Status and Future Prospects. *Int. J. Mol. Sci.* **2020**, *21*, 4522.

(99) Imaizumi, Y.; Kasahara, Y.; Fujita, H.; Kitadume, S.; Ozaki, H.; Endoh, T.; Kuwahara, M.; Sugimoto, N. Efficacy of Base-Modification on Target Binding of Small Molecule DNA Aptamers. *J. Am. Chem. Soc.* **2013**, *135*, 9412−9419.

(100) Wu, D.; Gordon, C. K. L.; Shin, J. H.; Eisenstein, M.; Soh, H. T. Directed Evolution of Aptamer Discovery Technologies. *Acc. Chem. Res.* **2022**, *55*, 685−695.

(101) Lipi, F.; Chen, S.; Chakravarthy, M.; Rakesh, S.; Veedu, R. N. In Vitro Evolution of Chemically-Modified Nucleic Acid Aptamers: Pros and Cons, and Comprehensive Selection Strategies. *RNA Biol.* **2016**, *13*, 1232−1245.

(102) Vaught, J. D.; Bock, C.; Carter, J.; Fitzwater, T.; Otis, M.; Schneider, D.; Rolando, J.; Waugh, S.; Wilcox, S. K.; Eaton, B. E. Expanding the Chemistry of DNA for in Vitro Selection. *J. Am. Chem. Soc.* **2010**, *132*, 4141−4151.

(103) Tang, X.; Feng, C.; Pan, Q.; Sun, F.; Zhu, X. Engineered Aptamer for the Analysis of Cells. *TrAC, Trends Anal. Chem.* **2021**, *145*, 116456.

(104) Egli, M.; Manoharan, M. Re-Engineering RNA Molecules into Therapeutic Agents. *Acc. Chem. Res.* **2019**, *52*, 1036−1047.

(105) Eremeeva, E.; Fikatas, A.; Margamuljana, L.; Abramov, M.; Schols, D.; Groaz, E.; Herdewijn, P. Highly Stable Hexitol Based XNA Aptamers Targeting the Vascular Endothelial Growth Factor. *Nucleic Acids Res.* **2019**, *47*, 4927−4939.

(106) Thirunavukarasu, D.; Chen, T.; Liu, Z.; Hongdilokkul, N.; Romesberg, F. E. Selection of 2'-Fluoro-Modified Aptamers with Optimized Properties. *J. Am. Chem. Soc.* **2017**, *139*, 2892−2895.

(107) Das, G.; Harikrishna, S.; Gore, K. R. Influence of Sugar Modifications on the Nucleoside Conformation and Oligonucleotide Stability: A Critical Review. *Chem. Rec.* **2022**, *22*, No. e202200174.

(108) Ochoa, S.; Milam, V. T. Modified Nucleic Acids: Expanding the Capabilities of Functional Oligonucleotides. *Molecules* **2020**, *25*, 4659.

(109) Ruckman, J.; Green, L. S.; Beeson, J.; Waugh, S.; Gillette, W. L.; Henninger, D. D.; Claesson-Welsh, L.; Janjic, N. 2'-Fluoropyrimidine RNA-Based Aptamers to the 165-Amino Acid Form of Vascular Endothelial Growth Factor (VEGF165): Inhibition of Receptor Binding and VEGF-Induced Vascular Permeability through Interactions Requiring the Exon 7-Encoded Domain. *J. Biol. Chem.* **1998**, *273*, 20556−20567.

(110) Pagratis, N. C.; Bell, C.; Chang, Y. F.; Jennings, S.; Fitzwater, T.; Jellinek, D.; Dang, C. Potent 2'-Amino-, and 2'-Fluoro-2'-Deoxyribonucleotide RNA Inhibitors of Keratinocyte Growth Factor. *Nat. Biotechnol.* **1997**, *15*, 68−73.

(111) Abeydeera, N. D.; Egli, M.; Cox, N.; Mercier, K.; Conde, J. N.; Pallan, P. S.; Mizurini, D. M.; Sierant, M.; Hibti, F.-E.; Hassell, T.; et al. Evoking Picomolar Binding in RNA by a Single Phosphorodithioate Linkage. *Nucleic Acids Res.* **2016**, *44*, 8052−8064.

(112) Gao, S.; Zheng, X.; Jiao, B.; Wang, L. Post-SELEX Optimization of Aptamers. *Anal. Bioanal. Chem.* **2016**, *408*, 4567−4573.

(113) Gawande, B. N.; Rohloff, J. C.; Carter, J. D.; von Carlowitz, I.; Zhang, C.; Schneider, D. J.; Janjic, N. Selection of DNA Aptamers with Two Modified Bases. *Proc. Natl. Acad. Sci. U. S. A.* **2017**, *114*, 2898−2903.

(114) Dolot, R.; Lam, C. H.; Sierant, M.; Zhao, Q.; Liu, F. W.; Nawrot, B.; Egli, M.; Yang, X. Crystal Structures of Thrombin in Complex with Chemically Modified Thrombin DNA Aptamers Reveal the Origins of Enhanced Affinity. *Nucleic Acids Res.* **2018**, *46*, 4819−4830.

(115) Yoshikawa, A. M.; Rangel, A.; Feagin, T.; Chun, E. M.; Wan, L.; Li, A.; Moeckl, L.; Wu, D.; Eisenstein, M.; Pitteri, S.; et al. Discovery of Indole-Modified Aptamers for Highly Specific Recognition of Protein Glycoforms. *Nat. Commun.* **2021**, *12*, 7106.

(116) Zhang, L.; Yang, Z.; Sefah, K.; Bradley, K. M.; Hoshika, S.; Kim, M. J.; Kim, H. J.; Zhu, G.; Jimenez, E.; Cansiz, S.; et al. Evolution of Functional Six-Nucleotide DNA. *J. Am. Chem. Soc.* **2015**, *137*, 6734−6737.

(117) Chawla, M.; Credendino, R.; Chermak, E.; Oliva, R.; Cavallo, L. Theoretical Characterization of the H-Bonding and Stacking Potential of Two Nonstandard Nucleobases Expanding the Genetic Alphabet. *J. Phys. Chem. B* **2016**, *120*, 2216−2224.

(118) Georgiadis, M. M.; Singh, I.; Kellett, W. F.; Hoshika, S.; Benner, S. A.; Richards, N. G. Structural Basis for a Six Nucleotide Genetic Alphabet. *J. Am. Chem. Soc.* **2015**, *137*, 6947−6955.

(119) Tan, J.; Zhao, M.; Wang, J.; Li, Z.; Liang, L.; Zhang, L.; Yuan, Q.; Tan, W. Regulation of Protein Activity and Cellular Functions Mediated by Molecularly Evolved Nucleic Acids. *Angew. Chem., Int. Ed.* **2019**, *58*, 1621−1625.

(120) Byun, J. Recent Progress and Opportunities for Nucleic Acid Aptamers. *Life* **2021**, *11*, 193.

(121) Zhao, L.; Qi, X.; Yan, X.; Huang, Y.; Liang, X.; Zhang, L.; Wang, S.; Tan, W. Engineering Aptamer with Enhanced Affinity by Triple Helix-Based Terminal Fixation. *J. Am. Chem. Soc.* **2019**, *141*, 17493−17497.

(122) Roloff, A.; Carlini, A. S.; Callmann, C. E.; Gianneschi, N. C. Micellar Thrombin-Binding Aptamers: Reversible Nanoscale Anticoagulants. *J. Am. Chem. Soc.* **2017**, *139*, 16442−16445.

(123) Lin, C.; Liu, Y.; Rinker, S.; Yan, H. DNA Tile Based Self-Assembly: Building Complex Nanoarchitectures. *ChemPhysChem* **2006**, *7*, 1641−1647.

(124) Meng, H.-M.; Liu, H.; Kuai, H.; Peng, R.; Mo, L.; Zhang, X.-B. Aptamer-Integrated DNA Nanostructures for Biosensing, Bioimaging and Cancer Therapy. *Chem. Soc. Rev.* **2016**, *45*, 2583−2602.

(125) Moreira, B. G.; You, Y.; Behlke, M. A.; Owczarzy, R. Effects of Fluorescent Dyes, Quenchers, and Dangling Ends on DNA Duplex Stability. *Biochem. Biophys. Res. Commun.* **2005**, *327*, 473−484.

(126) Cromie, G. A.; Connelly, J. C.; Leach, D. R. Recombination at Double-Strand Breaks and DNA Ends: Conserved Mechanisms from Phage to Humans. *Mol. Cell* **2001**, *8*, 1163−1174.

(127) Aldaye, F. A.; Palmer, A. L.; Sleiman, H. F. Assembling Materials with DNA as the Guide. *Science* **2008**, *321*, 1795−1799.

(128) Lin, C.; Liu, Y.; Yan, H. Designer DNA Nanoarchitectures. *Biochemistry* **2009**, *48*, 1663−1674.

(129) Lin, M.; Zhang, J.; Wan, H.; Yan, C.; Xia, F. Rationally Designed Multivalent Aptamers Targeting Cell Surface for Biomedical Applications. *ACS Appl. Mater. Interfaces* **2021**, *13*, 9369−9389.

(130) Li, Z.; Li, Q.; Wu, Y.; Yuan, K.; Shi, M.; Li, Y.; Meng, H.-M.; Li, Z. Multivalent Self-Assembled Nano String Lights for Tumor-Targeted Delivery and Accelerated Biomarker Imaging in Living Cells and in Vivo. *Analyst* **2022**, *147*, 811−818.

(131) Wang, Z.; Yang, X.; Lee, N. Z.; Cao, X. Multivalent Aptamer Approach: Designs, Strategies, and Applications. *Micromachines* **2022**, *13*, 436.

(132) Xu, Z.; Shi, T.; Mo, F.; Yu, W.; Shen, Y.; Jiang, Q.; Wang, F.; Liu, X. Programmable Assembly of Multivalent DNA-Protein Superstructures for Tumor Imaging and Targeted Therapy. *Angew. Chem., Int. Ed.* **2022**, *61*, No. e202211505.

(133) Xue, C.; Zhang, S.; Yu, X.; Hu, S.; Lu, Y.; Wu, Z. S. Periodically Ordered, Nuclease-Resistant DNA Nanowires Decorated with Cell-Specific Aptamers as Selective Theranostic Agents. *Angew. Chem., Int. Ed.* **2020**, *59*, 17540−17547.

(134) Li, W.; Yang, X.; He, L.; Wang, K.; Wang, Q.; Huang, J.; Liu, J.; Wu, B.; Xu, C. Self-Assembled DNA Nanocentipede as Multivalent Drug Carrier for Targeted Delivery. *ACS Appl. Mater. Interfaces* **2016**, *8*, 25733−25740.

(135) Wang, Z.; Lv, J.; Huang, H.; Xu, H.; Zhang, J.; Xue, C.; Zhang, S.; Wu, Z.-S. Structure-Switchable Aptamer-Arranged Reconfigurable DNA Nanonetworks for Targeted Cancer Therapy. *Nanomed. Nanotechnol. Biol. Med.* **2022**, *43*, 102553.

(136) Lv, Y.; Hu, R.; Zhu, G.; Zhang, X.; Mei, L.; Liu, Q.; Qiu, L.; Wu, C.; Tan, W. Preparation and Biomedical Applications of Programmable and Multifunctional DNA Nanoflowers. *Nat. Protoc.* **2015**, *10*, 1508−1524.

(137) Mahmoudpour, M.; Ding, S.; Lyu, Z.; Ebrahimi, G.; Du, D.; Ezzati Nazhad Dolatabadi, J.; Torbati, M.; Lin, Y. Aptamer Functionalized Nanomaterials for Biomedical Applications: Recent Advances and New Horizons. *Nano Today* **2021**, *39*, 101177.

(138) Song, W.; Hu, J. J.; Song, S. J.; Xu, Y.; Yang, H.; Yang, F.; Zhou, Y.; Yu, T.; Qiu, W. X. Aptamer-Gold Nanocage Composite for Photoactivated Immunotherapy. *ACS Appl. Mater. Interfaces* **2022**, *14*, 42931−42939.

(139) Sun, Y.; Hou, Y.; Cao, T.; Luo, C.; Wei, Q. A Chemiluminescence Sensor for the Detection of Alpha-Fetoprotein and Carcinoembryonic Antigen Based on Dual-Aptamer Functionalized Magnetic Silicon Composite. *Anal. Chem.* **2023**, *95*, 7387−7395.

(140) Zhang, Y.; Li, N.; Xu, Y.; Lu, P.; Qi, N.; Yang, M.; Hou, C.; Huo, D. An Ultrasensitive Dual-Signal Aptasensor Based on Functionalized Sb@ZIF-67 Nanocomposites for Simultaneously Detect Multiple Biomarkers. *Biosens. Bioelectron.* **2022**, *214*, 114508.

(141) Pei, Z.; Lei, H.; Cheng, L. Bioactive Inorganic Nanomaterials for Cancer Theranostics. *Chem. Soc. Rev.* **2023**, *52*, 2031−2081.

(142) Tan, X.; Sun, X.; Li, Y.; Zeng, Y.; Gong, J.; Wang, Z.; An, Y.; Li, H. Biomineralized $Mn_3(PO_4)_2$/Aptamer Nanosheets for Enhanced Electrochemical Determination of C-Reactive Protein. *Sensors Actuators B: Chem.* **2021**, *333*, 129510.

(143) Ye, R.; Chen, H.; Li, H. Biomimetic Synthesis of Protein-DNA-CaHPO₄ Hybrid Nanosheets for Biosensing: Detection of Thrombin as an Example. *Anal. Chim. Acta* **2022**, *1225*, 340227.

(144) Aravind, A.; Veeranarayanan, S.; Poulose, A. C.; Nair, R.; Nagaoka, Y.; Yoshida, Y.; Maekawa, T.; Kumar, D. S. Aptamer-Functionalized Silica Nanoparticles for Targeted Cancer Therapy. *BioNanoSci.* **2012**, *2*, 1−8.

(145) Chen, T.; Shukoor, M. I.; Chen, Y.; Yuan, Q.; Zhu, Z.; Zhao, Z.; Gulbakan, B.; Tan, W. Aptamer-Conjugated Nanomaterials for Bioanalysis and Biotechnology Applications. *Nanoscale* **2011**, *3*, 546−556.

(146) Oroval, M.; Coll, C.; Bernardos, A.; Marcos, M. D.; Martinez-Manez, R.; Shchukin, D. G.; Sancenon, F. Selective Fluorogenic Sensing of As(III) Using Aptamer-Capped Nanomaterials. *ACS Appl. Mater. Interfaces* **2017**, *9*, 11332−11336.

(147) Xia, F.; He, A.; Zhao, H.; Sun, Y.; Duan, Q.; Abbas, S. J.; Liu, J.; Xiao, Z.; Tan, W. Molecular Engineering of Aptamer Self-Assemblies Increases in Vivo Stability and Targeted Recognition. *ACS Nano* **2022**, *16*, 169−179.

(148) Chen, X.; Lisi, F.; Bakthavathsalam, P.; Longatte, G.; Hoque, S.; Tilley, R. D.; Gooding, J. J. Impact of the Coverage of Aptamers on a Nanoparticle on the Binding Equilibrium and Kinetics between Aptamer and Protein. *ACS Sens.* **2021**, *6*, 538−545.

(149) Sun, M.; Liu, S.; Song, T.; Chen, F.; Zhang, J.; Huang, J. A.; Wan, S.; Lu, Y.; Chen, H.; Tan, W.; et al. Spherical Neutralizing Aptamer Inhibits SARS-CoV-2 Infection and Suppresses Mutational Escape. *J. Am. Chem. Soc.* **2021**, *143*, 21541−21548.

(150) Khan, M. A.; Singh, D.; Ahmad, A.; Siddique, H. R. Revisiting Inorganic Nanoparticles as Promising Therapeutic Agents: A Paradigm Shift in Oncological Theranostics. *Eur. J. Pharm. Sci.* **2021**, *164*, 105892.

(151) Wang, Y.; Li, D.; Ren, W.; Liu, Z.; Dong, S.; Wang, E. Ultrasensitive Colorimetric Detection of Protein by Aptamer-Au Nanoparticles Conjugates Based on a Dot-Blot Assay. *Chem. Commun.* **2008**, *22*, 2520−2522.

(152) Chen, W. H.; Yang Sung, S.; Fadeev, M.; Cecconello, A.; Nechushtai, R.; Willner, I. Targeted VEGF-Triggered Release of an Anti-Cancer Drug from Aptamer-Functionalized Metal-Organic Framework Nanoparticles. *Nanoscale* **2018**, *10*, 4650−4657.

(153) Chen, W.-H.; Yu, X.; Liao, W.-C.; Sohn, Y. S.; Cecconello, A.; Kozell, A.; Nechushtai, R.; Willner, I. ATP-Responsive Aptamer-Based Metal-Organic Framework Nanoparticles (NMOFs) for the Controlled Release of Loads and Drugs. *Adv. Funct. Mater.* **2017**, *27*, 1702102.

(154) Liu, Q.; Jin, C.; Wang, Y.; Fang, X.; Zhang, X.; Chen, Z.; Tan, W. Aptamer-Conjugated Nanomaterials for Specific Cancer Cell Recognition and Targeted Cancer Therapy. *NPG Asia Mater.* **2014**, *6*, No. e95.

(155) Plourde, K.; Derbali, R. M.; Desrosiers, A.; Dubath, C.; Vallee-Belisle, A.; Leblond, J. Aptamer-Based Liposomes Improve Specific Drug Loading and Release. *J. Controlled Release* **2017**, *251*, 82−91.

(156) Abri Aghdam, M.; Bagheri, R.; Mosafer, J.; Baradaran, B.; Hashemzaei, M.; Baghbanzadeh, A.; de la Guardia, M.; Mokhtarzadeh, A. Recent Advances on Thermosensitive and pH-Sensitive Liposomes Employed in Controlled Release. *J. Controlled Release* **2019**, *315*, 1−22.

(157) Lukowski, J. K.; Weaver, E. M.; Hummon, A. B. Analyzing Liposomal Drug Delivery Systems in Three-Dimensional Cell Culture

Models Using Maldi Imaging Mass Spectrometry. *Anal. Chem.* **2017**, *89*, 8453−8458.

(158) Yin, W.; Chen, J.; Yang, H.; Zhang, Y.; Dai, Z.; Zou, X. Sensitive and Sustained Imaging of Intracellular Microrna in Living Cells by a High Biocompatible Liposomal Vehicle Introduced Isothermal Symmetric Exponential Amplification Reaction. *Chem. Commun.* **2019**, *55*, 11251−11254.

(159) Alshaer, W.; Hillaireau, H.; Vergnaud, J.; Ismail, S.; Fattal, E. Functionalizing Liposomes with Anti-CD44 Aptamer for Selective Targeting of Cancer Cells. *Bioconjugate Chem.* **2015**, *26*, 1307−1313.

(160) Farokhzad, O. C.; Jon, S.; Khademhosseini, A.; Tran, T. N.; Lavan, D. A.; Langer, R. Nanoparticle-Aptamer Bioconjugates: A New Approach for Targeting Prostate Cancer Cells. *Cancer Res.* **2004**, *64*, 7668−7672.

(161) Gunaratne, R.; Kumar, S.; Frederiksen, J. W.; Stayrook, S.; Lohrmann, J. L.; Perry, K.; Bompiani, K. M.; Chabata, C. V.; Thalji, N. K.; Ho, M. D.; et al. Combination of Aptamer and Drug for Reversible Anticoagulation in Cardiopulmonary Bypass. *Nat. Biotechnol.* **2018**, *36*, 606−613.

(162) Wang, D.; Li, Y.; Deng, X.; Torre, M.; Zhang, Z.; Li, X.; Zhang, W.; Cullion, K.; Kohane, D. S.; Weldon, C. B. An Aptamer-Based Depot System for Sustained Release of Small Molecule Therapeutics. *Nat. Commun.* **2023**, *14*, 2444.

(163) Zhou, F.; Wang, P.; Peng, Y.; Zhang, P.; Huang, Q.; Sun, W.; He, N.; Fu, T.; Zhao, Z.; Fang, X.; et al. Molecular Engineering-Based Aptamer-Drug Conjugates with Accurate Tunability of Drug Ratios for Drug Combination Targeted Cancer Therapy. *Angew. Chem., Int. Ed.* **2019**, *58*, 11661−11665.

(164) Holguín, A. R.; Delgado, D. R.; Martínez, F.; Marcus, Y. Solution Thermodynamics and Preferential Solvation of Meloxicam in Propylene Glycol + Water Mixtures. *J. Solution Chem.* **2011**, *40*, 1987−1999.

(165) Bergstrom, C. A.; Strafford, M.; Lazorova, L.; Avdeef, A.; Luthman, K.; Artursson, P. Absorption Classification of Oral Drugs Based on Molecular Surface Properties. *J. Med. Chem.* **2003**, *46*, 558−570.

(166) Shoghi, E.; Mirahmadi-Zare, S. Z.; Ghasemi, R.; Asghari, M.; Poorebrahim, M.; Nasr-Esfahani, M. H. Nanosized Aptameric Cavities Imprinted on the Surface of Magnetic Nanoparticles for High-Throughput Protein Recognition. *Mikrochim. Acta* **2018**, *185*, 241.

(167) Sullivan, M. V.; Allabush, F.; Bunka, D.; Tolley, A.; Mendes, P. M.; Tucker, J. H. R.; Turner, N. W. Hybrid Aptamer-Molecularly Imprinted Polymer (AptaMIP) Nanoparticles Selective for the Antibiotic Moxifloxacin. *Polym. Chem.* **2021**, *12*, 4394−4405.

(168) Matos, C. O.; Passos, Y. M.; do Amaral, M. J.; Macedo, B.; Tempone, M. H.; Bezerra, O. C. L.; Moraes, M. O.; Almeida, M. S.; Weber, G.; Missailidis, S.; et al. Liquid-Liquid Phase Separation and Fibrillation of the Prion Protein Modulated by a High-Affinity DNA Aptamer. *FASEB J.* **2020**, *34*, 365−385.

(169) Jia, W.; Xie, D.; Li, F.; Wu, X.; Wang, R.; Yang, L.; Liu, L.; Yin, W.; Chang, S. Evaluation the Effect of Nanoparticles on the Structure of Aptamers by Analyzing the Recognition Dynamics of Aptamer Functionalized Nanoparticles. *Anal. Chim. Acta* **2021**, *1183*, 338976.

(170) Ponzo, I.; Moller, F. M.; Daub, H.; Matscheko, N. A DNA-Based Biosensor Assay for the Kinetic Characterization of Ion-Dependent Aptamer Folding and Protein Binding. *Molecules* **2019**, *24*, 2877.

(171) Huang, M.; Song, J.; Huang, P.; Chen, X.; Wang, W.; Zhu, Z.; Song, Y.; Yang, C. Molecular Crowding Evolution for Enabling Discovery of Enthalpy-Driven Aptamers for Robust Biomedical Applications. *Anal. Chem.* **2019**, *91*, 10879−10886.

(172) Sakamoto, T.; Ennifar, E.; Nakamura, Y. Thermodynamic Study of Aptamers Binding to Their Target Proteins. *Biochimie* **2018**, *145*, 91−97.

(173) Englund, D.; Faraon, A.; Fushman, I.; Stoltz, N.; Petroff, P.; Vuckovic, J. Controlling Cavity Reflectivity with a Single Quantum Dot. *Nature* **2007**, *450*, 857−861.

(174) Lermé, J.; Bonnet, C.; Broyer, M.; Cottancin, E.; Manchon, D.; Pellarin, M. Optical Properties of a Particle above a Dielectric

Interface: Cross Sections, Benchmark Calculations, and Analysis of the Intrinsic Substrate Effects. *J. Phys. Chem. C* **2013**, *117*, 6383−6398.

(175) Kacherovsky, N.; Yang, L. F.; Dang, H. V.; Cheng, E. L.; Cardle, I. I.; Walls, A. C.; McCallum, M.; Sellers, D. L.; DiMaio, F.; Salipante, S. J.; et al. Discovery and Characterization of Spike N-Terminal Domain-Binding Aptamers for Rapid SARS-CoV-2 Detection. *Angew. Chem., Int. Ed.* **2021**, *60*, 21211−21215.

(176) Li, G.; Zeng, J.; Liu, H.; Ding, P.; Liang, J.; Nie, X.; Zhou, Z. A Fluorometric Aptamer Nanoprobe for Alpha-Fetoprotein by Exploiting the FRET between 5-Carboxyfluorescein and Palladium Nanoparticles. *Mikrochim. Acta* **2019**, *186*, 314.

(177) Liu, X.; Li, H.; Jia, W.; Chen, Z.; Xu, D. Selection of Aptamers Based on a Protein Microarray Integrated with a Microfluidic Chip. *Lab Chip* **2017**, *17*, 178−185.

(178) Olmsted, I. R.; Xiao, Y.; Cho, M.; Csordas, A. T.; Sheehan, J. H.; Meiler, J.; Soh, H. T.; Bornhop, D. J. Measurement of Aptamer-Protein Interactions with Back-Scattering Interferometry. *Anal. Chem.* **2011**, *83*, 8867−8870.

(179) Wu, B.; Jiang, R.; Wang, Q.; Huang, J.; Yang, X.; Wang, K.; Li, W.; Chen, N.; Li, Q. Detection of C-Reactive Protein Using Nanoparticle-Enhanced Surface Plasmon Resonance Using an Aptamer-Antibody Sandwich Assay. *Chem. Commun.* **2016**, *52*, 3568−3571.

(180) Ochsenkuhn, M. A.; Campbell, C. J. Probing Biomolecular Interactions Using Surface Enhanced Raman Spectroscopy: Label-Free Protein Detection Using a G-Quadruplex DNA Aptamer. *Chem. Commun.* **2010**, *46*, 2799−2801.

(181) Koyun, S.; Akgonullu, S.; Yavuz, H.; Erdem, A.; Denizli, A. Surface Plasmon Resonance Aptasensor for Detection of Human Activated Protein C. *Talanta* **2019**, *194*, 528−533.

(182) Perez-Ruiz, E.; Kemper, M.; Spasic, D.; Gils, A.; van Ijzendoorn, L. J.; Lammertyn, J.; Prins, M. W. Probing the Force-Induced Dissociation of Aptamer-Protein Complexes. *Anal. Chem.* **2014**, *86*, 3084−3091.

(183) Sun, D.; Wu, Y.; Chang, S. J.; Chen, C. J.; Liu, J. T. Investigation of the Recognition Interaction between Glycated Hemoglobin and Its Aptamer by Using Surface Plasmon Resonance. *Talanta* **2021**, *222*, 121466.

(184) Wang, S.; Dong, Y.; Liang, X. Development of a SPR Aptasensor Containing Oriented Aptamer for Direct Capture and Detection of Tetracycline in Multiple Honey Samples. *Biosens. Bioelectron.* **2018**, *109*, 1−7.

(185) Kim, S.; Lee, H. J. Gold Nanostar Enhanced Surface Plasmon Resonance Detection of an Antibiotic at Attomolar Concentrations via an Aptamer-Antibody Sandwich Assay. *Anal. Chem.* **2017**, *89*, 6624−6630.

(186) Zhou, W.; Jimmy Huang, P.-J.; Ding, J.; Liu, J. Aptamer-Based Biosensors for Biomedical Diagnostics. *Analyst* **2014**, *139*, 2627−2640.

(187) Jing, M.; Bowser, M. T. Methods for Measuring Aptamer-Protein Equilibria: A Review. *Anal. Chim. Acta* **2011**, *686*, 9−18.

(188) Yu, H.; Alkhamis, O.; Canoura, J.; Liu, Y.; Xiao, Y. Advances and Challenges in Small-Molecule DNA Aptamer Isolation, Characterization, and Sensor Development. *Angew. Chem., Int. Ed.* **2021**, *60*, 16800−16823.

(189) Gijs, M.; Penner, G.; Blackler, G. B.; Impens, N. R.; Baatout, S.; Luxen, A.; Aerts, A. M. Improved Aptamers for the Diagnosis and Potential Treatment of HER2-Positive Cancer. *Pharmaceuticals* **2016**, *9*, 29.

(190) Li, Y.; Lee, H. J.; Corn, R. M. Fabrication and Characterization of RNA Aptamer Microarrays for the Study of Protein-Aptamer Interactions with SPR Imaging. *Nucleic Acids Res.* **2006**, *34*, 6416−6424.

(191) Radhakrishnan, R.; Poltronieri, P. Fluorescence-Free Biosensor Methods in Detection of Food Pathogens with a Special Focus on Listeria Monocytogenes. *Biosensors* **2017**, *7*, 63.

(192) Chao, J.; Cao, W.; Su, S.; Weng, L.; Song, S.; Fan, C.; Wang, L. Nanostructure-Based Surface-Enhanced Raman Scattering Bio-

sensors for Nucleic Acids and Proteins. *J. Mater. Chem. B* **2016**, *4*, 1757−1769.

(193) He, J.; Li, G.; Hu, Y. Aptamer Recognition Induced Target-Bridged Strategy for Proteins Detection Based on Magnetic Chitosan and Silver/Chitosan Nanoparticles Using Surface-Enhanced Raman Spectroscopy. *Anal. Chem.* **2015**, *87*, 11039−11047.

(194) Zong, C.; Xu, M.; Xu, L. J.; Wei, T.; Ma, X.; Zheng, X. S.; Hu, R.; Ren, B. Surface-Enhanced Raman Spectroscopy for Bioanalysis: Reliability and Challenges. *Chem. Rev.* **2018**, *118*, 4946−4980.

(195) Taleat, Z.; Cristea, C.; Marrazza, G.; Mazloum-Ardakani, M.; Săndulescu, R. Electrochemical Immunoassay Based on Aptamer-Protein Interaction and Functionalized Polymer for Cancer Biomarker Detection. *J. Electroanal. Chem.* **2014**, *717−718*, 119−124.

(196) Muhammad, M.; Shao, C.-s.; Huang, Q. Aptamer-Functionalized Au Nanoparticles Array as the Effective SERS Biosensor for Label-Free Detection of Interleukin-6 in Serum. *Sensors Actuators B: Chem.* **2021**, *334*, 129607.

(197) Picault, L.; Laigre, E.; Gillon, E.; Tiertant, C.; Renaudet, O.; Imberty, A.; Goyard, D.; Dejeu, J. Characterization of the Interaction of Multivalent Glycosylated Ligands with Bacterial Lectins by Biolayer Interferometry. *Glycobiology* **2022**, *32*, 886−896.

(198) Murali, S.; Rustandi, R. R.; Zheng, X.; Payne, A.; Shang, L. Applications of Surface Plasmon Resonance and Biolayer Interferometry for Virus-Ligand Binding. *Viruses* **2022**, *14*, 717.

(199) Li, W.; Xu, S.; Li, Y.; Chen, J.; Ma, Y.; Liu, Z. High Mannose-Specific Aptamers for Broad-Spectrum Virus Inhibition and Cancer Targeting. *CCS Chem.* **2023**, *5*, 497−509.

(200) Liu, R.; Zhang, F.; Sang, Y.; Liu, M.; Shi, M.; Wang, X. Selection and Characterization of DNA Aptamers for Constructing Aptamer-AuNPs Colorimetric Method for Detection of AFM1. *Foods* **2022**, *11*, 1802.

(201) Zhang, H.; Li, W.; Luo, H.; Xiong, G.; Yu, Y. Quantitative Determination of Testosterone Levels with Biolayer Interferometry. *Chem. Biol. Interact.* **2017**, *276*, 141−148.

(202) Zhao, L.; Huang, Y.; Dong, Y.; Han, X.; Wang, S.; Liang, X. Aptamers and Aptasensors for Highly Specific Recognition and Sensitive Detection of Marine Biotoxins: Recent Advances and Perspectives. *Toxins (Basel)* **2018**, *10*, 427.

(203) Sharafeldin, M.; Davis, J. J. Characterising the Biosensing Interface. *Anal. Chim. Acta* **2022**, *1216*, 339759.

(204) Chen, J.; Liu, J.; Chen, X.; Qiu, H. Recent Progress in Nanomaterial-Enhanced Fluorescence Polarization/Anisotropy Sensors. *Chin. Chem. Lett.* **2019**, *30*, 1575−1580.

(205) Minagawa, H.; Shimizu, A.; Kataoka, Y.; Kuwahara, M.; Kato, S.; Horii, K.; Shiratori, I.; Waga, I. Fluorescence Polarization-Based Rapid Detection System for Salivary Biomarkers Using Modified DNA Aptamers Containing Base-Appended Bases. *Anal. Chem.* **2020**, *92*, 1780−1787.

(206) Zhang, D.; Lu, M.; Wang, H. Fluorescence Anisotropy Analysis for Mapping Aptamer-Protein Interaction at the Single Nucleotide Level. *J. Am. Chem. Soc.* **2011**, *133*, 9188−9191.

(207) Zhao, Q.; Bai, Y.; Wang, H. Directing a Rational Design of Aptamer-Based Fluorescence Anisotropy Assay for Sensitive Detection of Immunoglobulin E by Site-Specific Binding Study. *Talanta* **2020**, *217*, 121018.

(208) Funck, T.; Liedl, T.; Bae, W. Dual Aptamer-Functionalized 3D Plasmonic Metamolecule for Thrombin Sensing. *Appl. Sci.* **2019**, *9*, 3006.

(209) Das, P.; Krull, U. J. Detection of a Cancer Biomarker Protein on Modified Cellulose Paper by Fluorescence Using Aptamer-Linked Quantum Dots. *Analyst* **2017**, *142*, 3132−3135.

(210) Zhao, T.; Li, T.; Liu, Y. Silver Nanoparticle Plasmonic Enhanced Forster Resonance Energy Transfer (FRET) Imaging of Protein-Specific Sialylation on the Cell Surface. *Nanoscale* **2017**, *9*, 9841−9847.

(211) Chi, C. W.; Lao, Y. H.; Li, Y. S.; Chen, L. C. A Quantum Dot-Aptamer Beacon Using a DNA Intercalating Dye as the FRET Reporter: Application to Label-Free Thrombin Detection. *Biosens. Bioelectron.* **2011**, *26*, 3346−3352.

(212) Ueno, T.; Nagano, T. Fluorescent Probes for Sensing and Imaging. *Nat. Methods* **2011**, *8*, 642−645.

(213) Broude, N. E. Stem-Loop Oligonucleotides: A Robust Tool for Molecular Biology and Biotechnology. *Trends Biotechnol.* **2002**, *20*, 249−256.

(214) Mao, S.; Ying, Y.; Wu, X.; Krueger, C. J.; Chen, A. K. CRISPR/Dual-FRET Molecular Beacon for Sensitive Live-Cell Imaging of Non-Repetitive Genomic Loci. *Nucleic Acids Res.* **2019**, *47*, No. e131.

(215) Tyagi, S.; Kramer, F. R. J. N. b. Molecular Beacons: Probes That Fluoresce Upon Hybridization. *Nat. Biotechnol.* **1996**, *14*, 303−308.

(216) Zhang, Z.; Liu, N.; Zhang, Z.; Xu, D.; Ma, S.; Wang, X.; Zhou, T.; Zhang, G.; Wang, F. Construction of Aptamer-Based Molecular Beacons with Varied Blocked Structures and Targeted Detection of Thrombin. *Langmuir* **2021**, *37*, 8738−8745.

(217) Vicens, M. C.; Sen, A.; Vanderlaan, A.; Drake, T. J.; Tan, W. Investigation of Molecular Beacon Aptamer-Based Bioassay for Platelet-Derived Growth Factor Detection. *ChemBioChem.* **2005**, *6*, 900−907.

(218) Yamamoto, R.; Kumar, P. K. R. Molecular Beacon Aptamer Fluoresces in the Presence of Tat Protein of HIV-1. *Genes Cells* **2000**, *5*, 389−396.

(219) Mahani, M.; Faghihi-Fard, M.; Divsar, F.; Torkzadeh-Mahani, M.; Khakbaz, F. Ultrasensitive FRET-Based Aptasensor for Interleukin-6 as a Biomarker for COVID-19 Progression Using Nitrogen-Doped Carbon Quantum Dots and Gold Nanoparticles. *Mikrochim. Acta* **2022**, *189*, 472.

(220) Ghosh, S.; Datta, D.; Cheema, M.; Dutta, M.; Stroscio, M. A. Aptasensor Based Optical Detection of Glycated Albumin for Diabetes Mellitus Diagnosis. *Nanotechnology* **2017**, *28*, 435505.

(221) Gao, X.; Jiang, T.; Qin, W. Potentiometric Aptasensing of Escherichia Coli Based on Electrogenerated Chemiluminescence as a Highly Sensitive Readout. *Biosens. Bioelectron.* **2022**, *200*, 113923.

(222) Gao, X.; Qi, L.; Liu, K.; Meng, C.; Li, Y.; Yu, H. Z. Exonuclease I-Assisted General Strategy to Convert Aptamer-Based Electrochemical Biosensors from ″Signal-Off″ to ″Signal-On″. *Anal. Chem.* **2020**, *92*, 6229−6234.

(223) Tang, X.; Lu, C.; Xu, X.; Ding, Z.; Li, H.; Zhang, H.; Wang, Y.; Li, C. A Visible and Near-Infrared Light Dual Responsive ″Signal-Off″ and ″Signal-On″ Photoelectrochemical Aptasensor for Prostate-Specific Antigen. *Biosens. Bioelectron.* **2022**, *202*, 113905.

(224) Eissa, S.; Siddiqua, A.; Chinnappan, R.; Zourob, M. Electrochemical Selection of a DNA Aptamer, and an Impedimetric Method for Determination of the Dedicator of Cytokinesis 8 by Self-Assembly of a Thiolated Aptamer on a Gold Electrode. *Mikrochim. Acta* **2019**, *186*, 828.

(225) Li, J.; Wang, J.; Guo, X.; Zheng, Q.; Peng, J.; Tang, H.; Yao, S. Carbon Nanotubes Labeled with Aptamer and Horseradish Peroxidase as a Probe for Highly Sensitive Protein Biosensing by Postelectropolymerization of Insoluble Precipitates on Electrodes. *Anal. Chem.* **2015**, *87*, 7610−7617.

(226) Chai, H.; Cheng, W.; Xu, L.; Gui, H.; He, J.; Miao, P. Fabrication of Polymeric Ferrocene Nanoparticles for Electrochemical Aptasensing of Protein with Target-Catalyzed Hairpin Assembly. *Anal. Chem.* **2019**, *91*, 9940−9945.

(227) Hwang, M. T.; Park, I.; Heiranian, M.; Taqieddin, A.; You, S.; Faramarzi, V.; Pak, A. A.; van der Zande, A. M.; Aluru, N. R.; Bashir, R. Ultrasensitive Detection of Dopamine, IL-6 and SARS-CoV-2 Proteins on Crumpled Graphene FET Biosensor. *Adv. Mater. Technol.* **2021**, *6*, 2100712.

(228) Fang, S.; Dong, X.; Liu, S.; Penng, D.; He, L.; Wang, M.; Fu, G.; Feng, X.; Zhang, Z. A Label-Free Multi-Functionalized Electrochemical Aptasensor Based on a $Fe_3O_4$@3D-rGO@Plasma-Polymerized (4-Vinyl Pyridine) Nanocomposite for the Sensitive Detection of Proteins in Whole Blood. *Electrochim. Acta* **2016**, *212*, 1−9.

(229) Hosseini Ghalehno, M.; Mirzaei, M.; Torkzadeh-Mahani, M. Electrochemical Aptasensor for Activated Protein C Using a Gold

Nanoparticle - Chitosan/Graphene Paste Modified Carbon Paste Electrode. *Bioelectrochemistry* **2019**, *130*, 107322.

(230) Jo, H.; Her, J.; Lee, H.; Shim, Y. B.; Ban, C. Highly Sensitive Amperometric Detection of Cardiac Troponin I Using Sandwich Aptamers and Screen-Printed Carbon Electrodes. *Talanta* **2017**, *165*, 442−448.

(231) Meirinho, S. G.; Dias, L. G.; Peres, A. M.; Rodrigues, L. R. Voltammetric Aptasensors for Protein Disease Biomarkers Detection: A Review. *Biotechnol. Adv.* **2016**, *34*, 941−953.

(232) Tertiş, M.; Ciui, B.; Suciu, M.; Săndulescu, R.; Cristea, C. Label-Free Electrochemical Aptasensor Based on Gold and Polypyrrole Nanoparticles for Interleukin 6 Detection. *Electrochim. Acta* **2017**, *258*, 1208−1218.

(233) Yang, S.; Zhang, F.; Liang, Q.; Wang, Z. A Three-Dimensional Graphene-Based Ratiometric Signal Amplification Aptasensor for MUC1 Detection. *Biosens. Bioelectron.* **2018**, *120*, 85−92.

(234) Mascini, M. *Aptamers in Bioanalysis*; John Wiley & Sons: New York, 2009.

(235) Rodriguez, M. C.; Rivas, G. A. Label-Free Electrochemical Aptasensor for the Detection of Lysozyme. *Talanta* **2009**, *78*, 212−216.

(236) Wade, J. H.; Bailey, R. C. Applications of Optical Microcavity Resonators in Analytical Chemistry. *Annu. Rev. Anal. Chem.* **2016**, *9*, 1−25.

(237) Hasanzadeh, M.; Shadjou, N.; de la Guardia, M. Aptamer-Based Assay of Biomolecules: Recent Advances in Electro-Analytical Approach. *TrAC, Trends Anal. Chem.* **2017**, *89*, 119−132.

(238) Wang, H.; Sun, J.; Lu, L.; Yang, X.; Xia, J.; Zhang, F.; Wang, Z. Competitive Electrochemical Aptasensor Based on a cDNA-Ferrocene/MXene Probe for Detection of Breast Cancer Marker Mucin1. *Anal. Chim. Acta* **2020**, *1094*, 18−25.

(239) Wang, X.; Dong, P.; Yun, W.; Xu, Y.; He, P.; Fang, Y. A Solid-State Electrochemiluminescence Biosensing Switch for Detection of Thrombin Based on Ferrocene-Labeled Molecular Beacon Aptamer. *Biosens. Bioelectron.* **2009**, *24*, 3288−3292.

(240) Radi, A. E.; Acero Sanchez, J. L.; Baldrich, E.; O'Sullivan, C. K. Reagentless, Reusable, Ultrasensitive Electrochemical Molecular Beacon Aptasensor. *J. Am. Chem. Soc.* **2006**, *128*, 117−124.

(241) Song, S.; Wang, L.; Li, J.; Fan, C.; Zhao, J. Aptamer-Based Biosensors. *TrAC, Trends Anal. Chem.* **2008**, *27*, 108−117.

(242) Jiang, B.; Li, F.; Yang, C.; Xie, J.; Xiang, Y.; Yuan, R. Aptamer Pseudoknot-Functionalized Electronic Sensor for Reagentless and Single-Step Detection of Immunoglobulin E in Human Serum. *Anal. Chem.* **2015**, *87*, 3094−3098.

(243) Liu, Y.; Liu, Y.; Matharu, Z.; Rahimian, A.; Revzin, A. Detecting Multiple Cell-Secreted Cytokines from the Same Aptamer-Functionalized Electrode. *Biosens. Bioelectron.* **2015**, *64*, 43−50.

(244) Wu, Z. S.; Zheng, F.; Shen, G. L.; Yu, R. Q. A Hairpin Aptamer-Based Electrochemical Biosensing Platform for the Sensitive Detection of Proteins. *Biomaterials* **2009**, *30*, 2950−2955.

(245) Li, M.; Guo, X.; Li, H.; Zuo, X.; Hao, R.; Song, H.; Aldalbahi, A.; Ge, Z.; Li, J.; Li, Q.; et al. Epitope Binning Assay Using an Electron Transfer-Modulated Aptamer Sensor. *ACS Appl. Mater. Interfaces* **2018**, *10*, 341−349.

(246) Curti, F.; Fortunati, S.; Knoll, W.; Giannetto, M.; Corradini, R.; Bertucci, A.; Careri, M. A Folding-Based Electrochemical Aptasensor for the Single-Step Detection of the SARS-CoV-2 Spike Protein. *ACS Appl. Mater. Interfaces* **2022**, *14*, 19204−19211.

(247) Idili, A.; Parolo, C.; Alvarez-Diduk, R.; Merkoci, A. Rapid and Efficient Detection of the SARS-CoV-2 Spike Protein Using an Electrochemical Aptamer-Based Sensor. *ACS Sens.* **2021**, *6*, 3093−3101.

(248) Chen, G.; Shen, Y.; Xu, T.; Ban, F.; Yin, L.; Xiao, J.; Shu, Y. Rapid Detection of Acute Myocardial Infarction-Related Mirna Based on a Capture-InterCalation-ElectroCatalysis (3C) Strategy. *Biosens. Bioelectron.* **2016**, *77*, 1020−1025.

(249) Wang, L.; Zhang, G.; Pan, J.; Xiong, C.; Gong, D. Intercalation Binding of Food Antioxidant Butylated Hydroxyanisole

to Calf Thymus DNA. *J. Photochem. Photobiol., B* **2014**, *141*, 253−261.

(250) Bang, G. S.; Cho, S.; Kim, B. G. A Novel Electrochemical Detection Method for Aptamer Biosensors. *Biosens. Bioelectron.* **2005**, *21*, 863−870.

(251) Willner, I.; Zayats, M. Electronic Aptamer-Based Sensors. *Angew. Chem., Int. Ed.* **2007**, *46*, 6408−6418.

(252) Hianik, T.; Wang, J. Electrochemical Aptasensors - Recent Achievements and Perspectives. *Electroanalysis* **2009**, *21*, 1223−1235.

(253) Tabasi, A.; Noorbakhsh, A.; Sharifi, E. Reduced Graphene Oxide-Chitosan-Aptamer Interface as New Platform for Ultrasensitive Detection of Human Epidermal Growth Factor Receptor 2. *Biosens. Bioelectron.* **2017**, *95*, 117−123.

(254) Hianik, T.; Ostatna, V.; Zajacova, Z.; Stoikova, E.; Evtugyn, G. Detection of Aptamer-Protein Interactions Using QCM and Electrochemical Indicator Methods. *Bioorg. Med. Chem. Lett.* **2005**, *15*, 291−295.

(255) Xu, H.; Chen, R.; Sun, Q.; Lai, W.; Su, Q.; Huang, W.; Liu, X. Recent Progress in Metal-Organic Complexes for Optoelectronic Applications. *Chem. Soc. Rev.* **2014**, *43*, 3259−3302.

(256) Lim, Y. C.; Kouzani, A. Z.; Duan, W. Aptasensors: A Review. *J. Biomed. Nanotechnol.* **2010**, *6*, 93−105.

(257) E. Ferapontova, E.; V. Gothelf, K. Recent Advances in Electrochemical Aptamer-Based Sensors. *Curr. Org. Chem.* **2011**, *15*, 498−505.

(258) Cheng, A. K.; Ge, B.; Yu, H. Z. Aptamer-Based Biosensors for Label-Free Voltammetric Detection of Lysozyme. *Anal. Chem.* **2007**, *79*, 5158−5164.

(259) Maehashi, K.; Katsura, T.; Kerman, K.; Takamura, Y.; Matsumoto, K.; Tamiya, E. Label-Free Protein Biosensor Based on Aptamer-Modified Carbon Nanotube Field-Effect Transistors. *Anal. Chem.* **2007**, *79*, 782−787.

(260) Billinge, E. R.; Broom, M.; Platt, M. Monitoring Aptamer-Protein Interactions Using Tunable Resistive Pulse Sensing. *Anal. Chem.* **2014**, *86*, 1030−1037.

(261) Zhang, Y.; Mao, J.; Ji, W.; Feng, T.; Fu, Z.; Zhang, M.; Mao, L. Collision of Aptamer/Pt Nanoparticles Enables Label-Free Amperometric Detection of Protein in Rat Brain. *Anal. Chem.* **2019**, *91*, 5654−5659.

(262) Lim, R. R. X.; Ang, W. L.; Ambrosi, A.; Sofer, Z.; Bonanni, A. Electroactive Nanocarbon Materials as Signaling Tags for Electrochemical PCR. *Talanta* **2022**, *245*, 123479.

(263) Zhang, H.; Ma, L.; Li, P.; Zheng, J. A Novel Electrochemical Immunosensor Based on Nonenzymatic Ag@Au-Fe$_3$O$_4$ Nanoelectrocatalyst for Protein Biomarker Detection. *Biosens. Bioelectron.* **2016**, *85*, 343−350.

(264) Zhang, K.; Kirlikovali, K. O.; Le, Q. V.; Jin, Z.; Varma, R. S.; Jang, H. W.; Farha, O. K.; Shokouhimehr, M. Extended Metal-Organic Frameworks on Diverse Supports as Electrode Nanomaterials for Electrochemical Energy Storage. *ACS Appl. Nano Mater.* **2020**, *3*, 3964−3990.

(265) Zhang, Y.; Lai, B. S.; Juhas, M. Recent Advances in Aptamer Discovery and Applications. *Molecules* **2019**, *24*, 941.

(266) Baldrich, E.; Acero, J. L.; Reekmans, G.; Laureyn, W.; O'Sullivan, C. K. Displacement Enzyme Linked Aptamer Assay. *Anal. Chem.* **2005**, *77*, 4774−4784.

(267) Wang, Y.; Li, Z.; Yu, H. Aptamer-Based Western Blot for Selective Protein Recognition. *Front. Chem.* **2020**, *8*, 570528.

(268) Park, J. H.; Cho, Y. S.; Kang, S.; Lee, E. J.; Lee, G. H.; Hah, S. S. A Colorimetric Sandwich-Type Assay for Sensitive Thrombin Detection Based on Enzyme-Linked Aptamer Assay. *Anal. Biochem.* **2014**, *462*, 10−12.

(269) Hirao, I.; Kimoto, M.; Lee, K. H. DNA Aptamer Generation by ExSELEX Using Genetic Alphabet Expansion with a Mini-Hairpin DNA Stabilization Method. *Biochimie* **2018**, *145*, 15−21.

(270) Zhuang, G.; Katakura, Y.; Omasa, T.; Kishimoto, M.; Suga, K. Measurement of Association Rate Constant of Antibody-Antigen Interaction in Solution Based on Enzyme-Linked Immunosorbent Assay. *J. Biosci. Bioeng.* **2001**, *92*, 330−336.

(271) Drolet, D. W.; Moon-McDermott, L.; Romig, T. S. An Enzyme-Linked Oligonucleotide Assay. *Nat. Biotechnol.* **1996**, *14*, 1021−1025.

(272) Almeida, N. B. F.; Sousa, T.; Santos, V. C. F.; Lacerda, C. M. S.; Silva, T. G.; Grenfell, R. F. Q.; Plentz, F.; Andrade, A. S. R. DNA Aptamer Selection and Construction of an Aptasensor Based on Graphene FETs for Zika Virus NS1 Protein Detection. *Beilstein J. Nanotechnol.* **2022**, *13*, 873−881.

(273) Cavazzana, I.; Fredi, M.; Ceribelli, A.; Mordenti, C.; Ferrari, F.; Carabellese, N.; Tincani, A.; Satoh, M.; Franceschini, F. Testing for Myositis Specific Autoantibodies: Comparison between Line Blot and Immunoprecipitation Assays in 57 Myositis Sera. *J. Immunol. Methods* **2016**, *433*, 1−5.

(274) Marcon, E.; Jain, H.; Bhattacharya, A.; Guo, H.; Phanse, S.; Pu, S.; Byram, G.; Collins, B. C.; Dowdell, E.; Fenner, M.; et al. Assessment of a Method to Characterize Antibody Selectivity and Specificity for Use in Immunoprecipitation. *Nat. Methods* **2015**, *12*, 725−731.

(275) DeCaprio, J.; Kohl, T. O. Immunoprecipitation. *Cold Spring Harb. Protoc.* **2020**, *2020*, pdb.top098509.

(276) Wan, Q.; Zeng, Z.; Qi, J.; Zhao, Y.; Liu, X.; Chen, Z.; Zhou, H.; Zu, Y. Aptamer Targets Triple-Negative Breast Cancer through Specific Binding to Surface CD49c. *Cancers (Basel)* **2022**, *14*, 1570.

(277) Song, Z.; Mao, J.; Barrero, R. A.; Wang, P.; Zhang, F.; Wang, T. Development of a CD63 Aptamer for Efficient Cancer Immunochemistry and Immunoaffinity-Based Exosome Isolation. *Molecules* **2020**, *25*, 5585.

(278) Lin, C. N.; Tsai, Y. C.; Hsu, C. C.; Liang, Y. L.; Wu, Y. Y.; Kang, C. Y.; Lin, C. H.; Hsu, P. H.; Lee, G. B.; Hsu, K. F. An Aptamer Interacting with Heat Shock Protein 70 Shows Therapeutic Effects and Prognostic Ability in Serous Ovarian Cancer. *Mol. Ther. Nucleic Acids* **2021**, *23*, 757−768.

(279) Jain, A.; Liu, R.; Xiang, Y. K.; Ha, T. Single-Molecule Pull-Down for Studying Protein Interactions. *Nat. Protoc.* **2012**, *7*, 445−452.

(280) Yang, K. S.; Budin, G.; Tassa, C.; Kister, O.; Weissleder, R. Bioorthogonal Approach to Identify Unsuspected Drug Targets in Live Cells. *Angew. Chem., Int. Ed.* **2013**, *52*, 10593−10597.

(281) Jain, A.; Liu, R.; Ramani, B.; Arauz, E.; Ishitsuka, Y.; Ragunathan, K.; Park, J.; Chen, J.; Xiang, Y. K.; Ha, T. Probing Cellular Protein Complexes Using Single-Molecule Pull-Down. *Nature* **2011**, *473*, 484−488.

(282) Tinnefeld, P. Protein-Protein Interactions: Pull-Down for Single Molecules. *Nature* **2011**, *473*, 461−462.

(283) Ray, J.; Kruse, A.; Ozer, A.; Kajitani, T.; Johnson, R.; MacCoss, M.; Heck, M.; Lis, J. T. RNA Aptamer Capture of Macromolecular Complexes for Mass Spectrometry Analysis. *Nucleic Acids Res.* **2020**, *48*, No. e90.

(284) Hellman, L. M.; Fried, M. G. Electrophoretic Mobility Shift Assay (EMSA) for Detecting Protein-Nucleic Acid Interactions. *Nat. Protoc.* **2007**, *2*, 1849−1861.

(285) Ream, J. A.; Lewis, L. K.; Lewis, K. A. Rapid Agarose Gel Electrophoretic Mobility Shift Assay for Quantitating Protein: RNA Interactions. *Anal. Biochem.* **2016**, *511*, 36−41.

(286) Shaytan, A. K.; Xiao, H.; Armeev, G. A.; Gaykalova, D. A.; Komarova, G. A.; Wu, C.; Studitsky, V. M.; Landsman, D.; Panchenko, A. R. Structural Interpretation of DNA-Protein Hydroxyl-Radical Footprinting Experiments with High Resolution Using Hydroid. *Nat. Protoc.* **2018**, *13*, 2535−2556.

(287) Deng, B.; Lin, Y.; Wang, C.; Li, F.; Wang, Z.; Zhang, H.; Li, X. F.; Le, X. C. Aptamer Binding Assays for Proteins: The Thrombin Example-A Review. *Anal. Chim. Acta* **2014**, *837*, 1−15.

(288) Zhang, H.; Li, X. F.; Le, X. C. Tunable Aptamer Capillary Electrophoresis and Its Application to Protein Analysis. *J. Am. Chem. Soc.* **2008**, *130*, 34−35.

(289) Kakoti, A.; Goswami, P. Multifaceted Analyses of the Interactions between Human Heart Type Fatty Acid Binding Protein and Its Specific Aptamers. *Biochim. Biophys. Acta* **2017**, *1861*, 3289−3299.

(290) Hesselberth, J. R.; Chen, X.; Zhang, Z.; Sabo, P. J.; Sandstrom, R.; Reynolds, A. P.; Thurman, R. E.; Neph, S.; Kuehn, M. S.; Noble, W. S.; et al. Global Mapping of Protein-DNA Interactions in Vivo by Digital Genomic Footprinting. *Nat. Methods* **2009**, *6*, 283−289.

(291) Tijerina, P.; Mohr, S.; Russell, R. Dms Footprinting of Structured RNAs and RNA-Protein Complexes. *Nat. Protoc.* **2007**, *2*, 2608−2623.

(292) Chen, Y.; Corn, R. M. Dnazyme Footprinting: Detecting Protein-Aptamer Complexation on Surfaces by Blocking Dnazyme Cleavage Activity. *J. Am. Chem. Soc.* **2013**, *135*, 2072−2075.

(293) Chinnapen, D. J.; Sen, D. Hemin-Stimulated Docking of Cytochrome C to a Hemin-DNA Aptamer Complex. *Biochemistry* **2002**, *41*, 5202−5212.

(294) Bayramoglu, G.; Kilic, M.; Yakup Arica, M. Selective Isolation and Sensitive Detection of Lysozyme Using Aptamer Based Magnetic Adsorbent and a New Quartz Crystal Microbalance System. *Food Chem.* **2022**, *382*, 132353.

(295) Bell, D. R.; Weber, J. K.; Yin, W.; Huynh, T.; Duan, W.; Zhou, R. In Silico Design and Validation of High-Affinity RNA Aptamers Targeting Epithelial Cellular Adhesion Molecule Dimers. *Proc. Natl. Acad. Sci. U. S. A.* **2020**, *117*, 8486−8493.

(296) Liu, Y.; Liu, N.; Ma, X.; Li, X.; Ma, J.; Li, Y.; Zhou, Z.; Gao, Z. Highly Specific Detection of Thrombin Using an Aptamer-Based Suspension Array and the Interaction Analysis via Microscale Thermophoresis. *Analyst* **2015**, *140*, 2762−2770.

(297) Wang, Q.; Liu, L.; Yang, X.; Wang, K.; Chen, N.; Zhou, C.; Luo, B.; Du, S. Evaluation of Medicine Effects on the Interaction of Myoglobin and Its Aptamer or Antibody Using Atomic Force Microscopy. *Anal. Chem.* **2015**, *87*, 2242−2248.

(298) Lorenzo-Gomez, R.; Fernandez-Alonso, N.; Miranda-Castro, R.; de-Los-Santos-Alvarez, N.; Lobo-Castanon, M. J. Unravelling the Lipocalin 2 Interaction with Aptamers: May Rolling Circle Amplification Improve Their Functional Affinity? *Talanta* **2019**, *197*, 406−412.

(299) Cao, L.; Wang, Z.; Zhang, D.; Li, X.; Hou, C.; Ren, C. Phosphorylation of Myosin Regulatory Light Chain at Ser17 Regulates Actomyosin Dissociation. *Food Chem.* **2021**, *356*, 129655.

(300) Sett, A.; Borthakur, B. B.; Bora, U. Selection of DNA Aptamers for Extra Cellular Domain of Human Epidermal Growth Factor Receptor 2 to Detect HER2 Positive Carcinomas. *Clin. Transl. Oncol.* **2017**, *19*, 976−988.

(301) Slavkovic, S.; Churcher, Z. R.; Johnson, P. E. Nanomolar Binding Affinity of Quinine-Based Antimalarial Compounds by the Cocaine-Binding Aptamer. *Bioorg. Med. Chem.* **2018**, *26*, 5427−5434.

(302) Amano, R.; Takada, K.; Tanaka, Y.; Nakamura, Y.; Kawai, G.; Kozu, T.; Sakamoto, T. Kinetic and Thermodynamic Analyses of Interaction between a High-Affinity RNA Aptamer and Its Target Protein. *Biochemistry* **2016**, *55*, 6221−6229.

(303) Stein, J. A. C.; Ianeselli, A.; Braun, D. Kinetic Microscale Thermophoresis for Simultaneous Measurement of Binding Affinity and Kinetics. *Angew. Chem., Int. Ed.* **2021**, *60*, 13988−13995.

(304) Mao, Y.; Yu, L.; Yang, R.; Qu, L.-b.; Harrington, P. d. B. A Novel Method for the Study of Molecular Interaction by Using Microscale Thermophoresis. *Talanta* **2015**, *132*, 894−901.

(305) Pilipenko, I.; Korzhikov-Vlakh, V.; Valtari, A.; Anufrikov, Y.; Kalinin, S.; Ruponen, M.; Krasavin, M.; Urtti, A.; Tennikova, T. Mucoadhesive Properties of Nanogels Based on Stimuli-Sensitive Glycosaminoglycan-Graft-pNIPAAm Copolymers. *Int. J. Biol. Macromol.* **2021**, *186*, 864−872.

(306) Ruscito, A.; DeRosa, M. C. Small-Molecule Binding Aptamers: Selection Strategies, Characterization, and Applications. *Front. Chem.* **2016**, *4*, 14.

(307) Yu, H.; Zhao, Q. Sensitive Microscale Thermophoresis Assay Using Aptamer Thermal Switch. *Anal. Chem.* **2022**, *94*, 16685−16691.

(308) Yu, H.; Zhao, Q. Dnazyme-Based Microscale Thermophoresis Sensor. *Anal. Chem.* **2023**, *95*, 2152−2156.

(309) He, P.; Liu, L.; Qiao, W.; Zhang, S. Ultrasensitive Detection of Thrombin Using Surface Plasmon Resonance and Quartz Crystal

Microbalance Sensors by Aptamer-Based Rolling Circle Amplification and Nanoparticle Signal Enhancement. *Chem. Commun.* **2014**, *50*, 1481−1484.

(310) Sun, W.; Song, W.; Guo, X.; Wang, Z. Ultrasensitive Detection of Nucleic Acids and Proteins Using Quartz Crystal Microbalance and Surface Plasmon Resonance Sensors Based on Target-Triggering Multiple Signal Amplification Strategy. *Anal. Chim. Acta* **2017**, *978*, 42−47.

(311) Zhang, X.; Chen, J.; Liu, H.; Zhang, S. Quartz Crystal Microbalance Detection of Protein Amplified by Nicked Circling, Rolling Circle Amplification and Biocatalytic Precipitation. *Biosens. Bioelectron.* **2015**, *65*, 341−345.

(312) Ding, Y.; Weindl, P.; Lenz, A. G.; Mayer, P.; Krebs, T.; Schmid, O. Quartz Crystal Microbalances (QCM) Are Suitable for Real-Time Dosimetry in Nanotoxicological Studies Using VITROCELL(R)Cloud Cell Exposure Systems. *Part. Fibre Toxicol.* **2020**, *17*, 44.

(313) Hosseini, M. S.; Iraji zad, A.; Vossoughi, M.; Hosseini, M. L-Lysine Biodetector Based on a Tocnfs-Coated Quartz Crystal Microbalance (QCM). *Eur. Polym. J.* **2023**, *186*, 111831.

(314) Wang, L.; Wang, Z.; Xiang, Q.; Chen, Y.; Duan, Z.; Xu, J. High Performance Formaldehyde Detection Based on a Novel Copper (II) Complex Functionalized QCM Gas Sensor. *Sensors Actuators B: Chem.* **2017**, *248*, 820−828.

(315) Lim, H. J.; Saha, T.; Tey, B. T.; Tan, W. S.; Ooi, C. W. Quartz Crystal Microbalance-Based Biosensors as Rapid Diagnostic Devices for Infectious Diseases. *Biosens. Bioelectron.* **2020**, *168*, 112513.

(316) Strehlitz, B.; Nikolaus, N.; Stoltenburg, R. Protein Detection with Aptamer Biosensors. *Sensors* **2008**, *8*, 4296−4307.

(317) Lin, Y. C.; Chen, W. Y.; Hwu, E. T.; Hu, W. P. In-Silico Selection of Aptamer Targeting SARS-CoV-2 Spike Protein. *Int. J. Mol. Sci.* **2022**, *23*, 5810.

(318) Alexander Reese, R.; Xu, B. Single-Molecule Detection of Proteins and Toxins in Food Using Atomic Force Microscopy. *Trends Food Sci. Technol.* **2019**, *87*, 26−34.

(319) Kasas, S.; Dietler, G. DNA-Protein Interactions Explored by Atomic Force Microscopy. *Semin. Cell Dev. Biol.* **2018**, *73*, 231−239.

(320) Senapati, S.; Manna, S.; Lindsay, S.; Zhang, P. Application of Catalyst-Free Click Reactions in Attaching Affinity Molecules to Tips of Atomic Force Microscopy for Detection of Protein Biomarkers. *Langmuir* **2013**, *29*, 14622−14630.

(321) Senapati, S.; Lindsay, S. Recent Progress in Molecular Recognition Imaging Using Atomic Force Microscopy. *Acc. Chem. Res.* **2016**, *49*, 503−510.

(322) Jiang, Y.; Zhu, C.; Ling, L.; Wan, L.; Fang, X.; Bai, C. Specific Aptamer-Protein Interaction Studied by Atomic Force Microscopy. *Anal. Chem.* **2003**, *75*, 2112−2116.

(323) Zhang, N.; Chen, Z.; Liu, D.; Jiang, H.; Zhang, Z. K.; Lu, A.; Zhang, B. T.; Yu, Y.; Zhang, G. Structural Biology for the Molecular Insight between Aptamers and Target Proteins. *Int. J. Mol. Sci.* **2021**, *22*, 4093.

(324) Daems, E.; Moro, G.; Campos, R.; De Wael, K. Mapping the Gaps in Chemical Analysis for the Characterisation of Aptamer-Target Interactions. *TrAC, Trends Anal. Chem.* **2021**, *142*, 116311.

(325) Ruigrok, V. J. B.; Levisson, M.; Hekelaar, J.; Smidt, H.; Dijkstra, B. W.; Van der Oost, J. Characterization of Aptamer-Protein Complexes by X-Ray Crystallography and Alternative Approaches. *Int. J. Mol. Sci.* **2012**, *13*, 10537−10552.

(326) Troisi, R.; Balasco, N.; Vitagliano, L.; Sica, F. Molecular Dynamics Simulations of Human Alpha-Thrombin in Different Structural Contexts: Evidence for an Aptamer-Guided Cooperation between the Two Exosites. *J. Biomol. Struct. Dyn.* **2021**, *39*, 2199−2209.

(327) Xu, Y.; Zhang, D.; Rogawski, R.; Nimigean, C. M.; McDermott, A. E. Identifying Coupled Clusters of Allostery Participants through Chemical Shift Perturbations. *Proc. Natl. Acad. Sci. U. S. A.* **2019**, *116*, 2078−2085.

(328) Foster, M. P.; Wuttke, D. S.; Clemens, K. R.; Jahnke, W.; Radhakrishnan, I.; Tennant, L.; Reymond, M.; Chung, J.; Wright, P.

E. Chemical Shift as a Probe of Molecular Interfaces: NMR Studies of DNA Binding by the Three Amino-Terminal Zinc Finger Domains from Transcription Factor Iiia. *J. Biomol. NMR* **1998**, *12*, 51−71.

(329) Khan, N. H.; Bui, A. A.; Xiao, Y.; Sutton, R. B.; Shaw, R. W.; Wylie, B. J.; Latham, M. P. A DNA Aptamer Reveals an Allosteric Site for Inhibition in Metallo-Beta-Lactamases. *PLoS One* **2019**, *14*, No. e0214440.

(330) Morozov, D.; Mironov, V.; Moryachkov, R. V.; Shchugoreva, I. A.; Artyushenko, P. V.; Zamay, G. S.; Kolovskaya, O. S.; Zamay, T. N.; Krat, A. V.; Molodenskiy, D. S.; et al. The Role of SAXS and Molecular Simulations in 3D Structure Elucidation of a DNA Aptamer against Lung Cancer. *Mol. Ther. Nucleic Acids* **2021**, *25*, 316−327.

(331) Napolitano, E.; Riccardi, C.; Gaglione, R.; Arciello, A.; Pirota, V.; Triveri, A.; Doria, F.; Musumeci, D.; Montesarchio, D. Selective Light-up of Dimeric G-Quadruplex Forming Aptamers for Efficient VEGF(165) Detection. *Int. J. Biol. Macromol.* **2023**, *224*, 344−357.

(332) Kim, Y. B.; Wacker, A.; Laer, K. V.; Rogov, V. V.; Suess, B.; Schwalbe, H. Ligand Binding to 2′-Deoxyguanosine Sensing Riboswitch in Metabolic Context. *Nucleic Acids Res.* **2017**, *45*, 5375−5386.

(333) Weisshoff, H.; Krylova, O.; Nikolenko, H.; Dungen, H. D.; Dallmann, A.; Becker, S.; Gottel, P.; Muller, J.; Haberland, A. Aptamer BC 007 - Efficient Binder of Spreading-Crucial SARS-CoV-2 Proteins. *Heliyon* **2020**, *6*, No. e05421.

(334) Nichols, P.; Born, A.; Henen, M.; Strotz, D.; Orts, J.; Olsson, S.; Güntert, P.; Chi, C.; Vögeli, B. The Exact Nuclear Overhauser Enhancement: Recent Advances. *Molecules* **2017**, *22*, 1176.

(335) Ren, J.; Sherry, A. D.; Malloy, C. R. Band Inversion Amplifies (31)P-(31)P Nuclear Overhauser Effects: Relaxation Mechanism and Dynamic Behavior of ATP in the Human Brain by (31)P Mrs at 7 T. *Magn. Reson. Med.* **2017**, *77*, 1409−1418.

(336) Adrian, M.; Winnerdy, F. R.; Heddi, B.; Phan, A. T. Rotation of Guanine Amino Groups in G-Quadruplexes: A Probe for Local Structure and Ligand Binding. *Biophys. J.* **2017**, *113*, 775−784.

(337) Mashima, T.; Nishikawa, F.; Kamatari, Y. O.; Fujiwara, H.; Saimura, M.; Nagata, T.; Kodaki, T.; Nishikawa, S.; Kuwata, K.; Katahira, M. Anti-Prion Activity of an RNA Aptamer and Its Structural Basis. *Nucleic Acids Res.* **2013**, *41*, 1355−1362.

(338) Kirberger, S. E.; Maltseva, S. D.; Manulik, J. C.; Einstein, S. A.; Weegman, B. P.; Garwood, M.; Pomerantz, W. C. K. Synthesis of Intrinsically Disordered Fluorinated Peptides for Modular Design of High-Signal (19)F Mri Agents. *Angew. Chem., Int. Ed.* **2017**, *56*, 6440−6444.

(339) Marsh, E. N.; Suzuki, Y. Using (19)F NMR to Probe Biological Interactions of Proteins and Peptides. *ACS Chem. Biol.* **2014**, *9*, 1242−1250.

(340) Boeszoermenyi, A.; Ogórek, B.; Jain, A.; Arthanari, H.; Wagner, G. The Precious Fluorine on the Ring: Fluorine NMR for Biological Systems. *J. Biomol. NMR* **2020**, *74*, 365−379.

(341) Chrominski, M.; Baranowski, M. R.; Chmielinski, S.; Kowalska, J.; Jemielity, J. Synthesis of Trifluoromethylated Purine Ribonucleotides and Their Evaluation as (19)F NMR Probes. *J. Org. Chem.* **2020**, *85*, 3440−3453.

(342) Baranowski, M. R.; Warminski, M.; Jemielity, J.; Kowalska, J. 5′-Fluoro(Di)Phosphate-Labeled Oligonucleotides Are Versatile Molecular Probes for Studying Nucleic Acid Secondary Structure and Interactions by (19)F NMR. *Nucleic Acids Res.* **2020**, *48*, 8209−8224.

(343) Huang, C.; Kalodimos, C. G. Structures of Large Protein Complexes Determined by Nuclear Magnetic Resonance Spectroscopy. *Annu. Rev. Biophys.* **2017**, *46*, 317−336.

(344) Izunobi, J. U.; Higginbotham, C. L. Polymer Molecular Weight Analysis by $^1$H NMR Spectroscopy. *J. Chem. Educ.* **2011**, *88*, 1098−1104.

(345) Sprangers, R.; Velyvis, A.; Kay, L. E. Solution NMR of Supramolecular Complexes: Providing New Insights into Function. *Nat. Methods* **2007**, *4*, 697−703.

(346) Pica, A.; Russo Krauss, I.; Parente, V.; Tateishi-Karimata, H.; Nagatoishi, S.; Tsumoto, K.; Sugimoto, N.; Sica, F. Through-Bond Effects in the Ternary Complexes of Thrombin Sandwiched by Two DNA Aptamers. *Nucleic Acids Res.* 2017, *45*, 461−469.

(347) Kato, K.; Ikeda, H.; Miyakawa, S.; Futakawa, S.; Nonaka, Y.; Fujiwara, M.; Okudaira, S.; Kano, K.; Aoki, J.; Morita, J.; et al. Structural Basis for Specific Inhibition of Autotaxin by a DNA Aptamer. *Nat. Struct. Mol. Biol.* 2016, *23*, 395−401.

(348) Smirnov, I.; Kolganova, N.; Troisi, R.; Sica, F.; Timofeev, E. Expanding the Recognition Interface of the Thrombin-Binding Aptamer HD1 through Modification of Residues T3 and T12. *Mol. Ther. Nucleic Acids* 2021, *23*, 863−871.

(349) Grau, F. C.; Jaeger, J.; Groher, F.; Suess, B.; Muller, Y. A. The Complex Formed between a Synthetic RNA Aptamer and the Transcription Repressor TetR Is a Structural and Functional Twin of the Operator DNA-TetR Regulator Complex. *Nucleic Acids Res.* 2020, *48*, 3366−3378.

(350) Garman, E. F. Developments in X-Ray Crystallographic Structure Determination of Biological Macromolecules. *Science* 2014, *343*, 1102−1108.

(351) Landau, E. M.; Rosenbusch, J. P. Lipidic Cubic Phases: A Novel Concept for the Crystallization of Membrane Proteins. *Proc. Natl. Acad. Sci. U. S. A.* 1996, *93*, 14532−14535.

(352) Buckley, G.; Gervinskas, G.; Taveneau, C.; Venugopal, H.; Whisstock, J. C.; de Marco, A. Automated Cryo-Lamella Preparation for High-Throughput in-Situ Structural Biology. *J. Struct. Biol.* 2020, *210*, 107488.

(353) Koning, R. I.; Vader, H.; van Nugteren, M.; Grocutt, P. A.; Yang, W.; Renault, L. L. R.; Koster, A. J.; Kamp, A. C. F.; Schwertner, M. Automated Vitrification of Cryo-EM Samples with Controllable Sample Thickness Using Suction and Real-Time Optical Inspection. *Nat. Commun.* 2022, *13*, 2985.

(354) Takvorian, P. M.; Han, B.; Cali, A.; Rice, W. J.; Gunther, L.; Macaluso, F.; Weiss, L. M. An Ultrastructural Study of the Extruded Polar Tube of Anncaliia Algerae (Microsporidia). *J. Eukaryot. Microbiol.* 2020, *67*, 28−44.

(355) Cheng, E. L.; Cardle, I. I.; Kacherovsky, N.; Bansia, H.; Wang, T.; Zhou, Y.; Raman, J.; Yen, A.; Gutierrez, D.; Salipante, S. J.; et al. Discovery of a Transferrin Receptor 1-Binding Aptamer and Its Application in Cancer Cell Depletion for Adoptive T-Cell Therapy Manufacturing. *J. Am. Chem. Soc.* 2022, *144*, 13851−13864.

(356) Kim, J.; Yunn, N. O.; Park, M.; Kim, J.; Park, S.; Kim, Y.; Noh, J.; Ryu, S. H.; Cho, Y. Functional Selectivity of Insulin Receptor Revealed by Aptamer-Trapped Receptor Structures. *Nat. Commun.* 2022, *13*, 6500.

(357) Cheng, Y. Single-Particle Cryo-EM at Crystallographic Resolution. *Cell* 2015, *161*, 450−457.

(358) Ma, H.; Jia, X.; Zhang, K.; Su, Z. Cryo-EM Advances in RNA Structure Determination. *Signal Transduct. Target. Ther.* 2022, *7*, 58.

(359) Hattne, J.; Shi, D.; Glynn, C.; Zee, C. T.; Gallagher-Jones, M.; Martynowycz, M. W.; Rodriguez, J. A.; Gonen, T. Analysis of Global and Site-Specific Radiation Damage in Cryo-EM. *Structure* 2018, *26*, 759−766.

(360) Renaud, J. P.; Chari, A.; Ciferri, C.; Liu, W. T.; Remigy, H. W.; Stark, H.; Wiesmann, C. Cryo-EM in Drug Discovery: Achievements, Limitations and Prospects. *Nat. Rev. Drug Discovery* 2018, *17*, 471−492.

(361) Benjin, X.; Ling, L. Developments, Applications, and Prospects of Cryo-Electron Microscopy. *Protein Sci.* 2020, *29*, 872−882.

(362) Callaway, E. The Revolution Will Not Be Crystallized: A New Method Sweeps through Structural Biology. *Nature* 2015, *525*, 172−174.

(363) Lin, K. Y.; Kwong, G. A.; Warren, A. D.; Wood, D. K.; Bhatia, S. N. Nanoparticles That Sense Thrombin Activity as Synthetic Urinary Biomarkers of Thrombosis. *ACS Nano* 2013, *7*, 9001−9009.

(364) Wei, L. H.; Chen, T. R.; Fang, H. B.; Jin, Q.; Zhang, S. J.; Hou, J.; Yu, Y.; Dou, T. Y.; Cao, Y. F.; Guo, W. Z.; et al. Natural Constituents of St. John's Wort Inhibit the Proteolytic Activity of Human Thrombin. *Int. J. Biol. Macromol.* 2019, *134*, 622−630.

(365) Nilsson, M.; Hamalainen, M.; Ivarsson, M.; Gottfries, J.; Xue, Y.; Hansson, S.; Isaksson, R.; Fex, T. Compounds Binding to the S2-S3 Pockets of Thrombin. *J. Med. Chem.* 2009, *52*, 2708−2715.

(366) Calnan, B. J.; Tidor, B.; Biancalana, S.; Hudson, D.; Frankel, A. D. Arginine-Mediated RNA Recognition: The Arginine Fork. *Science* 1991, *252*, 1167−1171.

(367) Reshetnikov, R.; Golovin, A.; Spiridonova, V.; Kopylov, A.; Sponer, J. Structural Dynamics of Thrombin-Binding DNA Aptamer d(GGTTGGTGTGGTTGG) Quadruplex DNA Studied by Large-Scale Explicit Solvent Simulations. *J. Chem. Theory Comput.* 2010, *6*, 3003−3014.

(368) Nagatoishi, S.; Isono, N.; Tsumoto, K.; Sugimoto, N. Loop Residues of Thrombin-Binding DNA Aptamer Impact G-Quadruplex Stability and Thrombin Binding. *Biochimie* 2011, *93*, 1231−1238.

(369) Valsangkar, V.; Vangaveti, S.; Lee, G. W.; Fahssi, W. M.; Awan, W. S.; Huang, Y.; Chen, A. A.; Sheng, J. Structural and Binding Effects of Chemical Modifications on Thrombin Binding Aptamer (TBA). *Molecules* 2021, *26*, 4620.

(370) Xiong, Y.; Liang, M.; Cheng, Y.; Zou, J.; Li, Y. An "Off-on" Phosphorescent Aptasensor for the Detection of Thrombin Based on Pret. *Analyst* 2019, *144*, 161−171.

(371) Gao, Y.; Zheng, H.; Li, L.; Feng, M.; Chen, X.; Hao, B.; Lv, Z.; Zhou, X.; Cao, Y. Prostate-Specific Membrane Antigen (PSMA) Promotes Angiogenesis of Glioblastoma through Interacting with ITGB4 and Regulating NF-kappaB Signaling Pathway. *Front. Cell Dev. Biol.* 2021, *9*, 598377.

(372) Wustemann, T.; Haberkorn, U.; Babich, J.; Mier, W. Targeting Prostate Cancer: Prostate-Specific Membrane Antigen Based Diagnosis and Therapy. *Med. Res. Rev.* 2019, *39*, 40−69.

(373) Ptacek, J.; Zhang, D.; Qiu, L.; Kruspe, S.; Motlova, L.; Kolenko, P.; Novakova, Z.; Shubham, S.; Havlinova, B.; Baranova, P.; et al. Structural Basis of Prostate-Specific Membrane Antigen Recognition by the A9g RNA Aptamer. *Nucleic Acids Res.* 2020, *48*, 11130−11145.

(374) Omer, M.; Andersen, V. L.; Nielsen, J. S.; Wengel, J.; Kjems, J. Improved Cancer Targeting by Multimerizing Aptamers on Nano-scaffolds. *Mol. Ther. Nucleic Acids* 2020, *22*, 994−1003.

(375) Dalvit, C.; Invernizzi, C.; Vulpetti, A. Fluorine as a Hydrogen-Bond Acceptor: Experimental Evidence and Computational Calculations. *Chem.—Eur. J.* 2014, *20*, 11058−11068.

(376) Ouedraogo, N. A. N.; Yan, H.; Han, C. B.; Zhang, Y. Influence of Fluorinated Components on Perovskite Solar Cells Performance and Stability. *Small* 2021, *17*, No. e2004081.

(377) Hennecke, U. Chemistry. Revealing the Positive Side of Fluorine. *Science* 2013, *340*, 41−42.

(378) Bao, H. L.; Ishizuka, T.; Yamashita, A.; Furukoji, E.; Asada, Y.; Xu, Y. Improving Thermodynamic Stability and Anticoagulant Activity of a Thrombin Binding Aptamer by Incorporation of 8-Trifluoromethyl-2'-Deoxyguanosine. *J. Med. Chem.* 2021, *64*, 711−718.

(379) Wang, Y.; Xiao, Y.; Ma, X.; Li, N.; Yang, X. Label-Free and Sensitive Thrombin Sensing on a Molecularly Grafted Aptamer on Graphene. *Chem. Commun.* 2012, *48*, 738−740.

(380) Chen, F.; Gülbakan, B.; Zenobi, R. Direct Access to Aptamer-Protein Complexes via MALDI-MS. *Chem. Sci.* 2013, *4*, 4071−4078.

(381) Kanakaraj, I.; Chen, W. H.; Poongavanam, M.; Dhamane, S.; Stagg, L. J.; Ladbury, J. E.; Kourentzi, K.; Strych, U.; Willson, R. C. Biophysical Characterization of VEGF-Aht DNA Aptamer Interactions. *Int. J. Biol. Macromol.* 2013, *57*, 69−75.

(382) Diehl, K. L.; Anslyn, E. V. Array Sensing Using Optical Methods for Detection of Chemical and Biological Hazards. *Chem. Soc. Rev.* 2013, *42*, 8596−8611.

(383) Guo, H.; Zhang, N.; Liu, D.; Wang, P.; Ma, X. Inhibitory Effect on the Proliferation of Human Heptoma Induced by Cell-Permeable Manganese Superoxide Dismutase. *Biomed. Pharmacother.* 2016, *83*, 1379−1386.

(384) Konzack, A.; Jakupovic, M.; Kubaichuk, K.; Gorlach, A.; Dombrowski, F.; Miinalainen, I.; Sormunen, R.; Kietzmann, T. Mitochondrial Dysfunction Due to Lack of Manganese Superoxide Dismutase Promotes Hepatocarcinogenesis. *Antioxid. Redox Signal.* 2015, 23, 1059–1075.

(385) Safar, W.; Tatar, A. S.; Leray, A.; Potara, M.; Liu, Q.; Edely, M.; Djaker, N.; Spadavecchia, J.; Fu, W.; Derouich, S. G.; et al. New Insight into the Aptamer Conformation and Aptamer/Protein Interaction by Surface-Enhanced Raman Scattering and Multivariate Statistical Analysis. *Nanoscale* 2021, 13, 12443–12453.

(386) Cottat, M.; D'Andrea, C.; Yasukuni, R.; Malashikhina, N.; Grinyte, R.; Lidgi-Guigui, N.; Fazio, B.; Sutton, A.; Oudar, O.; Charnaux, N.; et al. High Sensitivity, High Selectivity SERS Detection of MnSOD Using Optical Nanoantennas Functionalized with Aptamers. *J. Phys. Chem. C* 2015, 119, 15532–15540.

(387) Hatada, M.; Tsugawa, W.; Kamio, E.; Loew, N.; Klonoff, D. C.; Sode, K. Development of a Screen-Printed Carbon Electrode Based Disposable Enzyme Sensor Strip for the Measurement of Glycated Albumin. *Biosens. Bioelectron.* 2017, 88, 167–173.

(388) He, D.; Kuang, W.; Yang, X.; Xu, M. Association of Hemoglobin H (HbH) Disease with Hemoglobin A(1c) and Glycated Albumin in Diabetic and Non-Diabetic Patients. *Clin. Chem. Lab. Med.* 2021, 59, 1127–1132.

(389) Paria, D.; Convertino, A.; Mussi, V.; Maiolo, L.; Barman, I. Silver-Coated Disordered Silicon Nanowires Provide Highly Sensitive Label-Free Glycated Albumin Detection through Molecular Trapping and Plasmonic Hotspot Formation. *Adv. Healthcare Mater.* 2021, 10, No. e2001110.

(390) Sun, D.; Xie, J.; Chen, C. J.; Liu, J. T. Analyzation of the Binding Mechanism and the Isoelectric Point of Glycated Albumin with Self-Assembled, Aptamer-Conjugated Films by Using Surface Plasmon Resonance. *Colloids Surf. B Biointerfaces* 2022, 214, 112445.

(391) Du, Y.; Dong, S. Nucleic Acid Biosensors: Recent Advances and Perspectives. *Anal. Chem.* 2017, 89, 189–215.

(392) Razmi, N.; Baradaran, B.; Hejazi, M.; Hasanzadeh, M.; Mosafer, J.; Mokhtarzadeh, A.; de la Guardia, M. Recent Advances on Aptamer-Based Biosensors to Detection of Platelet-Derived Growth Factor. *Biosens. Bioelectron.* 2018, 113, 58–71.

(393) Xue, Y.; Lim, S.; Yang, Y.; Wang, Z.; Jensen, L. D.; Hedlund, E. M.; Andersson, P.; Sasahara, M.; Larsson, O.; Galter, D.; et al. PDGF-BB Modulates Hematopoiesis and Tumor Angiogenesis by Inducing Erythropoietin Production in Stromal Cells. *Nat. Med.* 2012, 18, 100–110.

(394) Lu, C.; Shahzad, M. M.; Moreno-Smith, M.; Lin, Y. G.; Jennings, N. B.; Allen, J. K.; Landen, C. N.; Mangala, L. S.; Armaiz-Pena, G. N.; Schmandt, R.; et al. Targeting Pericytes with a PDGF-B Aptamer in Human Ovarian Carcinoma Models. *Cancer Biol. Ther.* 2010, 9, 176–182.

(395) Vu, C. Q.; Rotkrua, P.; Soontornworajit, B.; Tantirungrotechai, Y. Effect of PDGF-B Aptamer on PDGFRbeta/PDGF-B Interaction: Molecular Dynamics Study. *J. Mol. Graph. Model.* 2018, 82, 145–156.

(396) Wang, J.; Meng, W.; Zheng, X.; Liu, S.; Li, G. Combination of Aptamer with Gold Nanoparticles for Electrochemical Signal Amplification: Application to Sensitive Detection of Platelet-Derived Growth Factor. *Biosens. Bioelectron.* 2009, 24, 1598–1602.

(397) Potty, A. S.; Kourentzi, K.; Fang, H.; Schuck, P.; Willson, R. C. Biophysical Characterization of DNA and RNA Aptamer Interactions with Hen Egg Lysozyme. *Int. J. Biol. Macromol.* 2011, 48, 392–397.

(398) Putnin, T.; Waiwinya, W.; Pimalai, D.; Chawjiraphan, W.; Sathirapongsasuti, N.; Japrung, D. Dual Sensitive and Rapid Detection of Glycated Human Serum Albumin Using a Versatile Lead/Graphene Nanocomposite Probe as a Fluorescence-Electrochemical Aptasensor. *Analyst* 2021, 146, 4357–4364.

(399) Riccardi, C.; Napolitano, E.; Platella, C.; Musumeci, D.; Melone, M. A. B.; Montesarchio, D. Anti-VEGF DNA-Based Aptamers in Cancer Therapeutics and Diagnostics. *Med. Res. Rev.* 2021, 41, 464–506.

(400) Uemachi, H.; Kasahara, Y.; Tanaka, K.; Okuda, T.; Yoneda, Y.; Obika, S. Discovery of Cell-Internalizing Artificial Nucleic Acid Aptamers for Lung Fibroblasts and Targeted Drug Delivery. *Bioorg. Chem.* 2020, 105, 104321.

(401) Egli, M.; Lybrand, T. P. Enhanced Dispersion and Polarization Interactions Achieved through Dithiophosphate Group Incorporation Yield a Dramatic Binding Affinity Increase for an RNA Aptamer-Thrombin Complex. *J. Am. Chem. Soc.* 2019, 141, 4445–4452.

(402) Hyjek-Skladanowska, M.; Vickers, T. A.; Napiorkowska, A.; Anderson, B. A.; Tanowitz, M.; Crooke, S. T.; Liang, X. H.; Seth, P. P.; Nowotny, M. Origins of the Increased Affinity of Phosphorothioate-Modified Therapeutic Nucleic Acids for Proteins. *J. Am. Chem. Soc.* 2020, 142, 7456–7468.

(403) Yang, X.; Dinuka Abeydeera, N.; Liu, F. W.; Egli, M. Origins of the Enhanced Affinity of RNA-Protein Interactions Triggered by RNA Phosphorodithioate Backbone Modification. *Chem. Commun.* 2017, 53, 10508–10511.

(404) Davies, D. R.; Gelinas, A. D.; Zhang, C.; Rohloff, J. C.; Carter, J. D.; O'Connell, D.; Waugh, S. M.; Wolk, S. K.; Mayfield, W. S.; Burgin, A. B.; et al. Unique Motifs and Hydrophobic Interactions Shape the Binding of Modified DNA Ligands to Protein Targets. *Proc. Natl. Acad. Sci. U. S. A.* 2012, 109, 19971–19976.

(405) De Groote, M. A.; Nahid, P.; Jarlsberg, L.; Johnson, J. L.; Weiner, M.; Muzanyi, G.; Janjic, N.; Sterling, D. G.; Ochsner, U. A. Elucidating Novel Serum Biomarkers Associated with Pulmonary Tuberculosis Treatment. *PLoS One* 2013, 8, No. e61002.

(406) Kukova, L. Z.; Mansour, S. G.; Coca, S. G.; de Fontnouvelle, C. A.; Thiessen-Philbrook, H. R.; Shlipak, M. G.; El-Khoury, J. M.; Parikh, C. R. Comparison of Urine and Plasma Biomarker Concentrations Measured by Aptamer-Based Versus Immunoassay Methods in Cardiac Surgery Patients. *J. Appl. Lab. Med.* 2019, 4, 331–342.

(407) Park, N. J.; Wang, X.; Diaz, A.; Goos-Root, D. M.; Bock, C.; Vaught, J. D.; Sun, W.; Strom, C. M. Measurement of Cetuximab and Panitumumab-Unbound Serum EGFR Extracellular Domain Using an Assay Based on Slow Off-Rate Modified Aptamer (SOMAmer) Reagents. *PLoS One* 2013, 8, No. e71703.

(408) Webber, J.; Stone, T. C.; Katilius, E.; Smith, B. C.; Gordon, B.; Mason, M. D.; Tabi, Z.; Brewis, I. A.; Clayton, A. Proteomics Analysis of Cancer Exosomes Using a Novel Modified Aptamer-Based Array (SOMAscan™) Platform. *Mol. Cell. Proteomics* 2014, 13, 1050–1064.

(409) Yum, J. H.; Ishizuka, T.; Fukumoto, K.; Hori, D.; Bao, H. L.; Xu, Y.; Sugiyama, H.; Park, S. Systematic Approach to DNA Aptamer Design Using Amino Acid-Nucleic Acid Hybrids (ANHs) Targeting Thrombin. *ACS Biomater. Sci. Eng.* 2021, 7, 1338–1343.

(410) Kimoto, M.; Shermane Lim, Y. W.; Hirao, I. Molecular Affinity Rulers: Systematic Evaluation of DNA Aptamers for Their Applicabilities in ELISA. *Nucleic Acids Res.* 2019, 47, 8362–8374.

(411) Bjerregaard, N.; Andreasen, P. A.; Dupont, D. M. Expected and Unexpected Features of Protein-Binding RNA Aptamers. *Wiley Interdiscip. Rev. RNA* 2016, 7, 744–757.

(412) Peng, Y.; Li, L.; Mu, X.; Guo, L. Aptamer-Gold Nanoparticle-Based Colorimetric Assay for the Sensitive Detection of Thrombin. *Sensors Actuators B: Chem.* 2013, 177, 818–825.

(413) Mangani, S.; Orioli, P. L.; Scozzafava, A.; Messori, L.; Carloni, P. EXAFS Studies of Fe (III)-Phosvitin at High Metal to Protein Ratios. *BioMetals* 1994, 7, 104–108.

(414) Terron, A.; Fiol, J.; Herrero, L.; García-Raso, A.; Apella, M.; Caubet, A.; Moreno, V. Metal-Amino Acid (or Peptide)-Nucleoside (or Related Bases) Ternary Complexes. *J. Inorg. Biochem.* 1997, 93, 1.

(415) Terrón, A.; Fiol, J. J.; García-Raso, A.; Barceló-Oliver, M.; Moreno, V. Biological Recognition Patterns Implicated by the Formation and Stability of Ternary Metal Ion Complexes of Low-Molecular-Weight Formed with Amino Acid/Peptides and Nucleobases/Nucleosides. *Coord. Chem. Rev.* 2007, 251, 1973–1986.

(416) Liu, S.; Zhang, M.; Jin, H.; Wang, Z.; Liu, Y.; Zhang, S.; Zhang, H. Iron-Containing Protein-Mimic Supramolecular Iron Delivery Systems for Ferroptosis Tumor Therapy. *J. Am. Chem. Soc.* 2023, 145, 160–170.

(417) Zhu, H.; Situ, J.; Guan, T.; Dou, Z.; Kong, G.; Jiang, Z.; Xi, P. A $C_2H_2$ Zinc Finger Protein PlCZF1 Is Necessary for Oospore Development and Virulence in Peronophythora Litchii. *Int. J. Mol. Sci.* **2022**, *23*, 2733.

(418) Mueller, A. L.; Corbi-Verge, C.; Giganti, D. O.; Ichikawa, D. M.; Spencer, J. M.; MacRae, M.; Garton, M.; Kim, P. M.; Noyes, M. B. The Geometric Influence on the $Cys_2His_2$ Zinc Finger Domain and Functional Plasticity. *Nucleic Acids Res.* **2020**, *48*, 6382−6402.

(419) Cassandri, M.; Smirnov, A.; Novelli, F.; Pitolli, C.; Agostini, M.; Malewicz, M.; Melino, G.; Raschella, G. Zinc-Finger Proteins in Health and Disease. *Cell Death Discovery* **2017**, *3*, 17071.

(420) Li, X.; Han, M.; Zhang, H.; Liu, F.; Pan, Y.; Zhu, J.; Liao, Z.; Chen, X.; Zhang, B. Structures and Biological Functions of Zinc Finger Proteins and Their Roles in Hepatocellular Carcinoma. *Biomark. Res.* **2022**, *10*, 2.

(421) de Paiva, R. E. F.; Du, Z.; Peterson, E. J.; Corbi, P. P.; Farrell, N. P. Probing the HIV-1 NCp7 Nucleocapsid Protein with Site-Specific Gold(I)-Phosphine Complexes. *Inorg. Chem.* **2017**, *56*, 12308−12318.

(422) Godet, J.; Kenfack, C.; Przybilla, F.; Richert, L.; Duportail, G.; Mely, Y. Site-Selective Probing of Ctar Destabilization Highlights the Necessary Plasticity of the HIV-1 Nucleocapsid Protein to Chaperone the First Strand Transfer. *Nucleic Acids Res.* **2013**, *41*, 5036−5048.

(423) Ouyang, W.; Okaine, S.; McPike, M. P.; Lin, Y.; Borer, P. N. Probing the RNA Binding Surface of the HIV-1 Nucleocapsid Protein by Site-Directed Mutagenesis. *Biochemistry* **2013**, *52*, 3358−3368.

(424) Weiss, T. C.; Zhai, G. G.; Bhatia, S. S.; Romaniuk, P. J. An RNA Aptamer with High Affinity and Broad Specificity for Zinc Finger Proteins. *Biochemistry* **2010**, *49*, 2732−2740.

(425) Niedzwiecki, D. J.; Iyer, R.; Borer, P. N.; Movileanu, L. Sampling a Biomarker of the Human Immunodeficiency Virus across a Synthetic Nanopore. *ACS Nano* **2013**, *7*, 3341−3350.

(426) Stockwell, B. R. Ferroptosis Turns 10: Emerging Mechanisms, Physiological Functions, and Therapeutic Applications. *Cell* **2022**, *185*, 2401−2421.

(427) Tan, J.; Li, H.; Ji, C.; Zhang, L.; Zhao, C.; Tang, L.; Zhang, C.; Sun, Z.; Tan, W.; Yuan, Q. Electron Transfer-Triggered Imaging of EGFR Signaling Activity. *Nat. Commun.* **2022**, *13*, 594.

(428) Zhang, L.; Chu, M.; Ji, C.; Wei, J.; Yang, Y.; Huang, Z.; Tan, W.; Tan, J.; Yuan, Q. In Situ Visualization of Epidermal Growth Factor Receptor Nuclear Translocation with Circular Bivalent Aptamer. *Anal. Chem.* **2022**, *94*, 17413−17421.

(429) Al-Akhrass, H.; Naves, T.; Vincent, F.; Magnaudeix, A.; Durand, K.; Bertin, F.; Melloni, B.; Jauberteau, M. O.; Lalloue, F. Sortilin Limits EGFR Signaling by Promoting Its Internalization in Lung Cancer. *Nat. Commun.* **2017**, *8*, 1182.

(430) Wheeler, S. E. Understanding Substituent Effects in Noncovalent Interactions Involving Aromatic Rings. *Acc. Chem. Res.* **2013**, *46*, 1029−1038.

(431) Gray, M. D.; Deore, P. S.; Chung, A. J.; Van Riesen, A. J.; Manderville, R. A.; Prabhakar, P. S.; Wetmore, S. D. Lighting up the Thrombin-Binding Aptamer G-Quadruplex with an Internal Cyanine-Indole-Quinolinium Nucleobase Surrogate. Direct Fluorescent Intensity Readout for Thrombin Binding without Topology Switching. *Bioconjugate Chem.* **2020**, *31*, 2596−2606.

(432) Blanco, C.; Bayas, M.; Yan, F.; Chen, I. A. Analysis of Evolutionarily Independent Protein-RNA Complexes Yields a Criterion to Evaluate the Relevance of Prebiotic Scenarios. *Curr. Biol.* **2018**, *28*, 526−537.

(433) Nomura, Y.; Sugiyama, S.; Sakamoto, T.; Miyakawa, S.; Adachi, H.; Takano, K.; Murakami, S.; Inoue, T.; Mori, Y.; Nakamura, Y.; et al. Conformational Plasticity of RNA for Target Recognition as Revealed by the 2.15 a Crystal Structure of a Human IgG-Aptamer Complex. *Nucleic Acids Res.* **2010**, *38*, 7822−7829.

(434) Platella, C.; Riccardi, C.; Montesarchio, D.; Roviello, G. N.; Musumeci, D. G-Quadruplex-Based Aptamers against Protein Targets in Therapy and Diagnostics. *Biochim. Biophys. Acta* **2017**, *1861*, 1429−1447.

(435) Song, J.; Zheng, Y.; Huang, M.; Wu, L.; Wang, W.; Zhu, Z.; Song, Y.; Yang, C. A Sequential Multidimensional Analysis Algorithm for Aptamer Identification Based on Structure Analysis and Machine Learning. *Anal. Chem.* **2020**, *92*, 3307−3314.

(436) Buglak, A. A.; Samokhvalov, A. V.; Zherdev, A. V.; Dzantiev, B. B. Methods and Applications of In Silico Aptamer Design and Modeling. *Int. J. Mol. Sci.* **2020**, *21*, 8420.

(437) Lee, G.; Jang, G. H.; Kang, H. Y.; Song, G. Predicting Aptamer Sequences That Interact with Target Proteins Using an Aptamer-Protein Interaction Classifier and a Monte Carlo Tree Search Approach. *PLoS One* **2021**, *16*, No. e0253760.

(438) Oh, I. H.; Park, D. Y.; Cha, J. M.; Shin, W. R.; Ahn, J. Y.; Kim, Y. H.; Kim, J. H.; Kim, S. C.; Cho, B. K. Docking Simulation and Sandwich Assay for Aptamer-Based Botulinum Neurotoxin Type C Detection. *Biosensors* **2020**, *10*, 98.

(439) Cole, J. C.; Murray, C. W.; Nissink, J. W.; Taylor, R. D.; Taylor, R. Comparing Protein-Ligand Docking Programs Is Difficult. *Proteins* **2005**, *60*, 325−332.

(440) Taylor, R. D.; Jewsbury, P. J.; Essex, J. W. A Review of Protein-Small Molecule Docking Methods. *J. Comput. Aided Mol. Des.* **2002**, *16*, 151−166.

(441) Thomsen, R.; Christensen, M. H. Moldock: A New Technique for High-Accuracy Molecular Docking. *J. Med. Chem.* **2006**, *49*, 3315−3321.

(442) Wang, Z.; Sun, H.; Yao, X.; Li, D.; Xu, L.; Li, Y.; Tian, S.; Hou, T. Comprehensive Evaluation of Ten Docking Programs on a Diverse Set of Protein-Ligand Complexes: The Prediction Accuracy of Sampling Power and Scoring Power. *Phys. Chem. Chem. Phys.* **2016**, *18*, 12964−12975.

(443) Jumper, J.; Evans, R.; Pritzel, A.; Green, T.; Figurnov, M.; Ronneberger, O.; Tunyasuvunakool, K.; Bates, R.; Žídek, A.; Potapenko, A.; et al. Highly Accurate Protein Structure Prediction with Alphafold. *Nature* **2021**, *596*, 583−589.

(444) Jumper, J.; Hassabis, D. Protein Structure Predictions to Atomic Accuracy with Alphafold. *Nat. Methods* **2022**, *19*, 11−12.